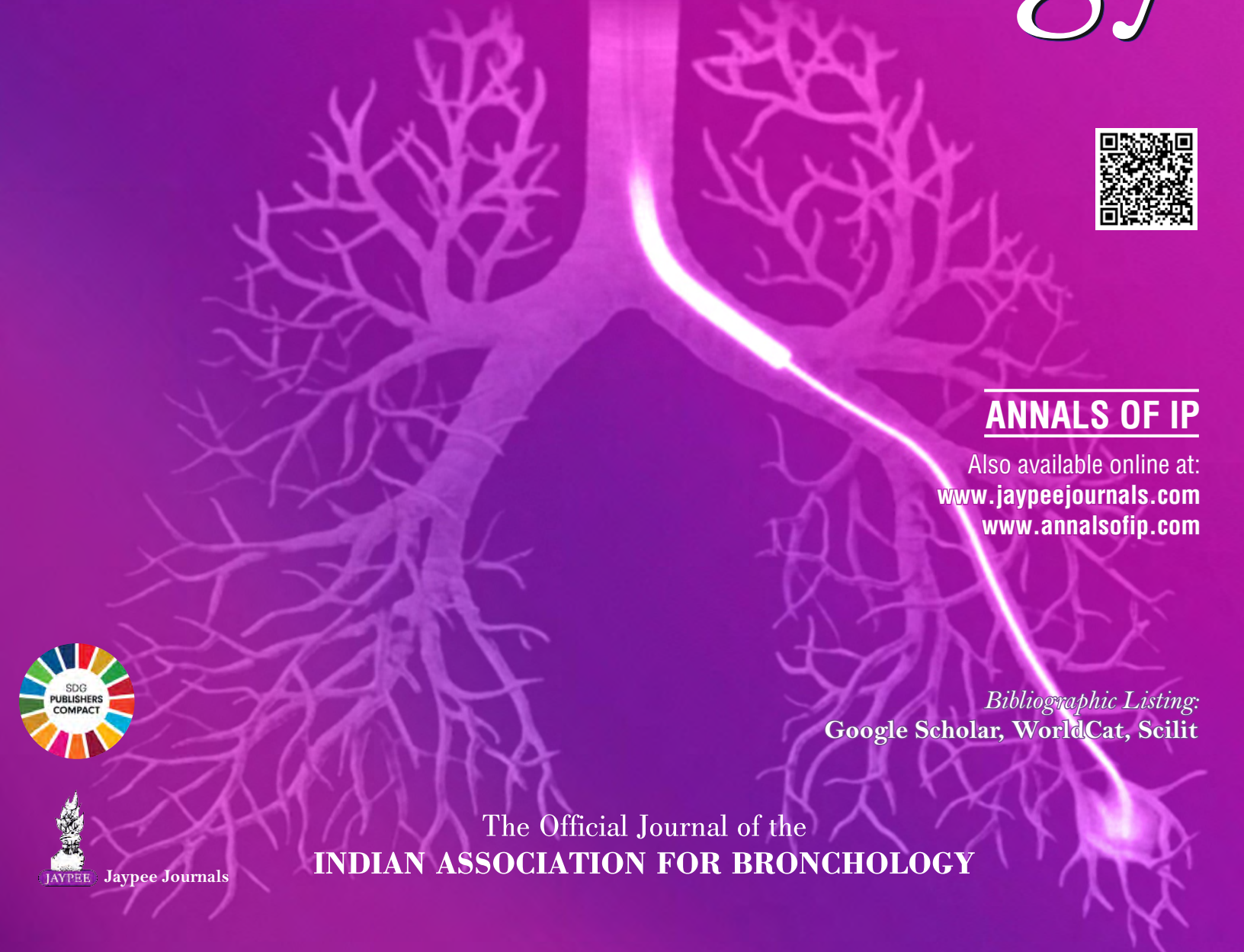
May–August 2026
Volume 2
Issue 2
eISSN: 3139-1583

Annals of Interventional Pulmonology



ANNALS OF IP

Also available online at:
www.jaypeejournals.com
www.annalsofip.com

Bibliographic Listing:
Google Scholar, WorldCat, Scilit

The Official Journal of the
INDIAN ASSOCIATION FOR BRONCHOLOGY

Jaypee Journals

Annals of Interventional Pulmonology

Volume 2 Issue 2 May–August 2026





www.jaypeebrothers.com
www.jaypeejournals.com

Annals of Interventional Pulmonology

1. Aims and Scope

Annals of Interventional Pulmonology is the official publication of the Indian Association for Bronchology. It is published triannually, with issues released in January–April, May–August, September–December. This Journal is born out of the need for a dedicated academic platform to support the growing discipline of interventional pulmonology in India and beyond. This journal is envisioned as a scholarly home for clinicians, researchers, and innovators involved in the evolving landscape of minimally invasive pulmonary diagnostics and therapeutics.

Over the past two decades, interventional pulmonology (IP) in India has witnessed a growth beyond imagination. From a specialty which was almost non-existent, it has now become one of the most sought-after fields in the domain of pulmonology. Technological advancements in this field of IP have changed the definitions of what is possible and what is not possible. With the introduction of navigational bronchoscopy platforms, thin and ultrathin scopes, cone-beam CT scans and robotic bronchoscopies, lesions—irrespective of the size and location—are being accurately diagnosed with precision. The introduction of portable and single-use flexible bronchoscopes has revolutionized the utility of bronchoscopy in the intensive care setups. Newer innovations integrated with the endobronchial ultrasonography have enabled us to procure biopsies from central mediastinal lesions and have changed our diagnostic algorithms. Therapeutic bronchoscopy for central airway lesions are also being increasingly performed to save and palliate people who were earlier considered incurable and nonpalliable.

Despite this rapid evolution of the IP sub-specialty in our country, and the sea change we are all witnessing, the growth in research contribution has not paralleled the growth in the number of procedures. This journal aims to bridge this gap, while providing a neutral platform for all those who are doing quality work to publish their research work. We aim to provide a platform for interventionalists—young as well as experienced—to share their experiences and innovations.

Timing and Scope of this Journal

The timing of this journal's launch is deliberate. We stand at a crucial juncture in the field of interventional pulmonology. The tools used in IP are becoming more sophisticated; the procedures are becoming more precise and the results more rewarding. While we incorporate the Western techniques into our practice, it is imperative to utilize them meaningfully and adapt to the local needs. There remains a paucity of region-specific data and guidelines tailored to local challenges. In the upcoming years we anticipate that this gap between practicing and publishing is minimized.

The scope of this new journal "*Annals of Interventional Pulmonology*" includes—but is not limited to—central airway interventions, pleural interventions, mediastinal sampling procedures, peripheral bronchoscopic interventions and interventions in the critical care setting. We welcome original articles, case series and reviews, educative case reports, case videos and images. A particular focus will be given to innovations in IP techniques and devices, original research work and guidelines and recommendations.

2. Subscription Information

• Subscription rates

For information on subscription rates and the other journal-related enquiries, please contact:
subscriptions@jaypeebrothers.com

• Orders

Journals Department
Jaypee Brothers Medical Publishers (P) Ltd.
4838/24, Ansari Road, Daryaganj
New Delhi 110 002, India
Phone: +91-11-4357 4357
Fax: +91-11-4357 4314
e-mail: subscriptions@jaypeebrothers.com

3. Electronic Media

An electronic edition of this journal is available at **www.annalsofip.com**

Manuscripts can be submitted online at **www.annalsofip.com**

4. Advertisement

For advertisement queries, please contact: Journals Department
Jaypee Brothers Medical Publishers (P) Ltd.
e-mail: sanjeev.kumar@jaypeebrothers.com

For any queries regarding online submission, please e-mail us at:
ayushi.goyal@jaypeebrothers.com

For editorial queries, please contact:
editor@jaypeebrothers.com

The Journal is printed on acid-free paper.

Copyright
© 2026 **Jaypee Brothers Medical Publishers (P) Ltd.**
www.jaypeebrothers.com
www.jaypeejournals.com

Annals of
Interventional Pulmonology

Editorial Board

Editor-in-Chief

Dr V Nagarjuna Maturu

Editor

Dr Amita Nene

Associate Editors

Dr Parvaiz A Koul

Dr Ravindra M Mehta

Dr VR Pattabhiraman

Dr Raja Dhar

Dr Arvind Kate

Dr Mehul Thakkar

Editorial Board

Dr Rakesh Chawla

Dr DJ Christopher

Dr Nitin Abhyankar

Dr Vivek Nangia

Dr Amit Dhamija

Dr Prashant Chhajed

Dr Nasser Yusuf

Dr RP Meena

Dr Rajesh Swarnakar

Dr Vikas Marwah

Dr Rajesh V

Dr Karan Madan

Dr Arjun Srinivasan

Dr Nitesh Gupta

Dr Santhakumar S

Dr Shyam Krishnan

Dr Viswesvaran B

Dr Sameer Bansal

Dr V Pratibh Prasad

Dr Ajay Ravi

Annals of
Interventional Pulmonology

IAB Governing Council 2026–29

President

Dr Rakesh Chawla

Hon Secretary

Dr Amita Nene

Hon Treasurer

Dr Mehul Thakkar

President–Elect

Dr Vivek Nangia

Vice Presidents

Dr Nitin Abhyankar • Dr Shyamsunder Tampi

Hon Joint Secretaries

Dr Krishna K Sharma • Dr Vinod Chavhan • Dr Aditya Chawla

Governing Council Members

Dr Radha Munje • Dr Abhishek Tandon • Dr Manu Chopra
Dr Mrutyunjay Mahendrakar • Dr Praveen Kumar

Editor-in-Chief

Dr V Nagarjuna Maturu

Journal Associate Editor

Dr Arvind Kate

International Relations Director and Academic Coordinator

Dr Visweswaran Balasubramaniam

Digital Media Editors

Dr Kapil Iyer • Dr Kamlesh Pandey

Website Editors

Dr Kinjal Modi • Dr Avya Bansal

Annals of Interventional Pulmonology

Volume 2 | Issue 2 | May–August 2026

Contents

EDITORIALS

1. Video-assisted Pleural Intervention in the Management of Pleural Infection
Arjun Srinivasan, Vallandramam Ranganathan Pattabhiraman, Sivaramakrishnan Mahadevan 55

2. Tracheobronchopathia Osteochondroplastica: When Does the Rock-garden Airway Matter?
Virender Pratibh Prasad, Venkata Nagarjuna Maturu 58

ORIGINAL ARTICLES

3. From Imaging to Insight: Evaluation of Mediastinal Lymph Nodes Using Endobronchial Ultrasound Elastography: A Prospective Study
Saurabh Jain, Vishal Kumar Chitikeshi, Mahesh Gudelli, Lakshminarayana Jasti, Kranthi Kumar Shavagani 60

4. Clinical and Technical Predictors of Diagnostic Yield in Radial Endobronchial Ultrasound Sampling for Peripheral Pulmonary Lesions: A Prospective Observational Study
Sreeja Reddy Sudhini, Mahesh Gudelli, Vishal Kumar Chitikeshi, Lakshminarayana Jasti, Kranthi Kumar Shavagani 67

5. Role of Bronchoscopy and Image Guided Tissue Sampling in Diagnosing Post COVID Cavitary Lung Disease: A Prospective Multicentric Study
Sreetama Bandyopadhyay, Chandan Kumar Shit, Surajit Chatterjee, Subhankar Chatterjee, Biplab Chandra, Amitabha Sengupta 75

CASE REPORTS

6. The Benign Imposter: When Cancer is not the Answer
Manu Chopra, Siddhartha Chakraborty, Prerna Guleria, Rahul Tyagi, Kislay Kishore, Aseem Yadav, Srishti Tripathi 86

7. Invasive Pulmonary Aspergillosis in an Apparently Immunocompetent Host: A Diagnostic Challenge
Athul Francis 90

INNOVATION CORNER

8. Flip Y Self-expanding Metallic Stent Deployment for Complex Right-sided Malignant Central Airway Obstruction: A Two-patient Case Series
Shivalingaswamy Salimath, Rajendra Rao KM 94

9. Targeted Thoracoscopic Autologous Blood Patch for Persistent Air Leak in Secondary Spontaneous Pneumothorax: A Case Report
Avinash Anil Nair, Rennis Davis Kizhakkepeedika, Ajaykumar Kurumpelil Karunakaran, Akhila Joboy 100

CASE LETTERS

10. A Surprise beyond Bronchiectasis: Tracheobronchopathia Osteochondroplastica
Sai Sindhu Naru, Virender Pratibh Prasad, Venkata Nagarjuna Maturu 104

11. The Rock-garden Trachea: Tracheobronchopathia Osteochondroplastica Presenting as Recurrent Respiratory Infections
Huda Shamim, Anil Kumar Singh, Shishir Kumar, Rahul Sharma 106

IMAGE OF THE ISSUE

12. When the Trachea Hardens: "Rock Garden Trachea"
Spurthi K, Virender Pratibh Prasad, Venkata Nagarjuna Maturu 111

VIDEO OF THE ISSUE

13. Emergency Airway Rescue with Self-expandable Metallic Y Stent for Malignant Distal Tracheobronchial Compression in a Young Adult with Soft Tissue Sarcoma
Yasho Vardhan Mangisetty, Koripi Kondala Rao, Khazi Mohammed Athar 113

EDITORIAL

Video-assisted Pleural Intervention in the Management of Pleural Infection

Arjun Srinivasan[1], Vallandramam Ranganathan Pattabhiraman[2], Sivaramakrishnan Mahadevan[3]

Keywords: Empyema, Multiloculated effusion, Video-assisted pleural intervention.
Annals of Interventional Pulmonology (2026): 10.5005/annalsofip-11045-0054

This is not the patient with a small, free-flowing parapneumonic effusion that has just been diagnosed. Rather, these are patients in whom pleural infection has been "cooking" for a week or more. Despite antibiotics, they continue to deteriorate, remain hospitalized, or require transfer to the intensive care unit. The pleural collection is rarely simple. Imaging typically demonstrates a large, multiloculated effusion, often producing near-complete opacification of the affected hemithorax. Inflammatory markers are markedly elevated, and many patients already have a chest tube or pigtail catheter *in situ*, yet without meaningful drainage. Simple tube thoracostomy has clearly failed, and time is no longer on the clinician's side. Once the pleural space becomes multiloculated and drainage is ineffective, the inflammatory process progresses relentlessly towards organization, making subsequent treatment increasingly difficult. There is a narrow therapeutic window during which intervention is most effective. Patients may initially be considered "too early" for definitive intervention; by the time a decision is made, they may be perceived as "too late," with a far more complex pleural space and fewer minimally invasive options remaining.

At this stage, the goal should not be merely to place another drain or temporize the situation. These patients require a definitive strategy that achieves complete pleural clearance, permits removal of any indwelling drain, controls sepsis, and enables discharge without the need for further pleural intervention. Current terminology does not adequately describe procedures that are substantially more extensive than conventional medical thoracoscopy yet deliberately stop short of pulmonary resection and other lung parenchymal procedures performed during video-assisted thoracoscopic surgery (VATS). This gap in nomenclature warrants the introduction of a new term: Video-assisted pleural intervention (VAPI).

The term is intentionally descriptive. Video-assisted pleural intervention is performed by an interventional pulmonologist entirely under direct thoracoscopic vision and is confined to the pleural cavity. Unlike conventional medical thoracoscopy, it encompasses interventions on both the parietal and visceral pleura. However, it explicitly excludes procedures involving the lung parenchyma, including wedge resection, anatomical lung resection, and the use of stapling devices. This boundary is the principal distinction between VAPI and VATS.

Video-assisted pleural intervention is intended primarily for patients with advanced pleural infection and complex pleural organization in whom simple drainage or conventional medical thoracoscopy is unlikely to provide adequate source control. The procedure is typically performed under general anesthesia with lung isolation, and multiple thoracoscopic ports are routinely used. Its objective is complete restoration of the pleural space through systematic release of all restrictive adhesions. Adhesions involving the chest wall and diaphragm are divided; the diaphragm is separated from the adjacent lung where necessary; and dense pleural adhesions are meticulously lysed. A thick visceral pleural peel that limits lung expansion is carefully removed to permit maximal re-expansion of the underlying lung. At the end of the procedure, one or two chest drains are placed under direct vision.

Conceptually, VAPI occupies the therapeutic space between medical thoracoscopy and VATS. It extends pleural intervention beyond diagnostic procedures and simple septal disruption. The proposed indications, technical scope, and distinguishing features of VAPI, medical thoracoscopy, and VATS are summarized in Table 1.

In patients with established pleural infection, initial treatment comprises appropriate antimicrobial therapy and image-guided chest-tube drainage. When drainage remains inadequate because of septations or residual loculated collections, intrapleural fibrinolytic therapy (IPFT) is an important next step. The strongest randomized evidence comes from MIST-2, which demonstrated that combined intrapleural tPA and DNase improved radiographic clearance and reduced both surgical referral and length of hospital stay.[1] Importantly, neither tPA nor DNase alone produced the same benefit, establishing that the evidence-based regimen is the fibrinolytic–DNase combination rather than fibrinolytic monotherapy.

This creates a significant therapeutic challenge in India, where dornase alfa is unavailable. Monotherapy with streptokinase, urokinase, or alteplase has been associated with favorable clinical and radiological outcomes in several small studies, including reports from the Indian subcontinent.[2–4] However, these findings must be interpreted in the context of MIST-1, the largest randomized trial of streptokinase, which found no reduction in mortality, requirement for surgery, or length of hospital stay.[5] The overall evidence for

[1–3]Centre for Advanced Pulmonary Interventions, Royal Care Hospital, Coimbatore, Tamil Nadu, India

Corresponding Author: Arjun Srinivasan, Centre for Advanced Pulmonary Interventions, Royal Care Hospital, Coimbatore, Tamil Nadu, India, Phone: +91 9791022549, e-mail: drarjun81@gmail.com

How to cite this article: Srinivasan A, Pattabhiraman VR, Mahadevan S. Video-assisted Pleural Intervention in the Management of Pleural Infection. Ann Interv Pulmonol 2026;2(2):55–57.

Source of support: Nil

Conflict of interest: None

© The Author(s). 2026 Open Access. This article is distributed under the terms of the Creative Commons Attribution-NonCommercial 4.0 International License (https://creativecommons.org/licenses/by-nc/4.0/). This license permits non-commercial use, distribution, and reproduction in any medium, provided the original author and source are credited, a link to the license is included, and any changes are indicated.

Table 1: Proposed distinctions among medical thoracoscopy, VAPI and VATS

Parameter	*Medical thoracoscopy*	*VAPI (proposed)*	*VATS*
Primary objective	Diagnosis, pleural biopsy, pleurodesis, and limited septal disruption	Complete pleural clearance and source control without parenchymal surgery	Pleural clearance with surgical management of the pleura and lung as required
Anesthesia	Usually local anesthesia with conscious sedation; general anesthesia in selected cases	General anesthesia	General anesthesia
Lung isolation	Not routine	Routine (bronchial blocker or double-lumen tube)	Routine
Ports	Usually one; a second port may be added	Usually two; an additional port may be used if required	One to three, depending on the procedure
Setting	Dedicated procedure suite or operating theater	Procedure suite or Operating theater, with anesthetic support and immediate thoracic surgical backup	Operating theater
Operator	Pulmonologist or interventional pulmonologist	Experienced interventional pulmonologist meeting the proposed competency criteria	Thoracic surgeon
Typical disease stage	Selected stage II (fibrinopurulent)	Advanced stage II or selected stage III, including organized disease identified at entry	Stage II–III, particularly organized stage III or when parenchymal intervention is required
Parietal pleura	Biopsy and limited adhesiolysis	Systematic adhesiolysis and debridement under direct vision	Systematic adhesiolysis and debridement
Visceral pleura	Generally, not addressed	Targeted removal of restrictive peels to permit lung re-expansion	Formal decortication as required
Diaphragm	Not routinely mobilized	Adhesions divided; lung and diaphragm fully released	Mobilized or released as required
Lung parenchyma	Not addressed	Explicitly excluded: No wedge or anatomical resection	Resection or repair as indicated
Stapling devices	Not used	Explicitly excluded	Used as indicated
Thoracic surgical backup	Available according to institutional practice	Immediate on-site thoracic surgical backup required	Integral to the procedure
Drainage at completion	Usually, one chest drain	One or two chest drains placed under direct vision	One or more drains, as indicated
Escalation if inadequate or unsafe	VAPI or VATS if adequate clearance is not achieved	Immediate escalation to VATS or thoracotomy if clearance is incomplete or complications occur	Thoracotomy if required
Prerequisite experience	Formal training and demonstrated competency in medical thoracoscopy	Regular diagnostic medical thoracoscopy practice; detailed knowledge of pleural anatomy and port positioning; at least 20 VAPI or VATS procedures assisted before independent practice	Accredited thoracic surgical training

VAPI, video-assisted pleural intervention; VATS, video-assisted thoracoscopic surgery

fibrinolytic monotherapy is nevertheless more nuanced. A Cochrane review found that intrapleural fibrinolytics may reduce treatment failure and the need for surgical intervention; however, no mortality benefit was demonstrated, and substantial heterogeneity existed among the included studies.[6]

Evidence comparing primary surgery with medical management is also limited. A Cochrane review of surgical vs non-surgical treatment found no convincing difference in mortality, although VATS may shorten hospital stay compared with treatment based on tube thoracostomy. The available trials were small, predominantly pediatric, and provided insufficient evidence to determine the independent benefit of fibrinolytic therapy.[7] Thus, given its low cost, ready availability, and widespread use as monotherapy in India, streptokinase may be considered a pragmatic alternative when access to tPA–DNase is limited; however, it should not be regarded as evidence-equivalent to tPA–DNase.

Medical thoracoscopy has shown variable efficacy in the management of empyema, with reported success rates of 75–95%; however, these data relate predominantly to stage II disease. For more challenging multiloculated pleural infections, the available evidence and recent pleural disease guidance favor VATS over medical thoracoscopy when stage III empyema is established.[8]

In practice, however, the stages may overlap substantially, and neither imaging nor clinical history can reliably define the stage before intervention.

Ravaglia et al.[9] reported improved overall outcomes when medical thoracoscopy was followed by IPFT to optimize pleural clearance. Nevertheless, this approach was successful in only 58.1% of patients with stage III empyema. This limitation is biologically plausible: Increased visceral pleural thickness on computed tomography has been identified as an independent predictor of IPFT failure, and the visceral pleural peel is not addressed by conventional medical thoracoscopy.[10,11] The addition of a second port and appropriate instruments may allow this peel to be addressed directly. If such an extension enables more complete pleural clearance without entering the lung parenchyma, should it necessarily remain exclusively within the domain of VATS?

Tuberculous empyema, which contributes substantially to the pleural disease burden in the Indian subcontinent, is even less well studied. Small reports have described streptokinase monotherapy in selected patients, with one series reporting an overall success rate of 62.7%.[4] In another study of 30 patients, 15 received intrapleural streptokinase and had a mean time to chest-tube removal of 32 ± 19.5 days.[12] This limited data do not permit firm conclusions regarding efficacy or patient selection.

Although medical thoracoscopy is commonly defined as a single-port procedure performed under sedation, literature dating back to 1998 acknowledges the use of a second port.[13] A survey by Madan et al. of medical thoracoscopy practices among more than 100 pulmonologists in India revealed several noteworthy findings. Rigid thoracoscopy was available to 68% of respondents, either alone or alongside flexi-rigid thoracoscopy. The procedure was performed in an operating theater by 48% and under general anesthesia by 18%. A second entry port was used most of the time by 8.2% and occasionally by a further 35%; 74% listed adhesiolysis among their indications, and 81% had access to an on-site thoracic surgeon.[14] These findings indicate that the practice and scope of medical thoracoscopy in India are heterogeneous and that several procedural elements required for VAPI are already in use. Lung isolation is also within the skillset of appropriately trained interventional pulmonologists, addressing the final procedural requirement for VAPI.

These existing practice patterns support the procedural feasibility of VAPI; the next question is who should perform it. We propose that clinicians undertaking VAPI should be experienced medical thoracoscopists who perform the procedure regularly for diagnostic indications. They should possess a detailed knowledge of pleural anatomy and port positioning and should have assisted in at least 20 VAPI or VATS procedures before performing VAPI independently.

Delayed intervention is consistently associated with poor outcomes in pleural infection. In resource-constrained settings such as India, where access to VATS is limited and streptokinase monotherapy remains widespread, early VAPI at appropriately equipped centers may offer a valuable option for carefully selected patients and reduce morbidity. The discussion should move beyond who performs VAPI or what it is called and focus on whether the right intervention is offered before the therapeutic window closes.

References

1. Rahman NM, Maskell NA, West A, et al. Intrapleural use of tissue plasminogen activator and DNase in pleural infection. N Engl J Med 2011;365(6):518–526. DOI: 10.1056/NEJMoa1012740.
2. Barthwal MS, Deoskar RB, Rajan KE, et al. Intrapleural streptokinase in complicated parapneumonic effusions and empyema. Indian J Chest Dis Allied Sci 2004;46(4):257–261. PMID: 15515826.
3. Adhikari S, Marwah V, Choudhary R, et al. Intrapleural fibrinolysis with urokinase versus alteplase in complicated pleural effusions and empyema: A prospective randomized controlled trial. Tuberc Respir Dis (Seoul) 2024;87(3):378–385. DOI: 10.4046/trd.2022.0168.
4. Barthwal MS, Marwah V, Chopra M, et al. A five-year study of intrapleural fibrinolytic therapy in loculated pleural collections. Indian J Chest Dis Allied Sci 2016;58(1):17–20. DOI: 10.5005/ijcdas-58-1-17.
5. Maskell NA, Davies CW, Nunn AJ, et al. U.K. Controlled trial of intrapleural streptokinase for pleural infection. N Engl J Med 2005;352(9):865–874. DOI: 10.1056/NEJMoa042473.
6. Altmann ES, Crossingham I, Wilson S, et al. Intra-pleural fibrinolytic therapy versus placebo, or a different fibrinolytic agent, in the treatment of adult parapneumonic effusions and empyema. Cochrane Database Syst Rev 2019;2019(10). DOI: 10.1002/14651858.CD002312.pub4.
7. Rodrigues A, Salomao IFA, Scabello IF, et al. Intrapleural fibrinolytics versus thoracic surgery for complicated pleural infections: A systematic review and meta-analysis. Heart Lung Circ 2025;34(6):627–638. DOI: 10.1016/j.hlc.2024.11.030.
8. Chaddha U, Agrawal A, Ghori U, et al. WABIP/AABIP statement on therapeutic indications of medical thoracoscopy for benign pleural disease. Eur Respir Rev 2026;35(180). DOI: 10.1183/16000617.0327-2025.
9. Ravaglia C, Ghirotti C, Puglisi S, et al. Medical thoracoscopy and intrapleural fibrinolytic therapy for the management of pleural empyema: A cohort study. Respiration 2023;102(1):46–54. DOI: 10.1159/000527409.
10. Khemasuwan D, Sorensen J, Griffin DC. Predictive variables for failure in administration of intrapleural tissue plasminogen activator/deoxyribonuclease in patients with complicated parapneumonic effusions/empyema. Chest 2018;154(3):550–556. DOI: 10.1016/j.chest.2018.01.037.
11. Abu-Daff S, Maziak DE, Alshehab D, et al. Intrapleural fibrinolytic therapy (IPFT) in loculated pleural effusions: Analysis of predictors for failure of therapy and bleeding: A cohort study. BMJ Open 2013;3(2). DOI: 10.1136/bmjopen-2012-001887.
12. Goel R, Singh GV, Shadrach BJ, et al. Efficacy and safety of intrapleural streptokinase in tubercular empyema thoracis: Old wine in new wineskin. Trop Doct 2022;52(1):23–26. DOI: 10.1177/00494755211050193.
13. Loddenkemper R, Schonfeld N. Medical thoracoscopy. Curr Opin Pulm Med 1998;4(4):235–238.
14. Madan K, Tiwari P, Thankgakunam B, et al. A survey of medical thoracoscopy practices in India. Lung India 2021;38(1):23–30. DOI: 10.4103/lungindia.lungindia_295_20.

EDITORIAL

Tracheobronchopathia Osteochondroplastica: When Does the Rock-garden Airway Matter?

Virender Pratibh Prasad[1], Venkata Nagarjuna Maturu[2]

Key words: Cobble stone appearance, Lung cancer, Recurrent infections, Rock-garden airway, Tracheobronchopathia Osteochondroplastica.
Annals of Interventional Pulmonology (2026): 10.5005/annalsofip-11045-0060

Tracheobronchopathia osteochondroplastica (TO) is an uncommon benign disorder of the large airways characterized by multiple submucosal cartilaginous and osseous nodules projecting into the tracheobronchial lumen. These lesions predominantly involve the anterior and lateral walls of the trachea and proximal bronchi, with characteristic relative sparing of the posterior membranous wall.[1] Although TO has been recognized for more than a century, its true prevalence remains uncertain. Reported prevalence varies considerably between studies, partly because many patients are asymptomatic, symptoms are nonspecific, and the diagnosis is often made incidentally during computed tomography (CT) or bronchoscopy.[2]

The three cases of TO in the present issue of the Annals of Interventional Pulmonology are therefore important not simply because they describe a rare disease, but because they demonstrate different clinical contexts in which TO may be encountered. Together, these cases raise a clinically relevant question: When TO is identified, is it merely an incidental bronchoscopic finding, or is it contributing to the patient's respiratory disease?[3–5]

Computed tomography may demonstrate irregular or nodular thickening of the anterolateral tracheal wall, often accompanied by calcification and variable luminal narrowing. However, calcification is not universally present, and a normal or apparently nonspecific CT does not exclude TO.[2,6] In the French multicenter series of 36 patients, radiological abnormality was observed in 97% of patients.[6] In the Korean series of 40 patients, 32.4% of patients had a normal CT chest.[2] More recent studies have similarly emphasized that TO may be under-recognized radiologically and only become apparent during bronchoscopy.[7]

Bronchoscopy therefore remains central to the diagnosis of this disease. Tracheobronchopathia osteochondroplastica has one of the most recognizable bronchoscopic appearances among benign airway disorders. Multiple firm, whitish or yellowish sessile nodules protrude into the lumen, giving rise to descriptions such as a "cobblestone," "stalactite," or "rock-garden" airway. The nodules arise predominantly from the cartilaginous portion of the tracheobronchial wall.[1] The differential diagnosis includes tracheobronchial amyloidosis, relapsing polychondritis, endobronchial tuberculosis, papillomatosis, sarcoidosis, and malignant infiltration. Posterior membranous wall sparing is an important clue but should not be regarded as an isolated diagnostic criterion.

The morphology, distribution of lesions, CT findings, clinical context, and, where necessary, histopathology should be considered together.[1,6] This is particularly relevant in tuberculosis-endemic countries, where chronic cough, airway nodularity, and recurrent respiratory symptoms may otherwise lead to an incorrect diagnosis of endobronchial tuberculosis.

The role of biopsy deserves some nuance. Histology typically demonstrates mature cartilage, bone, calcification, and occasionally marrow elements within the submucosa.[1] However, TO nodules may be extremely hard, making biopsy technically difficult and sometimes yielding inadequate tissue. When CT and bronchoscopy show a classical pattern of hard anterolateral nodules with posterior wall sparing, a biopsy need not be performed. Histological confirmation becomes more important when the appearance is atypical or when an infiltrative or malignant disorder is being considered. This approach is supported by contemporary series in which biopsy provided additional diagnostic information in a subset of patients.[6,7] Thus, biopsy need not be routinely performed in every patient, and the decision should be individualized.

An equally important lesson from the cases in this issue is the need to avoid diagnostic anchoring. Tracheobronchopathia osteochondroplastica is visually striking, and once encountered during bronchoscopy, it can easily become the focus of attention. However, its presence does not mean that all symptoms are attributable to TO. Coexistence with lung malignancy has been reported, although there is currently no convincing evidence that TO predisposes to lung cancer or undergoes malignant transformation.[8] When TO is identified during evaluation of a pulmonary mass, lymphadenopathy, or other significant abnormality, investigation of the primary clinical problem should therefore continue independently. In many patients, TO may simply be a "fellow traveler" rather than the disease determining prognosis.

The relationship between TO and recurrent respiratory infection is more intriguing. Chronic cough, expectoration, and recurrent respiratory infections have repeatedly been reported in observational studies and case series.[1,6] A biologically plausible

[1,2]Department of Pulmonary Medicine, Yashoda Hospital, Hyderabad, Telangana, India

Corresponding Author: Venkata Nagarjuna Maturu, Department of Pulmonary Medicine, Yashoda Hospitals, Hitec City, Hyderabad, Telangana, India, Phone: +91 9000060507, e-mail: arjunjipmer@yahoo.co.in

How to cite this article: Prasad VP, Maturu VN. Tracheobronchopathia Osteochondroplastica: When Does the Rock-garden Airway Matter? Ann Interv Pulmonol 2026;2(2):58–59.

Source of support: Nil

Conflict of interest: None

© The Author(s). 2026 Open Access. This article is distributed under the terms of the Creative Commons Attribution-NonCommercial 4.0 International License (https://creativecommons.org/licenses/by-nc/4.0/). This license permits non-commercial use, distribution, and reproduction in any medium, provided the original author and source are credited, a link to the license is included, and any changes are indicated.

explanation exists. Osteocartilaginous projections disrupt the normally smooth airway surface and, when sufficiently extensive, may interfere with mucociliary transport and secretion drainage. Histological studies have also demonstrated epithelial alteration, squamous metaplasia, and chronic inflammatory changes overlying the nodules.[1] These abnormalities could theoretically promote secretion retention and recurrent infection.

The reverse relationship is equally possible. Chronic airway inflammation and recurrent infection have long been proposed as potential contributors to the development of TO. Thus, chronic inflammation may promote structural change, while established structural abnormalities may in turn impair airway clearance. A bidirectional relationship is attractive conceptually, but longitudinal evidence is needed before it can be accepted.

Most patients with TO have a benign and slowly progressive clinical course. In the Korean cohort, most patients required no disease-specific treatment, and only two underwent laser therapy for significant tracheal stenosis.[2] Similarly, in the French multicenter series, bronchoscopic reassessment demonstrated stability in the small number of patients who underwent repeat procedures, and only three required specific treatments.[6] These observations support conservative management for asymptomatic or mildly symptomatic disease.

Extensive disease may produce fixed airway narrowing with central airway obstruction, dyspnea, wheeze, and retention of secretions. Tracheobronchopathia osteochondroplastica may also have procedural implications. Difficult endotracheal intubation has been described, and severe nodularity or stenosis may limit passage of a bronchoscope.

Management should be guided by the clinical features rather than the bronchoscopic appearance alone. It is often the associated cardiorespiratory diseases which cause symptoms, and these should be identified and promptly treated. Patients with incidental, nonobstructive TO usually require observation. Those with recurrent infection should undergo appropriate microbiological evaluation, culture-directed antimicrobial therapy when indicated, and measures to improve secretion clearance. Bronchoscopic interventions should be reserved for clinically significant stenosis or obstruction.[2,6]

The three cases in this issue therefore offer three practical lessons. First, TO should be recognized promptly from its characteristic radiological and bronchoscopic appearance, and when in doubt, a biopsy may be performed for confirmation. Second, identification of TO should not end the diagnostic process, because important conditions such as malignancy, bronchiectasis, and infection may coexist. Third, its clinical relevance should be judged individually. Tracheobronchopathia osteochondroplastica may be incidental in one patient, contribute to recurrent infection or airway symptoms in another, and cause significant obstruction in a small minority.[3–5]

Despite increasing recognition, several questions remain unanswered. The true prevalence of TO, predictors of progression, relationship between bronchoscopic disease burden and physiological impairment, and possible association with chronic infection and bronchiectasis remain unclear. Prospective longitudinal studies would help answer these questions. Until then, TO should be approached not simply as a memorable "rock-garden" airway, but as a structural airway disorder whose importance depends on its clinical context. For the interventional pulmonologist, the central question is not merely whether TO is present, but whether it is the disease, a contributor to disease, or simply a fellow traveler.

Orcid

Virender Pratibh Prasad https://orcid.org/0000-0001-8017-3697
Venkata Nagarjuna Maturu https://orcid.org/0000-0002-3679-9497

References

1. Ulasli SS, Kupeli E. Tracheobronchopathia osteochondroplastica: A review of the literature. Clin Respir J 2015;9(4):386–391. DOI: 10.1111/crj.12166.
2. Cho HK, Jeong BH, Kim H. Clinical course of tracheobronchopathia osteochondroplastica. J Thorac Dis 2020;12(10):5571–5579. DOI: 10.21037/jtd-20-1898.
3. Shamim H, Singh AK, Kumar S, et al. The rock-garden trachea: Tracheobronchopathia osteochondroplastica presenting as recurrent respiratory infections. Ann Interv Pulmonol 2026; 2(2):106–110. DOI: 10.5005/annalsofip-11045-0055.
4. Spurthi K, Prasad VP, Maturu VN. When the trachea hardens: "Rock Garden Trachea". Ann Interv Pulmonol 2026;2(2):111–112. DOI: 10.5005/annalsofip-11045-0049.
5. Naru SS, Prasad VP, Maturu VN. A Surprise beyond bronchiectasis: Tracheobronchopathia Osteochondroplastica. Ann Interv Pulmonol 2026;2(2):104–105. DOI: 10.5005/annalsofip-11045-0057.
6. Dumazet A, Launois C, Lebargy F, et al. Tracheobronchopathia osteochondroplastica: Clinical, bronchoscopic, and comorbid features in a case series. BMC Pulm Med 2022;22(1):423. DOI: 10.1186/s12890-022-02225-2.
7. Nair AA, Gupta R, Irodi A, et al. Tracheobronchopathia osteochondroplastica: To biopsy or not to biopsy? A relook at the rare disease. J Bronchology Interv Pulmonol 2024;31(1):57–62. DOI: 10.1097/LBR.0000000000000931.
8. Feng Y, Wang L, Jia R, et al. Tracheobronchopathia osteochondroplastica concurrent with peripheral lung cancer: A case report and perioperative considerations. Transl Cancer Res 2024;13(4):2064–2072. DOI: 10.21037/tcr-24-410.

ORIGINAL ARTICLE

From Imaging to Insight: Evaluation of Mediastinal Lymph Nodes Using Endobronchial Ultrasound Elastography: A Prospective Study

Saurabh Jain[1], Vishal Kumar Chitikeshi[2], Mahesh Gudelli[3], Lakshminarayana Jasti[4], Kranthi Kumar Shavagani[5]

Received on: 28 July 2026; *Accepted on*: 09 September 2026; *Published on*: 26 September 2026

Abstract

Background: Endobronchial ultrasound (EBUS) elastography is an emerging imaging modality that enables real-time assessment of tissue stiffness and provides additional information for the characterization of mediastinal lymph nodes. Its ability to discriminate malignant from benign lymph nodes is of particular clinical relevance in tuberculosis (TB)-endemic settings, where granulomatous lymphadenopathies may closely mimic malignant disease. Histopathological features such as fibrosis, necrosis, and chronic inflammation can alter tissue stiffness and contribute to overlapping elastographic patterns, thereby limiting diagnostic specificity.

Materials and methods: This prospective observational study included 51 patients undergoing EBUS evaluation, encompassing 93 mediastinal lymph nodes. The study was designed as a prospective observational study and reported in accordance with the STROBE recommendations. Elastographic assessment was performed before tissue acquisition, and lymph nodes were qualitatively classified according to the Izumo classification as type I (predominantly green/soft), type II (mixed), or type III (predominantly blue/hard). All lymph nodes underwent EBUS-guided transbronchial needle aspiration (TBNA), while cryonodal biopsy was performed in selected cases when additional tissue architecture was required. Final diagnoses were established on the basis of cytopathological, histopathological, microbiological, and immunohistochemical findings.

Results: Among the 93 lymph nodes evaluated, 62 (66.7%) were benign, and 31 (33.3%) were malignant. Type I, type II and type III elastographic patterns were observed in 24, 39, and 30 lymph nodes, respectively. Benign pathology predominated among type I and type II nodes, accounting for 83.3 and 82.1%, respectively, whereas 66.7% of type III nodes demonstrated malignant pathology. The association between elastographic pattern and final pathological diagnosis was statistically significant ($p < 0.001$). Among malignant type III nodes, adenocarcinoma was the predominant histopathological diagnosis (40%), followed by poorly differentiated carcinoma (20%), squamous carcinoma (15%), and small-cell carcinoma (15%). Meanwhile, among benign pathology, tuberculous lymph nodes exhibited considerable elastographic heterogeneity, with substantial overlap between type II and type III patterns. When type III elastography was considered predictive of malignancy, the sensitivity was 64.5%, and specificity was 83.9%.

Conclusion: Qualitative EBUS elastography demonstrated a significant association with final pathological diagnosis for malignant lymphadenopathy. Type III elastography was associated with an increased likelihood of malignancy, whereas type I and type II patterns were predominantly observed in benign lymph nodes. Nevertheless, substantial overlap between malignant and benign lymphadenopathies limits the specificity of elastography. Accordingly, EBUS elastography should be regarded as an adjunctive diagnostic modality, with its findings integrated with clinical, radiological, microbiological, cytological, and histopathological information to optimize nodal selection and diagnostic yield.

Keywords: Cryonodal biopsy, Endobronchial ultrasound, Endobronchial ultrasound elastography, Endobronchial ultrasound-guided transbronchial needle aspiration, Granulomatous lymphadenopathy, Malignancy, Mediastinal lymphadenopathy, Tuberculosis.

Annals of Interventional Pulmonology (2026): 10.5005/annalsofip-11045-0058

Introduction

Mediastinal lymphadenopathy poses a significant diagnostic problem in thoracic practice because of the diverse nature of its causes, which span the spectrum of malignancy, infection, granuloma, lymphoproliferation, and reactive inflammation.[1,2] The accurate characterization of mediastinal nodes is not only important for correct oncologic staging but also for making a diagnosis of alternative conditions.[3] Endobronchial ultrasound-guided transbronchial needle aspiration (EBUS-TBNA) has been considered the mainstay of minimally invasive assessment of mediastinal lymphadenopathy. Evidence has consistently reported that EBUS-TBNA is an excellent tool in terms of diagnostic sensitivity,

[1–5]Department of Interventional Pulmonology, KIMS Hospitals, Secunderabad, Telangana, India

Corresponding Author: Mahesh Gudelli, Department of Interventional Pulmonology, KIMS Hospitals, Secunderabad, Telangana, India, Phone: +91 8897976190, e-mail: maheshg28@gmail.com

How to cite this article: Jain S, Chitikeshi VK, Gudelli M, *et al*. From Imaging to Insight: Evaluation of Mediastinal Lymph Nodes Using Endobronchial Ultrasound Elastography: A Prospective Study. Ann Interv Pulmonol 2026;2(2):60–66.

Source of support: Nil

Conflict of interest: None

© The Author(s). 2026 Open Access. This article is distributed under the terms of the Creative Commons Attribution-NonCommercial 4.0 International License (https://creativecommons.org/licenses/by-nc/4.0/). This license permits non-commercial use, distribution, and reproduction in any medium, provided the original author and source are credited, a link to the license is included, and any changes are indicated.

specificity, and procedural safety for diagnosing mediastinal lymphadenopathy for both benign and malignant processes.[4,5] In tuberculosis (TB) endemic regions in particular, EBUS-TBNA is widely recognized as an essential diagnostic modality in the assessment of granulomatous mediastinal disease (TB, sarcoidosis).[6]

When evaluating mediastinal nodes, the typical B-mode endobronchial ultrasound (EBUS) characteristics that may be helpful in discriminating between malignant and benign causes of mediastinal lymphadenopathy are nodal size, margins, echogenicity, presence/absence of hilar central structure, coagulation necrosis sign, and vascular pattern.[7] B-mode EBUS findings are often highly similar in malignant vs benign disease and can lack specificity for differentiation, especially in populations with a high incidence of granulomatous inflammation.[8] Therefore, an additional imaging technique capable of real-time characterization of tissue may prove clinically useful. Endobronchial ultrasound elastography is an ultrasonographic modality that assesses the tissue stiffness of mediastinal lymph nodes by evaluating their elastographic patterns.[9] Three-color qualitative EBUS elastography allows categorization of lymph nodes into predominantly type I (soft, green), type II (mixed, yellow/green/blue), and type III (hard, blue) by classifying their respective tissue stiffness and profiles.[10]

Studies looking at elastographic patterns across a wider spectrum of etiologies of mediastinal lymphadenopathy such as TB, sarcoidosis, lymphoma, and reactive lymphadenopathy are few.[11] This is of particular concern in the endemic populations for TB, wherein granulomatous inflammation may be stiffer secondary to fibrosis, caseation, and chronic inflammation remodeling, thus creating increased overlap with malignant lesions in terms of elasticity and limiting the specificity of EBUS elastography.[12]

Another limiting feature of traditional EBUS-TBNA is that it often fails to provide preserved histologic architecture, which is crucial in the diagnosis of lymphoma and granulomatous conditions.[13] An emerging tissue acquisition modality is EBUS-guided transbronchial mediastinal cryobiopsy (cryonodal biopsy), which provides larger, architecturally preserved specimens that are amenable to histopathology, immunohistochemistry, and microbiology evaluation.[14] Studies have reported enhanced diagnostic adequacy and histopathologic yield for cryobiopsy in various benign inflammatory disorders.[14,15]

Accordingly, the present prospective study was undertaken to evaluate the diagnostic utility of qualitative three-color EBUS elastography in mediastinal lymphadenopathy across diverse etiologies including malignancy, TB, sarcoidosis, lymphoma, and reactive conditions.

Materials and Methods

Study Design and Setting

This study was conducted at the Department of Interventional Pulmonology, KIMS Hospitals, between April 2025 and March 2026.

Institutional ethical approval was obtained prior to data collection.

Study Population

Fifty-one patients undergoing EBUS for evaluation of mediastinal lymphadenopathy were included.

Study Outcome

Association between qualitative elastographic patterns and final pathological diagnosis.

Inclusion Criteria

- Age ≥18 years.
- Mediastinal lymph node enlargement (short-axis diameter ≥10 mm) on contrast-enhanced computed tomography (CECT) or positron emission tomography-computed tomography (PET-CT).
- Patients undergoing EBUS for diagnostic evaluation.
- Informed consent.

Exclusion Criteria

- Contraindications to bronchoscopy, including severe hypoxemia, hemodynamic instability, or uncontrolled coagulopathy.
- Inadequate elastography image acquisition.
- Inadequate tissue sample for definitive diagnosis.

Endobronchial Ultrasound Procedure

All procedures were performed under general anesthesia by an experienced interventional pulmonologist team using an Olympus convex probe EBUS bronchoscope ME3 processor, Olympus BF-UC-190F with integrated i-elastography. Malignant lymph node stations were identified and classified according to the International Association for the Study of Lung Cancer (IASLC) nodal map.

The following conventional B-mode sonographic characteristics were documented:

- Short-axis diameter.
- Shape (round or oval).
- Margins (distinct or indistinct).
- Echogenicity (homogeneous or heterogeneous).

Elastography Assessment

Elastography was performed before needle puncture using integrated ultrasound elastography software. After stabilization of the ultrasound image, qualitative elastographic patterns were assessed according to predominant color distribution using Izumo classification (Fig. 1).[16]

- Type I: Predominantly soft (non-blue/green dominant).
- Type II: Mixed pattern.
- Type III: Predominantly hard (blue dominant).

Interpretation was performed in real time by the operating pulmonologist, and representative images were digitally archived.

Tissue Sampling Protocol

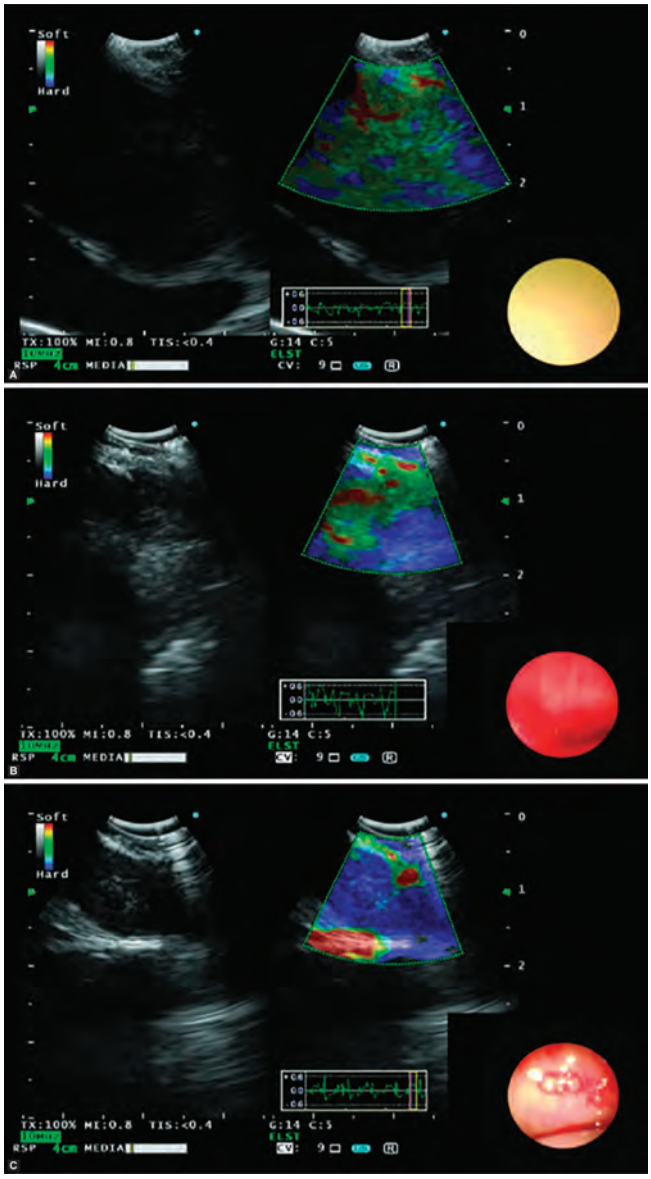
Endobronchial Ultrasound-guided Transbronchial Needle Aspiration

Following elastographic assessment, EBUS-TBNA was performed using a 21-gauge needle. A minimum of two passes per lymph node was performed, with additional passes obtained based on sample adequacy. Rapid on-site evaluation (ROSE) was utilized.

Cryonodal Biopsy

In selected cases where larger tissue samples were clinically indicated, wherein lymphoma or granulomatous diseases were suspected, or prior TBNA samples were inconclusive, EBUS-guided cryo-nodal biopsy was performed.

A flexible cryoprobe was introduced through the working channel following needle tract creation under EBUS guidance. The cryoprobe was activated for 3–5 seconds, and tissue samples were retrieved *en bloc*. Each node was assessed independently by a pathologist.



Figs 1A to C: (A) EBUS elastography image demonstrating a type I pattern, characterized predominantly by non-blue/green coloration suggestive of softer tissue consistency; (B) Type II elastography pattern showing a mixed blue and non-blue appearance, indicating intermediate tissue stiffness; (C) Type III elastography pattern demonstrating predominantly blue coloration, consistent with increased tissue stiffness and commonly associated with malignant lymph nodes

Final diagnosis was established using:

- Cytopathological and/or histopathological examination.
- Microbiological confirmation.
- Immunohistochemical analysis for lymphoma when required.

Diagnostic Classification

Lymph nodes were categorized into the following diagnostic groups:

- Malignancy.
- Benign.

Table 1: Baseline characteristics of study population and final diagnoses ($n = 51$)

Parameter	Value
Age (years), mean ± SD	57.6 ± 16.7 years
Gender	
Male, *n* (%)	31 (60.8 %)
Female, *n* (%)	20 (39.2 %)
Underlying disease	
No known disease	27 (52.9%)
Known malignancy	18 (35.3%)
Post CT/RT	5 (9.8%)
Lymphoma	1 (2.0%)
Final histo/cytologic diagnosis ($n = 93$)	
Benign etiology	62 (66.7%)
Granulomatous nodes	45 (48.4%)
Reactive lymphoid tissue	14 (15.1%)
Miscellaneous	3 (3.2%)
Malignant etiology	31 (33.3%)

Results

Patient Demographics and Baseline Characteristics

A total of 51 patients underwent EBUS evaluation during the study period. The mean age of the cohort was 57.6 ± 16.7 years. Males constituted the majority of patients ($n = 31$, 60.8%), while females accounted for 39.2% ($n = 20$). Regarding underlying disease, 58.8% of patients had no known prior disease. A significant proportion (35.3%, $n = 18$) had a known history of malignancy, 9.8% ($n = 5$) had undergone prior chemotherapy or radiotherapy for various malignancies, and 2.0% ($n = 1$) had a known diagnosis of lymphoma (Table 1).

Lymph Node Characteristics and Distribution

A total of 93 mediastinal lymph nodes were evaluated across the 51 patients. The mean short-axis diameter was 15.8 ± 6.4 mm. The majority of sampled nodes were located at mediastinal stations (67.7%, $n = 63$). Station 7 (subcarinal) was the most frequently sampled location, representing 33.3% ($n = 31$) of all lymph nodes, followed by station 4R (31.2%, $n = 29$) and station 11L (16.1%, $n = 15$). Less frequently sampled stations included 11RS (7.5%, $n = 7$), 10R (5.4%, $n = 5$), 4L (4.3%, $n = 4$), 10L (1.1%, $n = 1$) and 12R (1.1%, $n = 1$). Cryo-nodal biopsy was performed in 19 nodes (Table 2).

A definite histo/cytologic diagnosis was achieved in 79 nodes, and reactive lymphoid tissue was seen in the remaining 14 nodes. Of the 79 nodes with a definite histo/cytologic diagnosis, 48 nodes had a benign diagnoses, and 31 nodes had malignant diagnoses. Amongst benign nodes, 45 were granulomatous, and 3 had other etiologies. Amongst malignant nodes, 9 were poorly differentiated carcinomas, 12 were adenocarcinomas, 4 were squamous cell carcinomas, 4 were small cell carcinomas, and 2 were malignant carcinoid tumors. The 14 patients with reactive nodes were followed

Table 2: Characteristics of lymph nodes and elastography features

Lymph node characteristics	Values ($n = 93$)
Short-axis diameter (mm), mean ± SD	15.8 ± 6.4
Location (station-wise), *n* (%)	
7	31 (33.3)
10L	1 (1.1)
10R	5 (5.4)
11L	15 (16.1)
11RS	7 (7.5)
12R	1 (1.1)
4L	4 (4.3)
4R	29 (31.2)
Position, *n* (%)	
Mediastinal station (4R, 4L, 7)	64 (68.8)
Hilar stations (10R/L, 11R/L, 12R)	29 (31.2)
Elastography score, *n* (%)	
Type I	24 (25.8)
Type II	39 (41.9)
Type III	30 (32.3)

up for 3 months, and repeat imaging showed stability/resolution of nodes, thereby confirming them to be true reactive nodes. These true reactive nodes have also been included in the benign etiology group (Table 1).

Distribution of Elastographic Patterns

Qualitative elastographic assessment of all 93 lymph nodes demonstrated type I pattern in 24 (25.8%) nodes, type II pattern in 39 (41.9%) nodes and type III pattern in 30 (32.3%) nodes. Thus, type II was the most frequently observed elastographic pattern overall, followed by type III and type I. Analysis according to lymph node station demonstrated considerable variation in elastographic patterns. Station 7 was the most frequently sampled station ($n = 31$), with type II being the predominant pattern (14/31), followed by type I (12/31) and type III (5/31). Station 4R accounted for 29 nodes, type III pattern in 12 nodes, type II in 11 nodes and fewer type I nodes (6 nodes). Among the 15 nodes sampled from station 11L, type II was predominant (8 nodes), followed by type I (4 nodes) and type III (3 nodes). Station 11Rs included 7 nodes, with type III being the most frequent pattern (4 nodes), followed by type II (3 nodes), while no type I nodes were observed. The remaining nodes were distributed across stations 10R ($n = 5$), 4L ($n = 4$), 10L ($n = 1$), and 12R ($n = 1$), demonstrating additional heterogeneity in elastographic appearance across nodal stations (Fig. 2).

Correlation of Elastographic Patterns with Final Pathological Diagnosis

Elastographic Patterns in Malignant Lymph Nodes

Among the 31 malignant lymph nodes identified, type III elastographic pattern was the most frequently observed pattern, accounting for 20 (64.5%) nodes. Type II and type I patterns were observed in 7 (22.6%) and 4 (12.9%) malignant lymph nodes, respectively. Within the type III malignant group, adenocarcinoma constituted the predominant histopathological

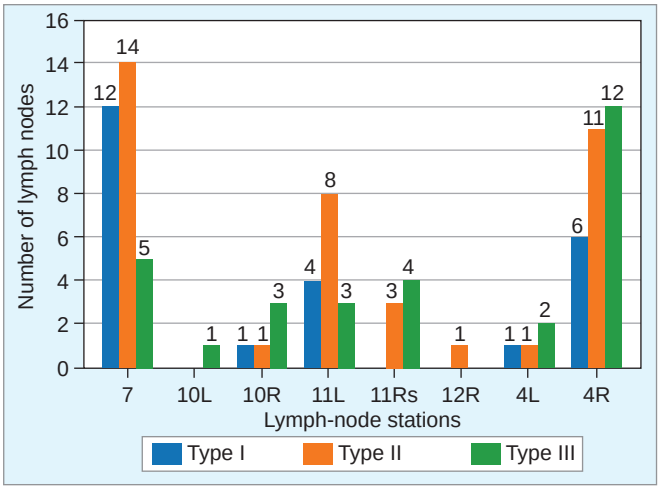


Fig. 2: Distribution of type I, type II, and type III EBUS elastographic patterns across the sampled lymph-node stations. Station 7 was the most frequently sampled lymph-node station ($n = 31$; 33.3%), followed by station 4R ($n = 29$; 31.2%) and station 11L ($n = 15$; 16.1%). Overall, type II elastography was the most frequently observed pattern ($n = 39$; 41.9%), followed by type III ($n = 30$; 32.3%) and type I ($n = 24$; 25.8%)

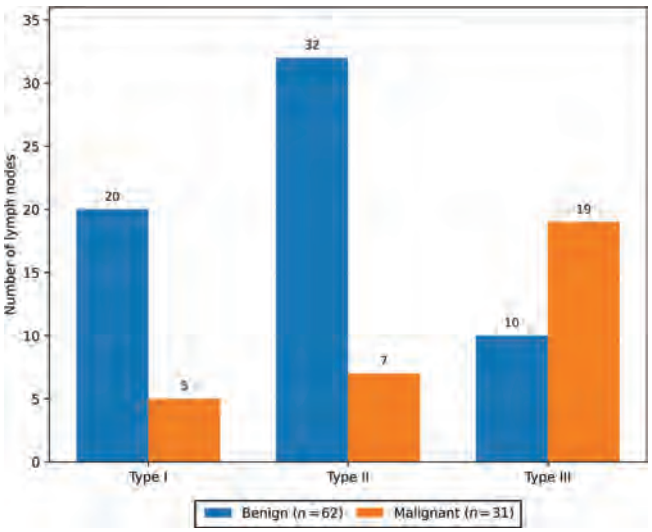


Fig. 3: Distribution of elastic patterns (types I, II, and III) in benign and malignant lymph nodes

diagnosis, accounting for 8 of 20 * 40%), followed by poorly differentiated carcinoma in 4 (20.0%), squamous carcinoma in 3 (15%), small-cell carcinoma in 3 (15%), and carcinoid tumor in 2 (10%). Overall, type III elastography demonstrated the strongest association with malignant pathology (Fig. 3).

Elastographic Patterns in Benign Conditions

Among the 62 benign lymph nodes, type II elastographic pattern was the most frequently observed, accounting for 32 (51.6%) nodes, followed by type I in 20 (32.3%) and type III in 10 (16.1%) nodes (Table 3). On pathological classification, granulomatous lymphadenopathy, comprising all lymph nodes diagnosed as TB or sarcoidosis, represented the predominant benign category, accounting for 42 (67.7%) nodes, followed by reactive lymphoid

Table 3: Correlation of elastography type with final diagnosis of lymph nodes

Elastography type	Benign, *n* (%)	Malignancy, *n* (%)	*p*-value
Type I (*n* = 24)	20 (83.3%)	4 (16.7%)	<0.001
Type II (*n* = 39)	32 (82.1%)	7 (17.9%)	
Type III (*n* = 30)	10 (33.3%)	20 (66.7%)	
Total (*n* = 93)	62 (66.7%)	31 (33.3%)	

The table demonstrates a significant association between EBUS elastography type and the final diagnosis of lymph nodes. Type I and type II elastography patterns were predominantly observed in benign lymph nodes (83.3 and 82.1%, respectively), whereas type III elastography was more frequently associated with malignant lymph nodes (66.7%)

Table 4: Diagnostic performance of EBUS elastography according to selected threshold (type III pattern)

ROC parameter	Result
AUC	0.745
95% CI	0.635–0.845
Best practical cut-off	≥Type III
Sensitivity	64.5%
Specificity	83.9%
Positive predictive value	66.7%
Negative predictive value	82.5%
Accuracy	77.4%

AUC, area under the curve; CI, confidence interval; EBUS, endobronchial ultrasound; ROC, receiver operating characteristic

Diagnostic performance of EBUS elastography according to the selected threshold. A type III pattern demonstrated a sensitivity of 64.5% and specificity of 83.9% for predicting malignant lymph-node pathology. A lower threshold of ≥type II increased sensitivity to 87.1% but reduced specificity to 32.3%

tissue in 14 (22.6%), anthracosis in 3 (4.8%) and non-tuberculous mycobacterial (NTM) infection in 3 (4.8%) nodes. Benign lymph nodes demonstrated considerable heterogeneity in elastographic appearance, with type I and type II patterns predominating overall. However, type III patterns were also observed in a subset of benign nodes, particularly those with granulomatous lymphadenopathy.

Diagnostic Performance of Elastography for Malignant Lymph Nodes

The diagnostic performance of qualitative EBUS elastography was assessed using type III elastography as the threshold for malignancy. Type III elastography yielded a sensitivity of 64.5%, specificity of 83.9%, positive predictive value of 66.7%, negative predictive value of 82.5%, and overall diagnostic accuracy of 77.4% for malignant nodal involvement. The association between elastographic pattern and final pathological diagnosis was statistically significant ($p < 0.001$). When elastography was analyzed as an ordinal variable, with type I, type II, and type III assigned increasing scores of tissue stiffness, the receiver operating characteristic analysis demonstrated an area under the curve of 0.745 (95% CI, 0.635–0.845), indicating moderate discriminatory ability (Table 4). These findings indicate that EBUS elastography provides useful adjunctive information for malignant nodal characterization and target selection. Figure 4 depicts the receiver operating characteristic (ROC) curve for EBUS elastography patterns in differentiating malignant from benign nodes.

Discussion

In our current study, we investigated qualitative three-color EBUS elastography in a mixed heterogeneous cohort of mediastinal lymphadenopathies of varied etiologies. Elastography patterns illustrated clinically significant discriminatory power for malignancy while showing significant overlap with granulomatous diseases.

Elastographic Characteristics in Malignant Lymphadenopathy

We illustrate that predominantly hard or blue-dominated elastographic patterns are seen with greater frequency in malignant lymph nodes. A number of recent, meta-analyses have suggested sensitivities ranging between 80 and 90% and specificities between 75 and 85% for differentiating malignant from benign mediastinal lymphadenopathy by EBUS elastography.[17–19] The pathological mechanisms underlying this phenomenon are believed to be primarily due to cellular density, tumor desmoplastic reaction and infiltration and altered matrix composition of malignant lymph nodes.[20] Recent multicenter data have further established that elastography-guided nodal selection can increase efficiency in mediastinal staging.[21] Our study aimed to incorporate varied disease spectra, namely TB, sarcoidosis, and lymphoma, which best correlate with real-life scenarios, especially in TB endemic regions.

Granulomatous Disease and Diagnostic Overlap

One of the most significant findings of the study was the substantial overlap of elastographic patterns between granulomatous(benign) and malignant lymphadenopathy. This is especially relevant for TB-endemic regions where TB constitutes a very common cause of enlarged mediastinal lymph nodes. Madan et al. have also demonstrated increased stiffness in granulomatous lymphadenopathies due to fibrosis, caseation, calcification, and chronic inflammatory remodeling, leading to mimicry of malignant elastographic patterns.[12] These similarities significantly limit elastography's ability to definitively differentiate malignant from granulomatous mediastinal disorders. Therefore, in such scenarios, EBUS elastographic findings must always be used in conjunction with conventional B-mode sonographic appearances, clinical presentation, radiology, and microbiological and histopathological diagnosis.[8]

Clinical Implications

The simple qualitative three-color Izumo EBUS elastography offers a straightforward and quick assessment tool during an EBUS procedure. Predominantly hard nodes might warrant higher sampling priority. However, due to the substantial overlap, elastography should not be relied upon as a definitive diagnostic modality. Instead, it is a useful real-time procedural tool that can aid selection of the nodal station during EBUS-TBNA. Similarly, inclusion of cryo-nodal biopsy in selected cases allows procedural flexibility to transition from cytological sampling to histology as per indication.

Strengths of the Study

Several strengths characterized the current study: A heterogeneous mixed disease cohort, inclusion of cryo-nodal biopsy to increase tissue adequacy, and the use of microbiologic, cytopathologic, and histopathologic references.

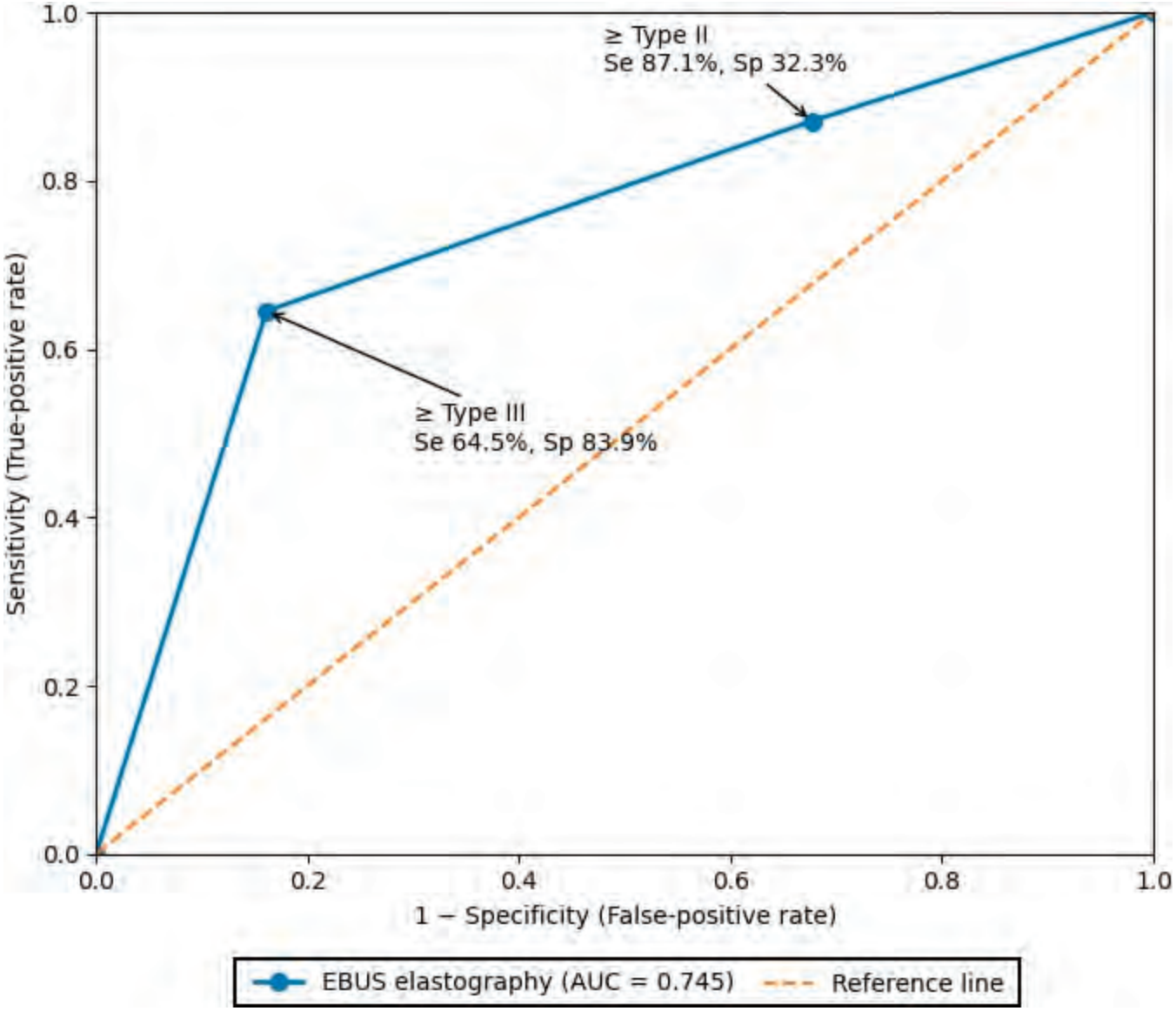


Fig. 4: Receiver operating characteristic curve for EBUS elastography patterns in differentiating malignant from benign lymph nodes. Elastography pattern was analyzed as an ordinal variable (type I < type II < type III). The area under the ROC curve was 0.745, indicating moderate discriminatory ability. A threshold of ≥type III yielded a sensitivity of 64.5% and specificity of 83.9%

Limitations

The study was monocentric with a relatively limited patient cohort. Endobronchial ultrasound-guided cryo-nodal biopsy was performed based on individual case indication, which may lead to procedural heterogeneity and selection bias. Additionally, qualitative elastography can be subject to operator variability.

Conclusion

Qualitative three-color EBUS elastography demonstrates moderate diagnostic utility in differentiating malignant from benign mediastinal lymphadenopathy but shows overlapping patterns in granulomatous diseases. Integration of cryo-nodal biopsy enhances tissue adequacy and diagnostic confidence, particularly in suspected lymphoma and granulomatous lesions. Elastography should be considered a complementary tool within a comprehensive EBUS diagnostic strategy rather than a standalone modality.

Clinical Significance

Qualitative three-colour EBUS Elastography interpretation is helpful as an adjunct in differentiating Benign and Malignant lymph nodes. Type III elastography is more frequently associated with malignancy; however, overlap with granulomatous disease limits its use as a standalone diagnostic modality. Elastography findings should therefore be interpreted together with clinical, radiological, microbiological, cytological, and histopathological findings.

Ethics Declaration

This prospective observational study was conducted at a tertiary pulmonology center in TB-endemic South India between June 2025 and April 2026. The study was approved by the Institutional Ethics

Committee (EC No.: KIMS/IEC-BHR/2026/128-03), and all patients provided written informed consent.

Data Declaration

All the relevant data are available in this document as a master chart. All the authors are available and ready to supply any additional data upon request through the corresponding author.

Artificial Intelligence (AI) Disclosure

Artificial intelligence was not used for this article.

Acknowledgments

The authors thank the nursing and technical staff of the Bronchoscopy Unit for their support during procedures. No funding was received for this work. All the authors declare that there are no conflicts of interest related to this study, including financial, academic, institutional, or personal relationships that could have influenced the conduct, analysis, interpretation, or reporting of the research.

Authors' Contribution

All the authors have contributed equally in terms of Manuscript content. Saurabh Jain – Data collection, protocol, data analysis and manuscript manufacturing. Vishal Kumar Chitikeshi – Methodology, analysis, review. Mahesh Gudelli – Methodology, conceptualization, supervision and critical manuscript review. Lakshminarayana Jasti – Data collection, interpretation and review. Kranthi Kumar Shavagani – data collection, interpretation and review.

Orcid

Mahesh Gudelli https://orcid.org/0000-0001-9108-2571

References

1. Iyer H, Anand A, Sryma PB, et al. Mediastinal lymphadenopathy: A practical approach. Expert Rev Respir Med 2021;15(10):1317–1334. DOI: 10.1080/17476348.2021.1920404.
2. Mohan A, Madan K, Hadda V, et al. Guidelines for endobronchial ultrasound-transbronchial needle aspiration (EBUS-TBNA): Joint Indian Chest Society (ICS)/Indian Association for Bronchology (IAB) recommendations. Lung India 2023;40(4):368–400. DOI: 10.4103/lungindia.lungindia_510_22.
3. Scano V, Fois AG, Manca A, et al. Role of EBUS-TBNA in non-neoplastic mediastinal lymphadenopathy: Review of literature. Diagnostics (Basel) 2022;12(2):512. DOI: 10.3390/diagnostics12020512.
4. Fielding D, Kurimoto N, Annema JT. Advances in EBUS-guided mediastinal sampling. Respirology 2022;27:225–236.
5. Silvestri GA, Gonzalez AV, Jantz MA, et al. Methods for staging non-small cell lung cancer: Diagnosis and management of lung cancer, 3rd ed: American College of Chest Physicians evidence-based clinical practice guidelines. Chest 2013;143(5 Suppl):e211S–e250S. DOI: 10.1378/chest.12-2355.
6. Madan M, Mittal S, Tiwari P, et al. The diagnostic utility of ultrasound elastography to differentiate tuberculosis and sarcoidosis during endobronchial ultrasound-guided transbronchial needle aspiration (EBUS-TBNA). Lung India 2022;39(6):532–536. DOI: 10.4103/lungindia.lungindia_214_22.
7. Fujiwara T, Yasufuku K, Nakajima T, et al. The utility of sonographic features during endobronchial ultrasound-guided transbronchial needle aspiration for lymph node staging in patients with lung cancer: a standard endobronchial ultrasound image classification system. Chest 2010;138(3):641–647. DOI: 10.1378/chest.09-2006.
8. Wang L, Wu W, Teng J, et al. Sonographic features of endobronchial ultrasound in differentiation of benign lymph nodes. Ultrasound Med Biol 2016;42(12):2785–2793. DOI: 10.1016/j.ultrasmedbio.2016.07.019.
9. Rozman A, Malovrh MM, Adamic K, et al. Endobronchial ultrasound elastography strain ratio for mediastinal lymph node diagnosis. Radiol Oncol 2015;49(4):334–340. DOI: 10.1515/raon-2015-0020.
10. Gupta R, Joshi S, Bhatia A, etal. Qualitative role of endobronchial elastography with endobronchial ultrasound in differentiating malignant and benign lesions: a retrospective single-center study from India. Egypt J Bronchol 2019;13:630–635. DOI: 10.4103/ejb.ejb_49_19.
11. Madan K, Madan M, Iyer H, et al. Utility of elastography for differentiating malignant and benign lymph nodes during EBUS-TBNA: A systematic review and meta-analysis. J Bronchology Interv Pulmonol 2022;29(1):18–33. DOI: 10.1097/LBR.0000000000000781.
12. Mittal S, Mohan A, Hadda V, et al. Endobronchial ultrasound elastography in mediastinal lymphadenopathy: Report of two cases and systematic review of literature. Lung India 2019;36(2):149–153. DOI: 10.4103/lungindia.lungindia_349_17.
13. Labarca G, Sierra-Ruiz M, Kheir F, Folch E, et al. Diagnostic Accuracy of Endobronchial Ultrasound Transbronchial Needle Aspiration in Lymphoma: A Systematic Review and Meta-Analysis. Ann Am Thorac Soc 2019;16(11):1432–1439. DOI: 10.1513/AnnalsATS.201902-175OC.
14. Genova C, Tagliabue E, Mora M, et al. Potential application of cryobiopsy for histo-molecular characterization of mediastinal lymph nodes in patients with thoracic malignancies: A case presentation series and implications for future developments. BMC Pulm Med 2022;22:5. DOI: 10.1186/s12890-021-01814-x.
15. Chandragiri PS, Tayal A, Mittal S, et al. Utility and safety of endobronchial ultrasound-guided transbronchial mediastinal cryobiopsy (EBUS-TMC): A systematic review and meta-analysis. Lung India 2024;41(4):288–298. DOI: 10.4103/lungindia.lungindia_606_23.
16. Izumo T, Sasada S, Chavez C, et al. Endobronchial ultrasound elastography in the diagnosis of mediastinal and hilar lymph nodes. Jpn J Clin Oncol 2014;44(10):956–962. DOI: 10.1093/jjco/hyu105.
17. Chen YF, Mao XW, Zhang YJ, et al. Endobronchial ultrasound elastography differentiates intrathoracic lymph nodes: A meta-analysis. Ann Thorac Surg 2018;106(4):1251–1257. DOI: 10.1016/j.athoracsur.2018.04.003.
18. Verhoeven RLJ, Trisolini R, Leoncini F, et al. Predictive Value of Endobronchial Ultrasound Strain Elastography in Mediastinal Lymph Node Staging: The E-Predict Multicenter Study Results. Respiration 2020;99(6):484–492. DOI: 10.1159/000507592.
19. Wu J, Sun Y, Wang Y, et al. Diagnostic value of endobronchial ultrasound elastography for differentiating benign and malignant hilar and mediastinal lymph nodes: A systematic review and meta-analysis. Med Ultrason 2022;24(1):85–94. DOI: 10.11152/mu-2971.
20. Nakajima T, Inage T, Sata Y, et al. Elastography for predicting and localizing nodal metastases during endobronchial ultrasound. Respiration 2015;90(6):499–506. DOI: 10.1159/000441798.
21. Dietrich CF, Jenssen C, Herth FJ. Endobronchial ultrasound elastography. Endosc Ultrasound 2016;5(4):233–238. DOI: 10.4103/2303-9027.187866.

ORIGINAL ARTICLE

Clinical and Technical Predictors of Diagnostic Yield in Radial Endobronchial Ultrasound Sampling for Peripheral Pulmonary Lesions: A Prospective Observational Study

Sreeja Reddy Sudhini[1], Mahesh Gudelli[2], Vishal Kumar Chitikeshi[3], Lakshminarayana Jasti[4], Kranthi Kumar Shavagani[5]

Received on: 26 August 2026; *Accepted on:* 17 September 2026; *Published on:* 26 September 2026

Abstract

Background: Radial endobronchial ultrasound (r-EBUS) is a key modality for diagnosing peripheral pulmonary lesions (PPLs), yet technical factors affecting diagnostic yield and the accuracy of pre-procedure clinical assessment remain incompletely characterized.

Objectives: To evaluate the combined impact of computed tomography (CT) bronchus sign and r-EBUS probe position on diagnostic yield and concordance between provisional clinical and final pathological diagnosis.

Materials and methods: This prospective study enrolled 50 consecutive adults with PPLs (≥1 cm) undergoing r-EBUS-guided forceps biopsy at a tertiary center in tuberculosis-endemic South India (June 2025–April 2026). Computed tomography bronchus sign and probe position (concentric/eccentric) were assessed. Final diagnoses were established through histopathology and clinical-radiological follow-up.

Results: Overall diagnostic yield was 80.0% (40/50; 95% CI: 66.3–90.0%). Stratified yields showed a gradient: Bronchus sign present + eccentric 100%, present + concentric 83.3%, absent + eccentric 77.8%, absent + concentric 50% (four-group $p = 0.074$). All 21 malignancies were solid nodule/mass lesions; all 19 benign lesions had non-nodular morphologies ($p < 0.001$). Clinical–pathological concordance was 92.5% (37/40; $\kappa = 0.85$), and discordance was 7.5% (3/40), with 90.5% sensitivity for predicting malignancy.

Conclusions: Combined bronchus sign and probe position stratification revealed yields ranging from 50 to 100%. Pre-procedure clinical assessment showed 92.5% concordance with final diagnosis. A 7.5% (3/40) discordance rate supports routine tissue confirmation, particularly in tuberculosis-endemic settings.

Keywords: Bronchus sign, Diagnostic concordance, Diagnostic yield, Lung cancer, Peripheral pulmonary lesions, Probe position, Radial endobronchial ultrasound, Tuberculosis.

Annals of Interventional Pulmonology (2026): 10.5005/annalsofip-11045-0061

Introduction

Peripheral pulmonary lesions (PPLs) represent a diagnostic challenge requiring integration of clinical assessment, radiological evaluation, and tissue confirmation.[1,2] Increasing detection through computed tomography (CT) screening has intensified the need for minimally invasive techniques balancing accuracy with safety.[3–5] Radial endobronchial ultrasound (r-EBUS) has emerged as an important technology, offering real-time visualization and enabling targeted transbronchial biopsy.[6,7]

Meta-analyses have established r-EBUS as a widely used diagnostic modality, with pooled diagnostic yields ranging from 70 to 73% across diverse clinical settings.[1,8] However, substantial heterogeneity exists in reported outcomes, with individual study yields varying from 54% to over 80%.[2,9] This variability reflects both technical factors affecting procedural success and the inherent complexity of distinguishing malignant from benign lesions based on clinical and radiological features alone.

Technical factors influencing r-EBUS diagnostic yield have been extensively studied. Computed tomography bronchus sign—indicating a bronchus leading to the lesion—has emerged as a consistent predictor, with meta-analyses reporting odds ratios of 2.5–3.0 for diagnostic success.[1,7] Probe position during ultrasound examination, classified as concentric (probe centered within lesion) or eccentric (probe at lesion periphery), has also shown associations with yield, though findings remain inconsistent.[10,11] Critically, the combined influence of these factors remains inadequately characterized, limiting our ability to predict procedural success and optimize technique.

Parallel to technical considerations, the accuracy of pre-procedure clinical assessment and its role in managing diagnostic uncertainty remain poorly characterized. Contemporary diagnostic approaches integrate clinical presentation, CT characteristics, and laboratory findings to formulate provisional diagnoses guiding management decisions.[12] Understanding the correlation between provisional clinical diagnosis and final pathological diagnosis has important implications for clinical decision-making, resource allocation, and patient counseling.[13,14] This knowledge gap is

[1–5]Department of Interventional Pulmonology, KIMS Hospitals, Secunderabad, Hyderabad, Telangana, India

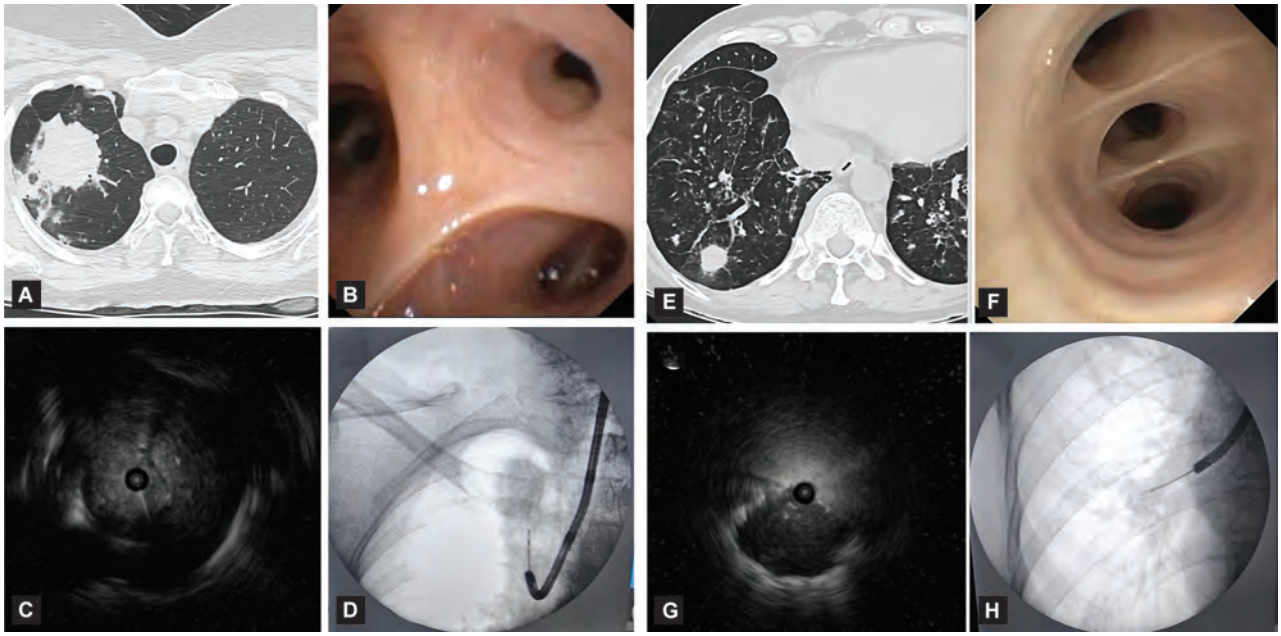
Corresponding Author: Mahesh Gudelli, Department of Interventional Pulmonology, KIMS Hospitals, Secunderabad, Hyderabad, Telangana, India, Phone: +91 8897976190, e-mail: maheshg28@gmail.com

How to cite this article: Sudhini SR, Gudelli M, Chitikeshi VK, *et al*. Clinical and Technical Predictors of Diagnostic Yield in Radial Endobronchial Ultrasound Sampling for Peripheral Pulmonary Lesions: A Prospective Observational Study. Ann Interv Pulmonol 2026;2(2): 67–74.

Source of support: Nil

Conflict of interest: None

© The Author(s). 2026 Open Access. This article is distributed under the terms of the Creative Commons Attribution-NonCommercial 4.0 International License (https://creativecommons.org/licenses/by-nc/4.0/). This license permits non-commercial use, distribution, and reproduction in any medium, provided the original author and source are credited, a link to the license is included, and any changes are indicated.



Figs 1A to H: (LEFT SIDE) (A) Computed tomography chest (lung window, axial section) showing a well-defined mass in the apical segment of the right upper lobe with a visible bronchus sign, indicating a bronchus leading directly to the lesion—a favorable predictor of r-EBUS diagnostic yield; (B) Bronchoscopy image of right upper lobe; (C) Radial endobronchial ultrasound showing concentric lesion along with bronchoscope; (D) Fluoroscopic image with forceps *in-situ*; (RIGHT SIDE) (E) Computed tomography chest (lung window, axial section) showing nodule in posterior basal segment of the right lower lobe; (F) Bronchoscopy image of right lower lobe; (G) Radial endobronchial ultrasound showing eccentric lesion; (H) Fluoroscopic image

particularly relevant in tuberculosis-endemic regions where inflammatory conditions frequently mimic malignancy.[15,16]

This study addresses both dimensions of diagnostic accuracy in r-EBUS by evaluating: (1) the combined impact of CT bronchus sign and probe position on diagnostic yield; (2) concordance between provisional clinical diagnosis and final pathological diagnosis; and (3) patterns and predictors of diagnostic misclassification. We hypothesized that technical factors would demonstrate a gradient effect on yield, while clinical assessment would show good overall accuracy but with clinically significant misclassification rates supporting routine tissue confirmation.

Materials and Methods

Study Design and Setting

This prospective observational study was conducted at a tertiary care center for Interventional Pulmonology in tuberculosis-endemic South India between June 2025 and April 2026. The study was approved by the Institutional Ethics Committee (EC No.: KIMS/IEC-BHR/2026/128-02), and all patients provided written informed consent. The study was conducted in accordance with the Declaration of Helsinki (1975, revised 2013).

Patient Selection

We enrolled 50 consecutive adult patients (≥18 years) undergoing r-EBUS for evaluation of PPLs. Inclusion criteria: (1) radiologically confirmed PPL on chest CT; (2) lesion size ≥1 cm; (3) lesion amenable to r-EBUS sampling; (4) no prior tissue diagnosis; and (5) clinical indication for tissue confirmation. Exclusion criteria: (1) contraindications to bronchoscopy (severe hypoxemia, uncorrected coagulopathy, and hemodynamic instability); (2) central lesions accessible by conventional bronchoscopy; (3) prior treatment for the current lesion; and (4) inability to provide informed consent.

Clinical Assessment and Provisional Diagnosis

Before r-EBUS, provisional diagnoses were assigned based on comprehensive clinical evaluation including: Patient demographics, smoking history, symptom profile, comorbidities, CT characteristics (size, morphology, location, bronchus sign, cavitation, and ground-glass opacity), and laboratory findings (inflammatory markers, tumor markers when available). Provisional diagnoses were categorized as "suspected malignancy" or "suspected nonmalignant diagnosis" based on the most likely diagnosis guiding initial management planning.

CT Imaging Protocol and Bronchus Sign Assessment

All patients underwent contrast-enhanced chest CT within 4 weeks before r-EBUS. Computed tomography scans were independently reviewed by radiologists blinded to clinical outcomes. Bronchus sign was defined as a bronchus visibly leading to or contained within the lesion on CT images, classified as present or absent. While several sub-classification systems exist, including the six-subtype scheme by Imabayashi et al., our study used the traditional binary classification (present vs absent) as defined by Kurimoto et al.[10,17] Type IIa (compressed bronchus adjacent to the lesion) was classified as bronchus sign absent. Disagreements were resolved by consensus. Lesion size was measured as maximum diameter on axial images. Lesion morphology was classified as solid nodule/mass, consolidation, cavitary lesion, or ground-glass opacity. Representative CT images illustrating lesion morphology are shown in Figure 1.

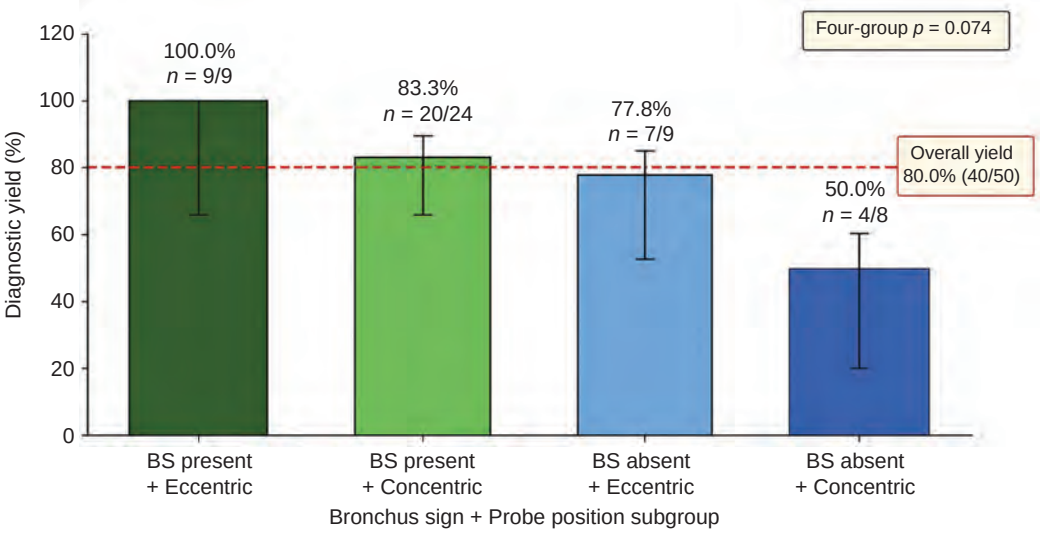


Fig. 2: Diagnostic yield (%) by bronchus sign (BS) and probe position subgroups (n = 50). Error bars = 95% CI. Dashed line = overall diagnostic yield 80.0% (40/50). Four-group p = 0.074

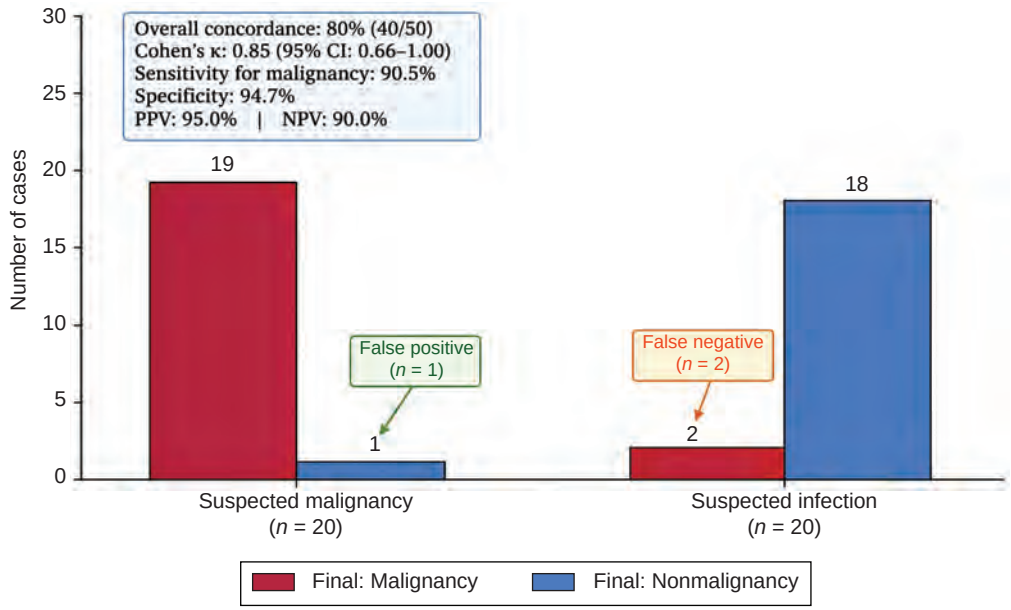


Fig. 3: Clinical–pathological concordance (n = 40). Grouped bars show final diagnosis (malignancy vs nonmalignancy) within each provisional diagnosis group

r-EBUS Procedure and Technical Parameters

Radial endobronchial ultrasound procedures were performed by experienced bronchoscopists using a flexible bronchoscope (Olympus BF-IT 190, BF-MP 190, BF-P190, Olympus Corporation, Tokyo, Japan) with a 20 MHz radial ultrasound probe (MAJ-1720, Olympus Corporation, Tokyo, Japan) and guide sheath system. Lesion localization was confirmed by characteristic ultrasound patterns. Probe position was classified in real-time as concentric (probe-centered within lesion with circumferential ultrasound signal) or eccentric (probe at lesion periphery with asymmetric signal). Representative r-EBUS images are shown in Figure 2. Transbronchial biopsies (4–6 samples) were obtained under fluoroscopic guidance (Fig. 3). All procedures were performed under general anesthesia with I-gel and continuous monitoring. Tissue sampling was performed predominantly using conventional transbronchial forceps biopsy (4–6 samples per case); in four cases, the operating bronchoscopist elected transbronchial cryo-biopsy (4–5 samples per case) based on intra-procedural judgment. The decision to use cryo-biopsy was guided by intra-procedural findings: Eccentric probe positioning with a peripheral tissue interface deemed suboptimal for forceps retrieval; lesion morphology—cavitary, consolidated, or diffusely infiltrative—suggesting that a

larger-core specimen would improve diagnostic representativeness; or anticipated difficulty in obtaining adequate tissue with standard forceps given lesion accessibility. The choice of biopsy modality was operator-directed and not prespecified in the study protocol. The primary study endpoints, diagnostic yield stratified by bronchus sign and probe position, were evaluated irrespective of sampling technique.

Pathological Diagnosis and Clinical Follow-up

Specimens underwent histopathological examination by pathologists. Final diagnoses were established through histopathology supported by clinical and radiological follow-up as needed, and classified as: Malignancy (primary lung cancer or metastatic disease), benign (tuberculosis, pneumonic consolidation, organizing pneumonia, hamartoma, and other granulomatous inflammation) and indeterminate or undiagnosed (nonspecific fibrosis, normal lung tissue). All patients with organizing pneumonia and pneumonic consolidation underwent a minimum of 6 months of clinical-radiological follow-up to confirm diagnostic stability or resolution before final diagnosis assignment.

Diagnostic yield was defined as obtaining tissue sufficient for specific pathological diagnosis. Nondiagnostic cases yielded only normal bronchial tissue or nonspecific fibrosis without clinical correlation.

Concordance Assessment

Concordance was defined as agreement between provisional clinical and final diagnostic categories. For primary analysis, diagnoses were dichotomized as malignancy vs nonmalignancy. Misclassification was categorized as: False positive (suspected malignancy, benign final diagnosis), false negative (suspected infection, malignancy final diagnosis), or reclassification within nonmalignant categories.

Statistical Analysis

Sample Size Justification

This was an exploratory prospective study; no formal *a priori* power calculation was performed, as the study was designed to generate preliminary estimates of diagnostic yield and concordance rather than to test a prespecified hypothesis. Consecutive eligible patients were enrolled over the study period to maximize available sample size. The resulting $n = 50$ cohort provides adequate precision for the primary yield estimate (80.0%; 95% CI: 66.3–90%) but may be underpowered for subgroup comparisons; all subgroup *p*-values should be interpreted with caution.

Descriptive statistics summarized patient characteristics and diagnostic outcomes. Diagnostic yield was calculated with 95% confidence intervals using the Wilson score method. Associations between yield and technical factors were assessed using Chi-square or Fisher's exact test. Univariable logistic regression evaluated predictors of diagnostic yield. Concordance was assessed using Cohen's kappa coefficient ($\kappa < 0.20$: Poor; 0.21–0.40: Fair; 0.41–0.60: Moderate; 0.61–0.80: Substantial; >0.80: Almost perfect agreement). Sensitivity, specificity, positive predictive value (PPV), and negative predictive value (NPV) with 95% confidence intervals were calculated for malignancy detection. Given the small number of misclassified cases ($n = 3$), only univariable analyses were performed to avoid overfitting. Statistical significance was set at $p < 0.05$. Analyses were performed using Python (version 3.9) with the scipy and statsmodels libraries.

Table 1: Baseline patient and lesion characteristics ($n = 50$)

Characteristic	Value
Demographics	
Age, years (mean ± SD)	59.4 ± 10.8
Male sex, *n* (%)	38 (76.0)
Ever-smoker, *n* (%)	31 (62.0)
Clinical presentation	
Cough, *n* (%)	34 (68.0)
Dyspnea, *n* (%)	27 (54.0)
Chest pain, *n* (%)	21 (42.0)
Hemoptysis, *n* (%)	14 (28.0)
Lesion characteristics	
Size, cm (mean ± SD)	4.2 ± 2.1
Lobe Location, *n* (%)	
Right upper lobe	16 (32.0)
Right middle lobe	7 (14.0)
Right lower lobe	12 (24.0)
Left upper lobe	11 (22.0)
Left lower lobe	4 (8.0)
Morphology, *n* (%)	
Solid nodule/mass	26 (52.0)
Consolidation	14 (28.0)
Cavitary lesion	6 (12.0)
Ground-glass opacity	4 (8.0)
CT bronchus sign, *n* (%)	
Present	33 (66.0)
Absent	17 (34.0)
Probe position, *n* (%)	
Concentric	32 (64.0)
Eccentric	18 (36.0)

Results

Patient Characteristics

The study included 50 patients (mean age 59.4 ± 10.8 years; 76% male; 62% ever-smokers). Common presenting symptoms included cough (68%), dyspnea (54%), chest pain (42%), and hemoptysis (28%). Mean lesion size was 4.2±2.1 cm (range 1.2–9.5 cm). Lesion distribution: Right upper lobe (32%), right lower lobe (24%), left upper lobe (22%), right middle lobe (14%), and left lower lobe (8%). Morphologically, 52% were solid nodules/masses, 28% consolidations, 12% cavitary lesions, and 8% ground-glass opacities. Computed tomography bronchus sign was present in 66% (33/50). Probe position was concentric in 64% (32/50) and eccentric in 36% (18/50). Detailed patient characteristics are presented in Table 1.

Diagnostic Yield and Technical Factors

Overall diagnostic yield was 80.0% (40/50; 95% CI: 66.3–90.0%). Final pathological diagnoses comprised malignancy in 42.0% (21/50), including 17 primary lung cancers and four metastatic lesions; benign etiologies in 38.0% (19/50), including tuberculosis, organizing pneumonia, granulomatous inflammation, hamartoma,

and pneumonic consolidation. Ten cases (20.0%) were undiagnosed. Full diagnostic distribution is presented in Table 2.

Stratified diagnostic yields by bronchus sign and probe position demonstrated a gradient (Table 3; Fig. 2): Bronchus sign present + eccentric probe 100.0% (9/9; 95% CI: 66.4–100.0%), present + concentric probe 83.3% (20/24; 95% CI: 62.6–95.3%), absent + eccentric probe 77.8% (7/9; 95% CI: 40.0–97.2%), and absent + concentric probe 50.0% (4/8; 95% CI: 15.7–84.3%). The four-group comparison yielded $p = 0.074$.

Individual factors, such as bronchus sign alone or probe position alone showed non-significant associations with diagnostic yield: Bronchus sign alone (present in 87.9% vs absent in 64.7%, $p = 0.052$); probe position alone (eccentric in 88.9% vs concentric in 75.0%, $p = 0.239$).

Lesion morphology demonstrated complete separation: All 21 malignancies were solid nodules/masses, while all 19 benign lesions had non-nodular morphologies (consolidations, cavitary lesions, and GGOs) ($p < 0.001$). Univariable logistic regression showed that lesion size was significantly associated with diagnostic yield (OR 1.91; 95% CI: 1.03–3.56; $p = 0.041$). Bronchus sign presence (OR 3.95; 95% CI: 0.93–16.74; $p = 0.062$) and eccentric probe position (OR 2.67; 95% CI: 0.50–14.22; $p = 0.251$) showed positive but non-significant associations with diagnostic yield. Age, male sex, lesion type, and lobe location were not significantly associated with diagnostic yield (Table 4).

Clinical–Pathological Concordance

Provisional diagnoses were: Suspected malignancy 50% (25/50) and suspected nonmalignant diagnosis 50% (25/50). Overall concordance between provisional and final diagnosis was 92.5% (37/40). Clinical–pathological concordance was high, with an observed agreement of 92.5% and Cohen's κappa of 0.85 (95% CI: 0.69–1.00), indicating substantial agreement between the provisional clinical diagnosis and definitive pathological diagnosis (Table 5; Fig. 3).

Among 40 evaluable definitive final diagnoses (21 malignancies, 19 benign), clinical prediction demonstrated a sensitivity of 90.5% (19/21; 95% CI: 68.6–98.0%), specificity of 94.7% (18/19; 95% CI: 74.0–99.9%), PPV of 95.0% (19/20; 95% CI: 75.1–99.9%), NPV of 90.0% (18/20; 95% CI: 68.3–98.8%), and overall accuracy of 92.5% (37/40; 95% CI: 79.6–98.4%). One false positive occurred (suspected malignancy without histological confirmation), and two false negatives occurred.

Table 2: Final pathological diagnoses ($n = 50$)

Diagnosis category	*n* (%)
Malignancy ($n = 21$)	21 (42.0)
Adenocarcinoma	9 (18.0)
Squamous cell carcinoma	5 (10.0)
Small cell lung cancer	3 (6.0)
Metastatic disease	4 (8.0)
Benign etiologies ($n = 19$)	19 (38.0)
Tuberculosis	8 (16.0)
Organizing pneumonia	5 (10.0)
Granulomatous inflammation (sarcoidosis)	2 (4.0)
Hamartoma	2 (4.0)
Pneumonic consolidation	2 (4.0)
Undiagnosed ($n = 10$)	10 (20.0)
Nonspecific fibrosis	4 (8.0)
Nondiagnostic*	6 (12.0)

*Nondiagnostic cases yielded only normal bronchial tissue or nonspecific inflammation without clinical correlation

Safety Outcomes

Minor self-limited bleeding occurred in 76% (38/50) of procedures. No major complications occurred: Zero cases of moderate/severe bleeding requiring intervention, pneumothorax, respiratory failure, or death.

Discussion

Principal Findings

This prospective study provides a dual-perspective evaluation of r-EBUS diagnostic accuracy for PPLs. Technical factors (bronchus sign and probe position) generated a non-significant gradient in diagnostic yield, and pre-procedure clinical assessment achieved 92.5% concordance with final pathology ($\kappa = 0.85$) with 90.5% sensitivity for malignancy detection. Despite this high accuracy, a 7.5% discordance rate underscores the continued necessity of tissue confirmation.

Technical Factors and Diagnostic Yield

Our overall yield of 80% is similar to 70–73% reported in contemporary meta-analyses.[1,8] The four-group stratification (Fig. 2)

Table 4: Univariable logistic regression for predictors of diagnostic yield

Variable	Odds ratio	95% CI	*p*-value
Age (per 10 years increase)	1.01	0.66–1.57	0.950
Male sex	0.90	0.22–3.70	0.886
Ever-smoker	0.78	0.12–5.01	0.745
Lesion size (per 1 cm increase)	1.91	1.03–3.56	0.041
Lesion type (solid vs non-nodular)	1.50	0.37–6.14	0.573
Lobe location (lower vs upper/middle)	0.72	0.17–3.01	0.655
Bronchus sign present	3.95	0.93–16.74	0.062
Eccentric probe position	2.67	0.50–14.22	0.251

CI, confidence interval

Table 3: Diagnostic yield stratified by bronchus sign and probe position

Bronchus sign	Probe position	Diagnostic cases/total	Yield (%)	95% CI
Present	Eccentric	9/9	100.0	66.4–100.0
Present	Concentric	20/24	83.3	62.6–95.3
Absent	Eccentric	7/9	77.8	40.0–97.2
Absent	Concentric	4/8	50.0	15.7–84.3
Overall		40/50	80.0	66.3–90.0

Statistical comparisons: Bronchus sign alone (present vs absent): $p = 0.052$; probe position alone (concentric vs eccentric): $p = 0.239$; combined four-group comparison: $p = 0.074$ (Chi-square test). CI, confidence interval

Table 5: Concordance between provisional clinical diagnosis and final pathological diagnosis

Provisional diagnosis	Final diagnosis: Malignancy	Final diagnosis: Nonmalignancy	Total
Suspected malignancy	19	1	20
Suspected infection	2	18	20
Total	21	19	40

Overall concordance: 80% (40/50). Cohen's kappa: 0.85 (95%CI: 0.69–1.00). Sensitivity for malignancy: 90.5%. Specificity: 94.7%. CI, confidence interval

revealed that the highest yield (100%) occurred when bronchus sign and eccentric probe position coincided, while the lowest (50%) corresponded to absent bronchus sign with concentric positioning. The four-group comparison did not reach statistical significance ($p = 0.074$); with only $n = 50$, the study was underpowered to detect a statistically significant difference across four subgroups. The individual-factor ORs (3.95 for bronchus sign, 2.67 for eccentric position) had wide confidence intervals spanning unity, and should be considered hypothesis-generating for future adequately powered studies.[10,11]

The individual-factor associations were not statistically significant. Bronchus sign was associated with higher diagnostic yield (87.9 vs 64.7%; OR 3.95; 95% CI: 0.93–16.74; $p = 0.062$), while eccentric probe positioning was associated with higher yield (88.9 vs 75.0%; OR 2.67; 95% CI: 0.50–14.22; $p = 0.251$). These findings suggest that neither factor should be interpreted as an independent determinant of diagnostic yield in this small cohort. The attenuated individual-factor associations (bronchus sign alone $p = 0.052$; probe position alone $p = 0.239$) suggest that neither predictor operates independently: Optimal yield requires favorable CT anatomy and optimal intra-procedural positioning simultaneously. These findings align with Hong et al., who reported that within-lesion probe positioning was the strongest predictor of diagnostic success (OR 28.50, $p < 0.001$), suggesting that any probe-to-lesion contact—whether concentric or eccentric—is more important than the geometry of contact.[18] Cases anticipated to have absent bronchus sign should prompt consideration of complementary approaches—CT-guided biopsy or enhanced navigation—rather than r-EBUS alone, regardless of anticipated probe position.[19]

The complete morphological separation (all 21 malignancies solid; all 19 benign lesions non-nodular; $p < 0.001$) is a notable but unexpected finding. While solid morphology is an established malignancy predictor complete separation is unusual and warrants cautious interpretation; it may reflect referral bias or cohort-specific characteristics rather than a generalizable rule, and requires validation in larger multi-center cohorts.[20,21]

In our cohort, the observed eccentric yield (88.9%) exceeding concentric yield (75.0%) is contrary to published literature and warrants careful interpretation, although this difference was not statistically significant ($p = 0.251$). The wide confidence intervals indicate substantial uncertainty around these estimates, compatible with sampling variability. With only 18 eccentric cases, the findings should not be interpreted as evidence of diagnostic superiority of eccentric positioning and instead highlight the need for larger studies to determine the independent contribution of probe position.

Clinical Assessment Accuracy and Concordance

The near-perfect kappa (0.85) and 90.5% malignancy sensitivity (Fig. 3) indicate that experienced clinicians at a tertiary center can reliably predict final pathological category in the majority of PPL cases, consistent with previously reported clinical prediction model sensitivities of 85–95%.[22,23]

The substantial clinical–pathological agreement ($\kappa = 0.85$; 95% CI: 0.69–1.00) and 90.5% sensitivity for malignancy indicate that experienced clinicians could reliably predict the final pathological category in the majority of evaluable PPL cases. Nevertheless, the 7.5% discordance rate (3/40 evaluable cases) represents clinically relevant diagnostic uncertainty. There was one false-positive case, in which granulomatous inflammation was provisionally considered malignant, and two false-negative cases, in which malignancy was provisionally considered infective. These findings illustrate the limitations of clinical assessment alone and reinforce the need for tissue confirmation when diagnostic uncertainty persists.[15,16]

Clinical Implications

Taken together, these findings support a risk-stratified procedural approach. Patients with bronchus sign present can be expected to achieve high diagnostic success with r-EBUS. Conversely, those with absent bronchus sign had lower diagnostic yields depending on probe position (77.8% with eccentric position and 50% with concentric positioning) and should be counseled about the higher likelihood of a nondiagnostic result and offered upfront complementary sampling strategies. Regardless of clinical confidence level, the 7.5% discordance rate (3/40) justifies routine tissue confirmation for all PPLs—a recommendation of particular relevance in tuberculosis-endemic regions where inflammatory mimicry is prevalent.[15,16,24] The zero major-complication rate further supports r-EBUS as a safe first-line modality when technical factors are favorable.[24,25]

Limitations

This study has several limitations. First, the single-center design and modest sample size ($n = 50$) limit generalizability and statistical power; all subgroup p-values should be interpreted cautiously, and the non-significant four-group comparison ($p = 0.074$) may reflect inadequate power. Second, provisional diagnoses were assigned by experienced tertiary-center pulmonologists, potentially overestimating accuracy relative to community or non-specialist settings.[14] Third, biopsy technique was not protocolized: Conventional forceps biopsy was used in the majority of cases, while four patients underwent cryo-biopsy at operator discretion based on intra-procedural assessment. Although no systematic difference in diagnostic outcome was observed between modalities and the primary analyses were technique-agnostic, a formal comparative analysis was not performed; the small number of cryobiopsy cases limits conclusions about relative yield, particularly for eccentric lesions.[26,27] Fourth, clinician confidence levels were not systematically captured, preventing graded concordance analysis. Fifth, the binary bronchus sign classification (Kurimoto, 2004) does not capture the six-subtype granularity proposed by Swensen et al.;[28] future studies should evaluate sub-classification

schemes. Sixth, the complete morphological separation between malignant and benign lesions is unusual and may reflect referral bias or cohort-specific characteristics; external validation is essential. Seventh, nondiagnostic cases with nonspecific benign histology ($n = 6$) require prolonged follow-up; 6 months of surveillance may be insufficient to exclude indolent malignancy.[29,30] Future multicenter studies incorporating larger cohorts, diverse geographic settings, cryo-biopsy, and integrated clinical-radiological-technical prediction models are needed to confirm these findings.

Ethics Declaration

This prospective observational study was conducted at a tertiary pulmonology center in TB-endemic South India between June 2025 and April 2026. The study was approved by the Institutional Ethics Committee (EC No.: KIMS/IEC-BHR/2026/128-02), and all patients provided written informed consent.

Conclusion

In this 50-patient prospective cohort, combined bronchus sign and probe position stratification revealed diagnostic yields ranging from 50 to 100%, though the four-group comparison did not reach statistical significance ($p = 0.074$). Pre-procedure clinical assessment demonstrated 92.5% concordance with final pathology ($\kappa = 0.85$), 90.5% sensitivity for diagnosing malignancy with 92.5% overall diagnostic accuracy. A 7.5% discordance rate concentrated in nonnodular lesion morphologies supports routine tissue confirmation for all PPLs, particularly in tuberculosis-endemic settings were inflammatory conditions mimic malignancy.However, given the limited sample size and non-significant subgroup differences, these factors should not be considered independent predictors. The findings also emphasize that tissue confirmation remains important when clinical and radiological assessment is uncertain, particularly in tuberculosis-endemic settings where benign inflammatory conditions may mimic malignancy. Future multicenter studies with larger cohorts are needed to confirm the results of this study.

Artificial Intelligence (AI) Disclosure

No AI was used in any step of preparing/writing of the manuscript.

Acknowledgement

None.

Orcid

Mahesh Gudelli https://orcid.org/0000-0001-9108-2571

References

1. Steinfort DP, Khor YH, Manser RL, et al. Radial probe endobronchial ultrasound for the diagnosis of peripheral lung cancer: Systematic review and meta-analysis. Eur Respir J 2011;37(4):902–910. DOI: 10.1183/09031936.00075310.
2. Wang Memoli JS, Nietert PJ, Silvestri GA. Meta-analysis of guided bronchoscopy for the evaluation of the pulmonary nodule. Chest 2012;142(2):385–393. DOI: 10.1378/chest.11-1764.
3. Gould MK, Donington J, Lynch WR, et al. Evaluation of individuals with pulmonary nodules: When is it lung cancer? Chest 2013;143(5 Suppl):e93S–e120S. DOI: 10.1378/chest.12-2351.
4. MacMahon H, Naidich DP, Goo JM, et al. Guidelines for management of incidental pulmonary nodules detected on CT images: From the Fleischner Society 2017. Radiology 2017;284(1):228–243. DOI: 10.1148/radiol.2017161659.
5. Ost D, Fein AM, Feinsilver SH. Clinical practice: The solitary pulmonary nodule. N Engl J Med 2003;348(25):2535–2542. DOI: 10.1056/nejmcp012290.
6. Rivera MP, Mehta AC, Wahidi MM. Establishing the diagnosis of lung cancer: Diagnosis and management of lung cancer, 3rd ed: American College of Chest Physicians evidence-based clinical practice guidelines. Chest 2013;143(5 Suppl):e142S–e165S. DOI: 10.1378/chest.12-2353.
7. Ali MS, Trick W, Mba BI, et al. Radial endobronchial ultrasound for the diagnosis of peripheral pulmonary lesions: A systematic review and meta-analysis. Respirology 2017;22(3):443–453. DOI: 10.1111/resp.12980.
8. Folch EE, Labarca G, Ospina-Delgado D, et al. Sensitivity and safety of electromagnetic navigation bronchoscopy for lung cancer diagnosis: Systematic review and meta-analysis. Chest 2020;158(4):1753–1769. DOI: 10.1016/j.chest.2020.05.534.
9. Oki M, Saka H, Ando M, et al. Ultrathin bronchoscopy with multimodal devices for peripheral pulmonary lesions: A randomized trial. Am J Respir Crit Care Med 2015;192(4):468–476. DOI: 10.1164/rccm.201502-0205oc.
10. Kurimoto N, Miyazawa T, Okimasa S, et al. Endobronchial ultrasonography using a guide sheath increases the ability to diagnose peripheral pulmonary lesions endoscopically. Chest 2004;126(3):959–965. DOI: 10.1378/chest.126.3.959.
11. Herth FJ, Ernst A, Becker HD. Endobronchial ultrasound-guided transbronchial lung biopsy in solitary pulmonary nodules and peripheral lesions. Eur Respir J 2002;20(4):972–974. DOI: 10.1183/09031936.02.00032001.
12. McWilliams A, Tammemagi MC, Mayo JR, et al. Probability of cancer in pulmonary nodules detected on first screening CT. N Engl J Med 2013;369(10):910–919. DOI: 10.1056/nejmoa1214726.
13. Ost DE, Gould MK. Decision making in patients with pulmonary nodules. Am J Respir Crit Care Med 2012;185(4):363–372. DOI: 10.1164/rccm.201104-0679ci.
14. Tanner NT, Aggarwal J, Gould MK, et al. Management of pulmonary nodules by community pulmonologists: A multicenter observational study. Chest 2015;148(6):1405–1414. DOI: 10.1378/chest.15-0630.
15. Sharma SK, Mohan A. Extrapulmonary tuberculosis. Indian J Med Res 2004;120(4):316–353. PMID: 15520485.
16. Nachiappan AC, Rahbar K, Shi X, et al. Pulmonary tuberculosis: Role of radiology in diagnosis and management. Radiographics 2017;37(1):52–72. DOI: 10.1148/rg.2017160032.
17. Imabayashi T, Matsumoto Y, Uchimura K, et al. Computed tomography bronchus sign subclassification during radial endobronchial ultrasound-guided transbronchial biopsy: A retrospective analysis. Diagnostics 2023;13(6):1064. DOI: 10.3390/diagnostics13061064.
18. Hong KS, Lee KH, Chung JH, et al. Utility of radial probe endobronchial ultrasound guided transbronchial lung biopsy in bronchus sign negative peripheral pulmonary lesions. J Korean Med Sci 2021;36(24):e176. DOI: 10.3346/jkms.2021.36.e176.
19. Choi SH, Chae EJ, Kim JE, et al. Percutaneous CT-guided aspiration and core biopsy of pulmonary nodules smaller than 1 cm: Analysis of outcomes of 305 procedures from a tertiary referral center. AJR Am J Roentgenol 2013;201(5):964–970. DOI: 10.2214/ajr.12.10156.
20. Henschke CI, Yankelevitz DF, Mirtcheva R, et al. CT screening for lung cancer: Frequency and significance of part-solid and nonsolid nodules. AJR Am J Roentgenol 2002;178(5):1053–1057. DOI: 10.2214/ajr.178.5.1781053.
21. Travis WD, Brambilla E, Noguchi M, et al. International Association for the Study of Lung Cancer/American Thoracic Society/European Respiratory Society international multidisciplinary classification of lung adenocarcinoma. J Thorac Oncol 2011;6(2):244-285. DOI: 10.1097/JTO.0b013e318206a221.

22. Gould MK, Ananth L, Barnett PG. A clinical model to estimate the pretest probability of lung cancer in patients with solitary pulmonary nodules. Chest 2007;131(2):383–388. DOI: 10.1378/chest.06-1261.
23. Schultz EM, Sanders GD, Trotter PR, et al. Validation of two models to estimate the probability of malignancy in patients with solitary pulmonary nodules. Thorax 2008;63(4):335–341. DOI: 10.1136/thx.2007.084731.
24. Daley CL, Iaccarino JM, Lange C, et al. Treatment of nontuberculous mycobacterial pulmonary disease: An official ATS/ERS/ESCMID/IDSA clinical practice guideline. Eur Respir J 2020;56(4):2000535. DOI: 10.1183/13993003.00535-2020.
25. Asano F, Aoe M, Ohsaki Y, et al. Complications associated with endobronchial ultrasound-guided transbronchial needle aspiration: A nationwide survey by the Japan Society for Respiratory Endoscopy. Respir Res 2013;14:50. DOI: 10.1186/1465-9921-14-50.
26. Kho SS, Chan SK, Yong MC, et al. Performance of transbronchial cryobiopsy in eccentrically and adjacently orientated radial endobronchial ultrasound lesions. ERJ Open Res 2019;5(4):00135–2019. DOI: 10.1183/23120541.00135-2019.
27. Sumi T, Yamada Y, Koshino Y, et al. Transbronchial cryobiopsy for small peripheral pulmonary lesions using EBUS and an ultrathin bronchoscope. Respir Investig 2024;62(1):77–84. DOI: 10.1016/j.resinv.2023.11.001.
28. Swensen SJ, Silverstein MD, Ilstrup DM, et al. The probability of malignancy in solitary pulmonary nodules: Application to small radiologically indeterminate nodules. Arch Intern Med 1997;157(8):849–855. DOI: 10.1001/archinte.1997.00440290031002.
29. Leonard KM, Low SW, Echanique CS, et al. Diagnostic yield vs diagnostic accuracy for peripheral lung biopsy evaluation. Chest 2024;165(4):920–927. DOI: 10.1016/j.chest.2023.12.024.
30. Lee KH, Lim KY, Suh YJ, et al. Nondiagnostic percutaneous transthoracic needle biopsy of lung lesions: A multicenter study of malignancy risk. Radiology 2019;290(3):814–823. DOI: 10.1148/radiol.2018181482.

ORIGINAL ARTICLE

Role of Bronchoscopy and Image Guided Tissue Sampling in Diagnosing Post COVID Cavitary Lung Disease: A Prospective Multicentric Study

Sreetama Bandyopadhyay[1], Chandan Kumar Shit[2], Surajit Chatterjee[3], Subhankar Chatterjee[4], Biplab Chandra[5], Amitabha Sengupta[6]

Received on: 05 August 2026; *Accepted on:* 16 September 2026; *Published on:* 26 September 2026

Abstract

Background: Cavitary lung disease is a serious post-acute COVID-19 complication, frequently caused by opportunistic infections in patients treated with corticosteroids. While steroids reduce inflammation, they predispose patients to invasive infections, which necessitate early diagnosis.

Materials and methods: This was a multicentric prospective observational study conducted at the Institute of Post Graduate Medical Education & Research and SSKM Hospital, and Calcutta Heart Clinic & Hospital, Kolkata, between November 2020 and January 2023. A total of 102 symptomatic post-acute COronaVIrus Disease (COVID) patients were included. Patients who had cavitary lesions in high-resolution computed tomography (HRCT) thorax were evaluated using fiberoptic bronchoscopy and bronchoalveolar lavage (BAL), computed tomography (CT)-guided biopsy, or surgical resection for etiological diagnosis.

Results: In total, 21 (20.6%) patients exhibited cavitary lung disease. Fungal infections were identified as the most common causative organism in 14 patients (66.7%). COVID-associated pulmonary aspergillosis (CAPA) was found in nine patients, while COVID-associated pulmonary mucormycosis (CAPM) was found in five. All mucormycosis cases were related to preexisting diabetes and prior corticosteroid exposure. Bacterial infections were isolated in five patients (23.8%), among which two were due to *Klebsiella*, two due to *Pseudomonas*, and one due to methicillin-resistant *Staphylococcus aureus* (MRSA) infection. Tuberculosis (TB) caused cavitary lung disease in one patient, and one remained undiagnosed. *Aspergillus* was diagnosed via BAL culture and BAL galactomannan, whereas mucor was confirmed by BAL and bronchoscopic biopsy tissue culture, histopathology, and polymerase chain reaction (PCR), with additional confirmation via CT-guided biopsy and lobectomy in two cases. This study found that interventional procedures were valuable for accurate diagnosis. In total, 19 patients survived, while two patients died—one mucormycosis patient who died while awaiting surgery and one patient with *Pseudomonas* infection.

Conclusion and clinical significance: In total, 21% of symptomatic post-acute COVID patients were complicated by cavitary lung lesions, predominantly of fungal etiology. Diabetics who received systemic corticosteroids were most likely to develop cavitary lung disease. Early interventions like bronchoscopy, CT, or surgical biopsy are essential for prompt and accurate diagnosis. Prompt diagnosis guides targeted therapy, improving outcomes in this high-risk population.

Keywords: Bronchoscopy, Cavitary lung disease, Computed tomography–guided Tru-Cut biopsy, Post-acute COVID-19.

Annals of Interventional Pulmonology (2026): 10.5005/annalsofip-11045-0059

Introduction

The COVID-19 pandemic has been associated with numerous complications occurring between 4 and 12 weeks after acute illness, collectively referred to as post-acute COronaVIrus Disease (COVID) complications.[1] The pandemic resulted in multisystem involvement during the post-COVID period, with pulmonary manifestations being particularly prominent. Cavitary lung disease has emerged as a potentially life-threatening pulmonary sequela.[2,3] Pulmonary cavities represent localized areas of lung tissue necrosis, which may be solitary or multiple and are most commonly caused by opportunistic bacterial or fungal infections. Among fungal etiologies, *Aspergillus* and Mucorales are particularly important, resulting in COVID-associated pulmonary aspergillosis (CAPA) and COVID-associated pulmonary mucormycosis (CAPM), respectively. Pulmonary cavitation may also occur due to reactivation of *Mycobacterium* tuberculosis (MTB).[4,5]

Accurate diagnosis of post-acute COVID cavitary lung disease remains challenging, as conventional sputum and blood cultures frequently yield negative results, particularly in the setting of altered lung architecture and prior antimicrobial exposure.[6] Consequently, interventional diagnostic procedures, including fiberoptic

[1]Department of Pulmonary Medicine, R. G. Kar Medical College and Hospital, Kolkata, West Bengal, India

[2]Department of Pulmonary Medicine and Critical Care, Calcutta Heart Clinic & Hospital, Kolkata, West Bengal, India

[3]Department of Respiratory Medicine, Institute of Post Graduate Medical Education and Research and SSKM Hospital, Kolkata, West Bengal, India

[4,5]Department of Internal Medicine and Critical Care, Calcutta Heart Clinic and Hospital, Kolkata, West Bengal, India

[6]Department of Pulmonary Medicine, Institute of Post Graduate Medical Education and Research, Kolkata, West Bengal, India

Corresponding Author: Chandan Kumar Shit, Department of Pulmonary Medicine and Critical Care, Calcutta Heart Clinic and Hospital, Kolkata, West Bengal, India, Phone: +91 8900537932, e-mail: chandansheet1986@gmail.com

How to cite this article: Bandyopadhyay S, Shit CK, Chatterjee S, *et al.* Role of Bronchoscopy and Image Guided Tissue Sampling in Diagnosing Post COVID Cavitary Lung Disease: A Prospective Multicentric Study. Ann Interv Pulmonol 2026;2(2):75–85.

Source of support: Nil

Conflict of interest: None

© The Author(s). 2026 Open Access. This article is distributed under the terms of the Creative Commons Attribution-NonCommercial 4.0 International License (https://creativecommons.org/licenses/by-nc/4.0/). This license permits non-commercial use, distribution, and reproduction in any medium, provided the original author and source are credited, a link to the license is included, and any changes are indicated.

bronchoscopy with bronchoalveolar lavage (BAL) and bronchoscopic biopsy, computed tomography (CT)-guided Tru-Cut biopsy, and surgical resection, have assumed an important role in establishing definitive microbiological and histopathological diagnoses.[7]

Corticosteroids became a standard component of therapy for moderate-to-severe COVID-19-associated acute respiratory distress syndrome (ARDS), based in part on their prior use in influenza-associated ARDS.[8,9] Although corticosteroids are lifesaving during acute illness, their immunosuppressive effects increase susceptibility to opportunistic infections, particularly among patients with diabetes mellitus, and contributed to the emergence of post-COVID pulmonary mucormycosis outbreaks in India.[10,11]

The primary objective of this study was to evaluate the etiological spectrum of post-COVID cavitary lung disease and assess the role of interventional diagnostic procedures in establishing an early diagnosis. Secondary objectives were to identify risk factors associated with the development of post-COVID cavitary lung disease, characterize the microbiological profile, and evaluate clinical outcomes.

Materials and Methods

Study Design and Setting

It was a multicentric, hospital-based, prospective observational study that included patients from West Bengal and the neighboring region, conducted between November 2020 and January 2023. All symptomatic post-acute COVID-19 patients aged ≥18 years who suffered from COVID-19 pneumonia and presented 4–12 weeks after recovery, attending outpatient as well as inpatient follow-up at the Department of Respiratory Medicine, Institute of Post Graduate Medical Education & Research (IPGME&R) and SSKM Hospital, and Calcutta Heart Clinic and Hospital, Kolkata, West Bengal, India, were included. IPGME&R and SSKM Hospital is a state-run academic institute as well as a tertiary care hospital, while Calcutta Heart Clinic and Hospital is a nonprofit private multispeciality hospital. Asymptomatic patients, those who were reinfected, and patients who refused to give consent were excluded.

As this was an observational study, a convenience sampling method was utilized, enrolling all eligible symptomatic patients who presented to the participating centers during the predefined study period.

Patient Flow

A total of 102 patients with persistent respiratory symptoms were initially assessed using the modified Medical Research Council (mMRC) dyspnea score and pulse oximetry. Hospitalization was considered where clinically indicated. Inflammatory parameters and radiological assessment were performed for all patients at follow-up. Functional assessment was performed using the 6-minute walk test, spirometry, and diffusing capacity for carbon monoxide (DLCO) in patients who were clinically fit to undergo these tests. However, spirometry and DLCO were predominantly performed in noncavitary cases, particularly in patients with interstitial or fibrotic lung pathology. These lung function tests were deliberately deferred in patients with cavitary lung disease because of the presence of acute, active infection and the associated risk of precipitating hemoptysis or clinical deterioration. Special investigations and interventions, including bronchoscopy and CT-guided Tru-Cut lung biopsy, were performed when clinically indicated. Treatment modalities, complications, and clinical outcomes were also recorded.

Detailed data pertaining to the acute COVID-19 period were collected retrospectively from medical records. This included demographic characteristics, presenting symptoms, comorbidities, laboratory parameters (total leukocyte count [TLC], neutrophil-to-lymphocyte ratio [NLR], C-reactive protein [CRP], and D-dimer), chest imaging findings [chest radiographs and high-resolution computed tomography (HRCT) of the chest], oxygen therapy, and respiratory support with non-invasive ventilation (NIV) or invasive positive-pressure ventilation (IPPV). Details of other treatment modalities, including corticosteroids, remdesivir, antibiotics, anticoagulation, and tocilizumab, were also recorded. All data were collected using a predesigned case record proforma and subsequently entered into a Microsoft Excel spreadsheet. The patient flow is depicted in Figure 1.

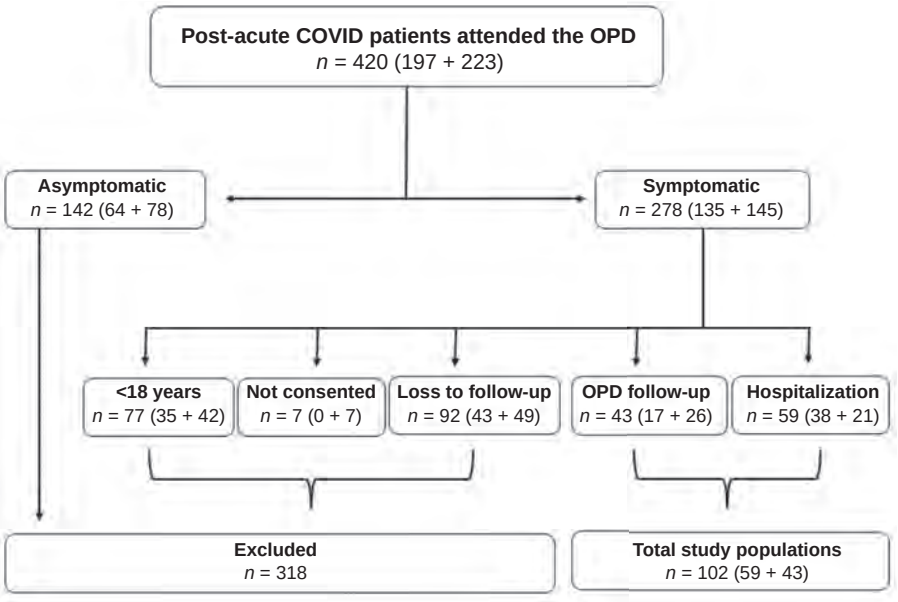


Fig. 1: Patient flow

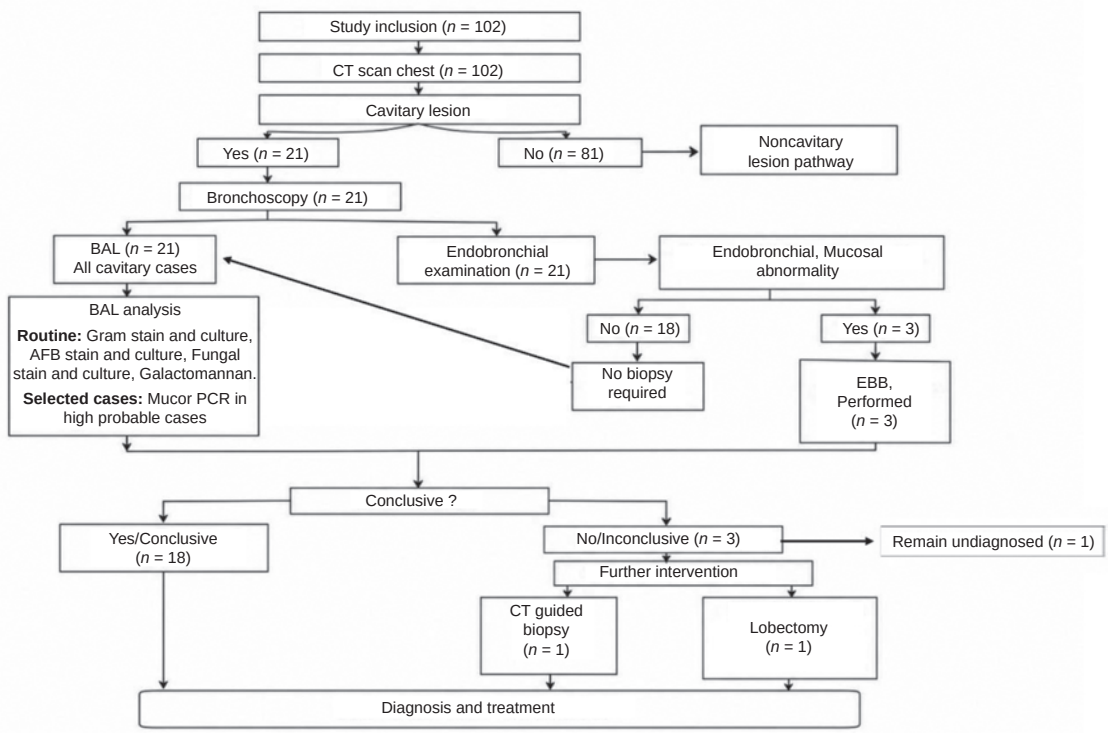


Fig. 2: Evaluation of different cavitary lung diseases

Evaluation of Cavitary Lung Disease

All patients included in the study ($n = 102$) underwent an HRCT scan of the chest. Based on the imaging results, 21 patients exhibited cavitary lesions and were subsequently subjected to bronchoscopy, while the remaining 81 patients followed a noncavitary lesion pathway. Fiberoptic bronchoscopy with BAL was performed for evaluation of all radiological cavities in 21 patients. During the bronchoscopy, a careful examination of the endobronchial tree was performed, and BAL fluid was collected from the appropriate segments in all patients. For BAL, a minimum of 60 mL of saline was used in all cases. Routine BAL analysis included a Gram stain and culture, acid-fast bacilli (AFB) smear and culture, GeneXpert Ultra (MTB and rifampicin resistance), fungal smear and culture, and galactomannan testing. In select cases with a high clinico-radiological or bronchoscopic probability of mucormycosis, a mucor polymerase chain reaction (PCR) was also performed.

Concurrently, when endobronchial examination identified endobronchial or mucosal abnormalities, an endobronchial biopsy (EBB) was also performed. A cautious approach was taken during flexible bronchoscopy while performing BAL and EBB in all patients who had hemoptysis or high clinico-radiological probability of mucormycosis or aspergillosis because of the high risk of bleeding.[12] When bronchoscopic investigations failed to confirm a diagnosis, additional investigations like CT-guided Tru-Cut biopsy or surgical excision biopsy were performed to achieve the diagnosis (Fig. 2).

Microbiological and Histopathological Evaluation

Aspergillus infections were confirmed using BAL fungal culture and/or galactomannan testing, with a BAL galactomannan cutoff of ≥1.0 optical density index (ODI).[13–15]

Mucor infections were confirmed using BAL and bronchoscopic biopsy samples for histopathology, fungal culture, and PCR. One case was diagnosed via CT-guided biopsy and another via surgical lobectomy.[15] Mucor PCR was used for rapid diagnosis and early initiation of antifungals due to the fulminant nature of pulmonary mucormycosis.

Bacterial infections were diagnosed using BAL bacterial culture, with simultaneous blood cultures in selected cases. Methicillin-resistant *Staphylococcus aureus* cavitary lung disease was diagnosed in one patient via both BAL and blood cultures. Tuberculosis was confirmed using BAL GeneXpert MTB/Rif.

Statistical Analysis

All clinical, radiological, and outcome data were initially recorded in a predesigned case record proforma and subsequently entered into a Microsoft Excel spreadsheet for data management and analysis. Descriptive statistics were employed to summarize the baseline demographic, clinical, and interventional characteristics of the study cohort. Continuous variables, such as patient age, were evaluated and expressed as means. Categorical variables, including the frequencies of specific etiologies of cavitary lung disease, preexisting comorbidities such as diabetes mellitus, prior systemic corticosteroid exposure rates, and 90-day mortality outcomes, were calculated and presented as absolute frequencies and percentages. Patients who were less than 18 years of age, asymptomatic, did not consent, or were lost to follow-up were excluded from the final analytical cohort. As this was a descriptive observational study, data analysis focused on the presentation of prevalence and clinical outcomes without complex comparative statistical hypothesis testing.

To identify potential risk factors and clinical differences, baseline characteristics, treatments, and functional assessments were compared between the cavitary ($n = 21$) and noncavitary ($n = 81$) groups. Categorical variables were analyzed using the

Table 1: Clinico-demographic features of cavitary and noncavitary groups

Variable	Cavitary group ($n = 21$)	Noncavitary group ($n = 81$)	*p*-value
Demographics			
Age (years), mean ± SD	52 ± 6.89	49.8 ± 11.95	0.277
Comorbidities, *n* (%)			
Diabetes	11 (52.4%)	44 (54.3%)	1.000
Immunosuppressant therapy	1 (4.8%)	2 (2.5%)	0.503
CKD	2 (9.5%)	4 (4.9%)	0.600
Obstructive airway disease	6 (28.6%)	24 (29.6%)	1.000
HTN	5 (23.8%)	28 (34.6%)	0.438
IHD	3 (14.3%)	11 (13.6%)	1.000
Arrhythmia	1 (4.8%)	6 (7.4%)	1.000
Chronic heart failure	1 (4.8%)	3 (3.7%)	1.000
Old CVA	2 (9.5%)	4 (4.9%)	0.600
COVID-19 severity, *n* (%)			
Mild	2 (9.5%)	11 (13.6%)	0.620
Moderate	11 (52.4%)	33 (40.7%)	0.620
Severe	8 (38.1%)	37 (45.7%)	0.620
Treatments during acute COVID, *n* (%)			
Hospitalization	16 (76.2%)	72 (88.9%)	0.157
ICU stay	14 (66.6%)	35 (43.2%)	0.055
Invasive ventilation	6 (28.5%)	12 (14.8%)	0.158
Systemic steroids	20 (95.2%)	79 (97.5%)	0.503
Remdesivir	16 (76.2%)	57 (70.4%)	0.787
Tocilizumab	10 (47.6%)	36 (44.4%)	0.811
Treatments during post-COVID, *n* (%)			
Hospitalization	10 (47.6%)	28 (34.5%)	0.287
ICU stay	6 (28.5%)	17 (20.9%)	0.548
Invasive ventilation	3 (14.2%)	9 (11.1%)	0.709
Functional assessment			
Restrictive defect in spirometry	Spirometry not done	60.0% (of 61 pts)	N/A
Obstructive defect in spirometry	Spirometry not done	12.0% (of 61 pts)	N/A
DLCO (%), mean ± SD	DLCO not done	Not done	N/A
6MWT desaturation ≥3%	18 (85.7%)	59.5% (of 74 pts)	0.037
6MWD distance (<350 m)	12 (57.1%)	29.1% (of 74 pts)	0.037

CKD, chronic kidney disease; CVA, cerebrovascular accident; DLCO, diffusing capacity for carbon monoxide; HTN, hypertension; IHD, ischemic heart disease; N/A, not available; SD, standard deviation

Chi-square or Fisher's exact test, and continuous variables were analyzed using the independent samples *t*-test or Mann–Whitney *U* test, as appropriate. A *p*-value of <0.05 was considered statistically significant.

Results

Clinical Profile

Of the 102 symptomatic post-acute COVID-19 patients evaluated, 21 (20.6%) had cavitary lung disease on HRCT chest and were included in this study. A comprehensive comparison of baseline demographics, disease severity, comorbidities, treatment modalities, and functional assessments between the cavitary ($n = 21$) and noncavitary ($n = 81$) groups is detailed in Table 1. The etiology of cavitary lung diseases is depicted in Figure 3.

The cavitary disease cohort exhibited a male predominance, with a mean age of 52 years. While functional assessments were compared between the cohorts, it is important to note that spirometry and DLCO data were largely unavailable for the cavitary group ($n = 21$) due to contraindications such as active infection and hemoptysis. There was no difference in demographics, comorbidities, or treatment received during the acute COVID phase between the cavitary and noncavitary groups (Table 1). Six-minute walk distance was significantly lower in the cavitary disease group.

Systemic corticosteroid therapy during the acute phase of COVID-19 was ubiquitous, having been administered to 98.2% of

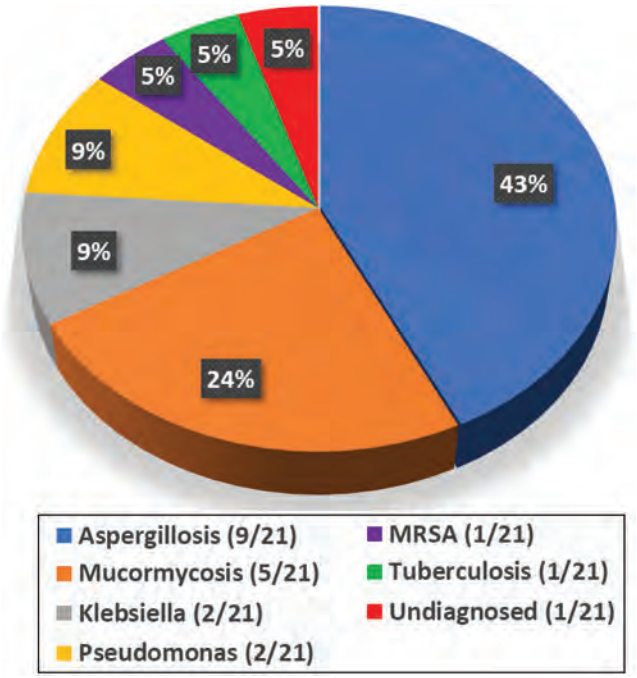


Fig. 3: Etiology of cavitary lung diseases

the affected patients. Notably, 100% of the patients diagnosed with CAPM presented with preexisting diabetes mellitus alongside prior corticosteroid exposure.

Of the 21 included patients, BAL was performed in all cases, and three patients underwent an EBB. The initial bronchoscopic evaluation and BAL analysis yielded a conclusive diagnosis for 18 of the 21 patients. The three cases that remained inconclusive required further interventions. One patient underwent a CT-guided Tru-Cut biopsy, and the other underwent a surgical lobectomy. The lobectomy was performed as a lifesaving measure due to extensive lung involvement and a high radiological probability of invasive mucormycosis, highlighted by the presence of a "bird's nest" sign. One patient refused further evaluation and remained undiagnosed (Fig. 2).

Clinical Presentation and Treatment Outcomes

CAPA

COVID-associated pulmonary aspergillosis was diagnosed in nine patients (42.85%). Patients typically presented after a median of 14 days, with cough being the predominant symptom (8/9), followed by fever (4/9). Most patients (8/9) required hospitalization during acute COVID-19 and received a median cumulative steroid dose of 450 mg over 12 days. The 90-day mortality was 0/9 (0.0%) (Table 2).

CAPM

COVID-associated pulmonary mucormycosis was diagnosed in five patients (23.8%). This group presented earliest, with a median interval of 10 days ($p = 0.08$), and had the highest steroid exposure, with a median dose of 600 mg over 14 days ($p = 0.09$). All five patients had fever and cough and had preexisting diabetes mellitus. Four out of five patients also presented with hemoptysis. The 90-day mortality was 1/5 (20.0%).

Bacterial Infections

Bacterial infections were identified in five patients who presented after a median symptom duration of 18 days. Gram-negative organisms predominated. Two patients had *Klebsiella* infections, both of which were carbapenem-resistant Enterobacteriaceae (CRE), and both improved following targeted antibiotic therapy (90-day mortality, 0/2). Two patients had *Pseudomonas* infections; one died from refractory septic shock complicated by pneumothorax (90-day mortality, 1/2). One patient with methicillin-resistant *Staphylococcus aureus* (MRSA) survived following targeted therapy (90-day mortality, 0/1).

TB and Undiagnosed Cases

Tuberculosis was confirmed in one patient by BAL GeneXpert MTB/Rif and was successfully treated (90-day mortality, 0/1). One patient remained undiagnosed and received empirical antibiotic therapy (90-day mortality, 0/1). Bronchoscopy was essential in this setting for excluding fungal and bacterial etiologies.

Radiological Features

CAPA

COVID-associated pulmonary aspergillosis was characterized by cavities with pericavitary consolidation. Multiple cavities were observed in most cases (6/9). Other prominent radiological findings included pericavitary consolidation (5/9), the halo sign (3/9), the reverse halo sign (2/9), and pneumothorax (2/9) (Fig. 4).

CAPM

All CAPM patients demonstrated multiple, necrotic, thick-walled cavities (5/5), with pericavitary consolidation present in all cases (5/5). Additional radiological features included the "bird's nest" sign (5/5), halo sign (2/5), reverse halo sign (1/5), and occasional pleural effusion (Fig. 4). Thick-walled cavities and bird's nest sign were more often observed in CAPM patients when compared to other etiologies (Table 2).

Bacterial Cavities

Bacterial cavities frequently presented as multiple cavities (3/5), which were predominantly thick-walled (3/5), with occasional air-fluid levels (1/5). *Klebsiella* infection and one *Pseudomonas* infection specifically presented with thick-walled cavities. One patient with *Pseudomonas* infection had multiple thin-walled cavities complicated by pneumothorax (1/5) and pneumomediastinum (1/5) (Fig. 4).

TB

The patient with TB demonstrated a single upper-lobe cavity with pericavitary consolidation on imaging (Fig. 4).

Bronchoscopic Findings

CAPA

Bronchoscopic airway evaluation predominantly revealed mucopurulent secretions (7/9), while purulent secretions were observed in a minority of cases (2/9) (Fig. 5).

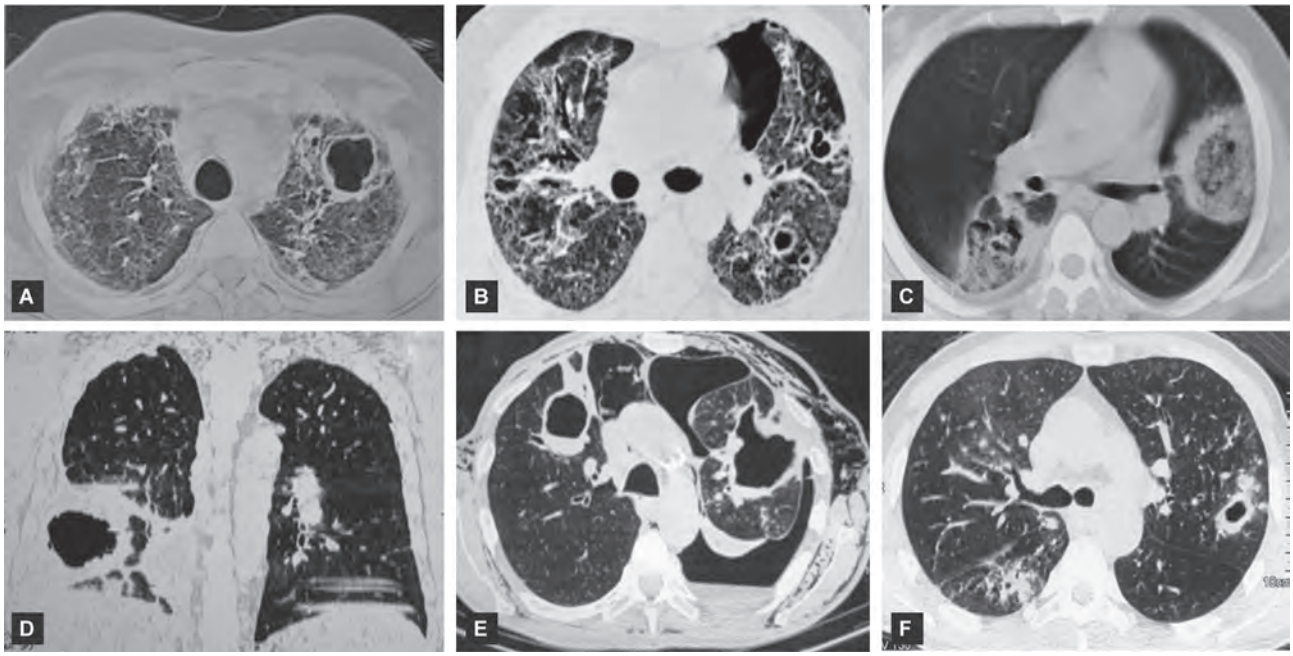
CAPM

Direct bronchoscopic visualization revealed whitish necrotic slough arising from the segmental bronchi, with sequelae of bleeding in

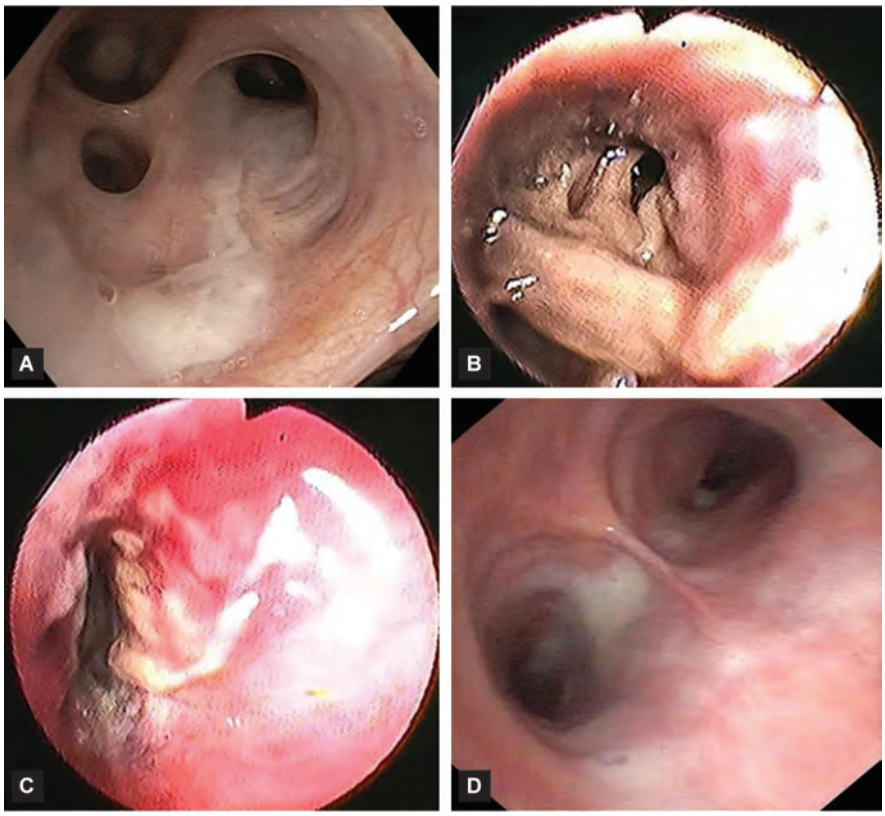
Table 2: Etiology, diagnosis, treatment, and outcomes of cavitary diseases

Variables	CAPA (*n* = 9)	CAPM (*n* = 5)	Bacterial and TB (*n* = 5+1)	*p*-value
Clinical presentation				
Fever	4/9	5/5	5/6	0.14
Cough	8/9	5/5	4/6	0.54
Dyspnea	4/9	4/5	5/6	0.63
Hemoptysis	3/9	4/5	1/6	0.29
Duration of symptoms (median, IQR)	14 days (10–18)	10 days (8–14)	19 days (16–22)	0.08
Respiratory failure	2/9	4/5	3/6	0.28
COVID severity during acute COVID				
• Mild	1/9	0/5	1/6	-
• Moderate	6/9	2/5	3/6	-
• Severe	2/9	3/5	2/6	-
Comorbidities				
Diabetes	4/9	5/5	2/6	0.28
Immunosuppressant therapy	1/9	0/5	0/6	0.61
CKD	0/9	0/5	2/6	0.16
Obstructive airway disease	2/9	2/5	2/6	0.91
HTN	3/9	1/5	1/6	0.77
IHD	2/9	1/5	0/6	0.54
Arrhythmia	1/9	0/5	0/6	0.61
Chronic heart failure	0/9	1/5	0/6	0.36
Old CVA	2/9	0/5	0/6	0.36
Treatment received during acute COVID				
Hospitalization	8/9	5/5	3/6	0.11
Steroid median cumulative dose (Prednisolone eq.)	450 mg (IQR: 300–600)	600 mg (IQR: 400–800)	270 mg (IQR: 240–360)	0.15
Steroid duration (median)	12 days (IQR: 8–16)	14 days (IQR: 10–18)	8.5days (IQR: 7–9)	0.09
Remdesivir	6/9	5/5	4/6	0.54
Tocilizumab	5/9	3/5	2/6	0.83
Radiology				
Number of cavities (multiple)	6/9	5/5	3/6	0.28
Location of cavities	Upper + middle + lower	Upper + lower	Upper + lower	Not applicable
Wall of the cavity (thick wall)	1/9	5/5	4/6	0.01
Pericavitary consolidation	5/9	5/5	2/6	0.14
Air-fluid level within cavity	0/9	0/5	1/6	0.36
Halo sign	3/9	2/5	0/6	0.29
Reverse halo sign	2/9	1/5	0/6	0.54
Bird's nest sign	0/9	5/5	0/6	<0.001
Pneumothorax	2/9	0/5	1/6	0.54
Pneumomediastinum	0/9	0/5	1/6	0.36
Pleural effusion	0/9	1/5	2/6	0.36
Bronchoscopic findings				
Type of secretions	Purulent (2/9) Mucopurulent (7/9)	Purulent (3/5) Mucopurulent (2/5)	Purulent (5/5) Mucopurulent (1/1)	Not applicable
Endobronchial/mucosal lesion	0/9	3/5	0/6	0.03
Necrotic slough	1/9	4/5	0/6	0.01
BAL performed	9/9	5/5	6/6	Not applicable
EBB performed	0/9	3/5	0/6	0.03
Outcomes				
90-day mortality	0/9 (0.0%)	1/5 (20.0%)	1/6 (16.7%)	0.45

CKD, chronic kidney disease; CVA, cerebrovascular accident; HTN, hypertension; IHD, ischemic heart disease; IQR, interquartile range; TB, tuberculosis



Figs 4A to F: HRCT findings of different cavitary lung diseases. (A) HRCT chest of CAPA showing a thin-walled empty cavity with surrounding consolidation in the left upper lobe and bilateral ground-glass opacity (GGO) with septal thickening; (B) HRCT of CAPA in another patient showing multiple bilateral cavities with surrounding GGO and septal thickening and left-sided pneumothorax; (C) HRCT chest of CAPM showing reverse halo sign with central cavitation (Bird's nest sign) at the left upper lobe and a necrotizing pneumonia in the right lower lobe superior segment with mild bilateral pleural effusion; (D) HRCT chest of cavitary disease due to *Klebsiella* showing a thick-walled hollow cavity with pericavitary consolidation; (E) HRCT chest of cavitary disease due to *Pseudomonas aeruginosa* showing multiple cavitary lesions with low air-fluid level. There is also left-sided pneumothorax and pneumomediastinum with subcutaneous emphysema; (F) HRCT chest of TB cavitary disease showing a single thick-walled cavitary lesion without air-fluid level and pericaviatary consolidation with multiple centrilobular nodules and tree-in-bud with patchy consolidation



Figs 5A to D: Bronchoscopy of different cavitary lung diseases. (A) Bronchoscopy of a CAPA showed mucopurulent secretions in the right upper lobe; (B and C) Bronchoscopy of a CAPM showed whitish necrotic slough from the segmental bronchi with sequelae of bleeding; (D) Bronchoscopy for *Pseudomonas aeruginosa* showed purulent secretions in the left main bronchus

three cases (Fig. 5). Bronchial secretions were either purulent (3/5) or mucopurulent (2/5).

Bacterial Cavities

All patients with bacterial cavities demonstrated purulent secretions on bronchoscopy (5/5) (Fig. 5D).

TB

Bronchoscopy in the patient with TB revealed mucopurulent secretions.

Despite the high-risk nature of this cohort, severe procedure-related complications were uncommon. Procedure-induced hypoxemia was the most frequently observed complication and occurred transiently in five patients overall. It was observed in 3/9 CAPA patients, 1/5 CAPM patients, and 1/5 patients with bacterial cavities. The single patient with TB did not develop hypoxemia. No procedure-related pneumothorax occurred across any of the etiological groups.

Diagnostic Confirmation

Early diagnosis using bronchoscopy and tissue sampling was essential for establishing definitive microbiological and histopathological diagnoses. These diagnostic interventions facilitated timely initiation of targeted therapy across the different etiological groups and contributed to the high overall survival rate.

CAPA

COVID-associated pulmonary aspergillosis was diagnosed using a BAL galactomannan cutoff of ≥1.0 ODI, which was positive in 8/9 patients (89%), and BAL fungal culture, which was positive in 5/9 patients (55.5%). The combined diagnostic yield was 100% (9/9) according to European Organization for Research and Treatment of Cancer/Mycoses Study Group Education and Research Consortium (EORTC/MSGERC) criteria.[14,15] However, according to disease-specific consensus criteria, all CAPA cases in this study are classified as probable CAPA because tissue biopsy was not available, as lung biopsies were not performed in these patients (Table 3).[5]

CAPM

COVID-associated pulmonary mucormycosis was diagnosed in five patients (23.8%), all of whom were classified as having proven CAPM based on histopathological confirmation of tissue invasion. Initial diagnosis was primarily established using BAL and bronchoscopic biopsy cultures, together with mucor PCR.

In three patients, EBB histopathology demonstrated aseptate fungal hyphae with tissue invasion, with corresponding positivity on biopsy culture and mucor PCR. Subsequently, one case was diagnosed by CT-guided biopsy, which demonstrated positive histopathology, culture, and PCR results; the initial BAL cultures and PCR were negative.

Another patient was confirmed following surgical lobectomy, which demonstrated positive histopathology, culture, and PCR results. This patient had severe lung involvement with a high radiological probability of mucormycosis, but BAL cultures and PCR were negative, and no visible endobronchial lesions were present for standard bronchoscopic biopsy (Table 4).

Bacterial Infections

Bacterial infections resulting in cavity formation were diagnosed by targeted microbiological investigations. *Klebsiella* (CRE) accounted for two cases, representing 9.5% of the total cohort, and was diagnosed using BAL bacterial culture. Similarly, *Pseudomonas* accounted for two cases (9.5%) and was diagnosed by BAL bacterial culture. Methicillin-resistant *Staphylococcus aureus* accounted for one case (4.8%) and was diagnosed using a combination of BAL and blood cultures.

TB

Tuberculosis was confirmed by BAL GeneXpert MTB/Rif.

Treatment

For primary therapy, all nine CAPA patients were initiated on voriconazole, with one later switching to amphotericin B, while all five CAPM patients received intravenous liposomal amphotericin B. The bacterial and TB group received targeted antibiotics or anti-tubercular therapy. Dosing regimens varied accordingly,

Table 3: Diagnostic confirmation of CAPA by different interventions

Diagnostics	CAPA ($n = 9$)	Percentage
BAL galactomannan ≥1.0 ODI positive	8/9	89%
BAL fungal culture positive	5/9	55.5%
Combined BAL (galactomannan + culture)	9/9	100%
Biopsy confirmation	0/9	0%

BAL, bronchoalveolar lavage; ODI, optical density index

Table 4: Diagnostic confirmation of CAPM by different interventions

Diagnostic modality	Number of CAPM ($n = 5$)	Diagnostic basis and findings	Additive and cumulative diagnostic yield
Bronchoscopy (BAL and EBB)	3/5	EBB histopathology demonstrated aseptate fungal hyphae with tissue invasion, alongside positive biopsy culture and mucor PCR	Primary diagnostic yield of 60% (3/5 CAPM cases)
CT-guided Tru-Cut biopsy	1/5	Confirmed via biopsy histopathology, culture, and PCR positivity after initial BAL results were negative	Additive diagnostic yield of 20% (1/5 CAPM cases)
Surgical resection (lobectomy)	1/5	Confirmed via lobectomy HPE, culture, and PCR positivity due to severe lung involvement and negative initial BAL/PCR	Additive diagnostic yield of 20%, achieving a 100% cumulative yield for the CAPM cohort

BAL, bronchoalveolar lavage; CAPM, COVID-associated pulmonary mucormycosis; HPE, histopathological examination; EBB, endobronchial biopsy; PCR, polymerase chain reaction

featuring a step-down schedule of voriconazole starting at 6 mg/kg every 12 hours for CAPA, renal-adjusted intravenous liposomal amphotericin B dosing of 3–5 mg/kg/day for CAPM, and culture-guided regimens were used for the bacterial cohort. Weight-band-based Isoniazid, Rifampicin, Pyrazinamide, Ethambutol (HRZE) was used for the treatment of one TB patient. Surgical intervention via lobectomy was performed in two out of five CAPM patients.

Overall Outcomes

In total, 19 out of 21 patients survived with appropriate therapy, resulting in an overall 90-day mortality rate of (2/21) 9.5%. The two fatalities were attributed to CAPM and *Pseudomonas* refractory sepsis, respectively (Table 2).

Discussion

In this prospective multicentric study, 21 of 102 symptomatic post-acute COronaVIrus Disease (COVID-19) patients (20.6%) developed cavitary lung disease. Fungal infection was the predominant etiology, accounting for 14 cases (66.7%). COVID-associated pulmonary aspergillosis was diagnosed in nine patients and CAPM in five. Bacterial infection accounted for five cases, while one patient had TB and one remained undiagnosed. Thus, fungal infection was the leading cause of post-COVID cavitary disease in our cohort. Radiology alone was insufficient to establish the etiology. Lower respiratory tract sampling and, in selected cases, tissue diagnosis were required.

Our study differs from most published Indian studies because it specifically evaluated cavitary disease in the post-acute COVID period. All 21 patients underwent bronchoscopy with BAL. Bronchoscopic biopsy, CT-guided Tru-Cut biopsy, or surgical resection was performed when required. This provided a systematic diagnostic pathway for fungal, bacterial, and mycobacterial causes.

COVID-associated pulmonary aspergillosis was identified in nine of the 21 patients with cavitary disease, and 88.8% received corticosteroids during acute COVID disease. An Indian study by Moni et al. reported 95 CAPA cases, with 88.4% having moderate-to-severe COVID-19 and 78.9% receiving corticosteroids. COVID-associated pulmonary aspergillosis was associated with increased mechanical ventilation and longer intensive care unit (ICU) and hospital stays. Their findings were corroborative of our study.[16]

In our study, all nine CAPA cases were diagnosed using BAL fungal culture and/or BAL galactomannan, with a BAL galactomannan cutoff of ≥1.0 ODI. This supports the role of BAL in establishing a microbiological diagnosis when imaging is suggestive but nonspecific. The ECMM/ISHAM criteria also recognize BAL culture and BAL galactomannan as important diagnostic tools for CAPA.[5]

More recent Indian data from Moni et al. further identified lymphopenia, host factors, and broad-spectrum antibiotic exposure as predictors of CAPA. COVID-associated pulmonary aspergillosis was also associated with increased mortality and ICU escalation.[17] Our study was not designed to assess predictors of CAPA. However, the identification of nine CAPA cases among patients with post-COVID cavitary disease supports targeted fungal evaluation in this setting.

COVID-associated pulmonary mucormycosis was diagnosed in five patients in our cohort, all of whom had diabetes and prior corticosteroid exposure, echoing the Indian multicenter findings of Patel et al.[10] This pattern closely mirrors broader multisite studies by other investigators showing that uncontrolled diabetes and glucocorticoid therapy serve as primary underlying risk factors.[10,18,19] Although work by Jeong et al. highlights these variables as strong individual drivers of the disease, evaluating them independently was difficult in our group because nearly all patients (98%) received systemic corticosteroids. Consequently, our findings demonstrate a clear clinical association with these predisposing conditions rather than proving direct causality.

Our study also adds to the emerging Indian literature on pulmonary mucormycosis. A recent multicenter Indian study reported 122 cases of COVID-CAPM and found diabetes, glucocorticoid exposure, and COVID-related hypoxemia among important risk factors. The reported 12-week mortality was 52.3%, and surgery was associated with improved survival.[7] In our study, CAPM involved only five patients, with a 90-day mortality of 1/5 (20%). Two patients required surgical lobectomy. The difference in mortality should be interpreted cautiously because of our small sample size and differences in patient characteristics and clinical setting.

The bronchoscopic and radiological findings in our CAPM patients further support tissue-based diagnosis. Necrotic thick-walled cavities and the bird's nest sign were observed radiologically. Bronchoscopy demonstrated whitish necrotic endobronchial tissue in affected patients. These findings are consistent with the Indian Delphi consensus on COVID-CAPM. The consensus also supports early bronchoscopy and CT-guided Tru-Cut biopsy when required.[7]

A major finding of our study was the value of an interventional diagnostic approach. All 21 patients underwent bronchoscopy with BAL. Bronchoscopic biopsy was required in three patients with visible endobronchial abnormalities. Computed tomography–guided Tru-Cut biopsy and surgical resection were used when bronchoscopy was inconclusive despite high clinical or radiological suspicion. This approach was particularly useful for diagnosing mucormycosis and obtaining tissue confirmation.

Bacterial infection was identified in five patients. Gram-negative organisms predominated, including *Klebsiella* and *Pseudomonas*, with one case of MRSA. One patient had pulmonary TB. These findings emphasize that post-COVID cavitation should not automatically be attributed to fungal infection. Comprehensive BAL evaluation can help distinguish fungal, bacterial, and mycobacterial causes and guide targeted treatment.

Overall, 19 of 21 patients survived, giving a 90-day mortality of 9.5%. COVID-associated pulmonary aspergillosis had a 90-day mortality of 0/9 (0%), whereas CAPM had a mortality of 1/5 (20%). The bacterial group accounted for the remaining death. Although the numbers are small, the favorable overall outcome may reflect early microbiological diagnosis and targeted treatment, with surgery when indicated. However, the observational design does not allow a causal relationship between the diagnostic strategy and outcome to be established.

Our findings extend the Indian literature in two important ways. First, they demonstrate that CAPA and CAPM were the predominant causes of post-COVID cavitary lung disease in our cohort. Second, they highlight the value of a structured interventional diagnostic pathway in the post-acute setting. Unlike studies focused mainly on acute COVID-19 or broader COVID-19-Associated Mucormycosis (CAM) syndromes, our study specifically addresses cavitary disease in a post-COVID scenario and integrates bronchoscopy, BAL, tissue sampling, CT-guided biopsy, and surgery.

The primary strengths of this study lie in its prospective, multicentric design and the systematic application of interventional

pulmonology. By utilizing BAL, bronchoscopic and CT-guided biopsies, and surgical specimens, we achieved comprehensive microbiological and histopathological confirmation. This allowed for the accurate differentiation of fungal, bacterial, and mycobacterial etiologies, highlighting the real-world clinical value of rigorous diagnostic pathways in post-acute COVID-19 settings.

However, our study has certain limitations. The relatively small sample size of patients with cavitary disease restricts robust statistical analysis and the evaluation of independent risk factors. In addition, reliance on limited tissue samples due to procedural risks may have affected pathogen detection in select cases. An additional clinical limitation of our study was the inability to perform comprehensive pulmonary function testing (spirometry and DLCO) on patients with cavitary disease. Because these patients presented with acute infections and occasional hemoptysis, forced expiratory maneuvers were contraindicated. Consequently, our functional data predominantly reflect the outcomes of the noncavitary group with interstitial or fibrotic sequelae. Finally, because the study was conducted at tertiary care centers with specialized procedural expertise, the findings may have limited generalizability to resource-constrained, lower-tier facilities. Despite these limitations, our results provide valuable clinical insights, strongly advocating for early, lower respiratory tract sampling in post-COVID patients presenting with cavitary lesions, particularly those with preexisting diabetes and a history of corticosteroid exposure.

Conclusion

Different interventional procedures were a cornerstone in diagnosing the cavitary lung lesions encountered during the COVID era, which complicated the clinical course and prognosis. Identifying the etiology and risk factors is key to managing such cases. This study observed that cavitary lung disease emerged as a significant complication in approximately 21% of the symptomatic post-acute COVID patients evaluated, predominantly due to fungal infections. Bronchoscopic sampling, CT-guided Tru-Cut, or surgical excision biopsy facilitated timely and accurate diagnoses and helped in improving patient outcomes.

Clinical Significance

Cavitary lung disease is a significant post-acute COVID complication frequently driven by opportunistic fungal infections, especially in patients exposed to corticosteroids. Early microbiological confirmation is essential because imaging and routine cultures alone are often non-diagnostic. Interventional procedures such as bronchoscopy, BAL, EBB, CT-guided biopsy, and surgical sampling markedly enhance diagnostic accuracy and facilitate prompt, targeted therapy. Identifying high-risk groups—particularly diabetics receiving steroids—supports earlier investigation and can substantially improve outcomes. This study reinforces the need for vigilant evaluation of persistent respiratory symptoms in the post-COVID period.

Ethical Approval

It was approved by the IPGME&R Institutional Ethics Committee (IPGME&R/IEC/2021/088).

Data Availability Declaration

The data supporting the findings of this study are available from the corresponding author upon reasonable request.

Artificial Intelligence (AI) Disclosure

ChatGPT (OpenAI) was used solely for language editing, grammatical correction, and improvement of the clarity and readability of the manuscript. The authors independently conducted the study, collected and analyzed the data, interpreted the findings, and take full responsibility for the accuracy, integrity, and final content of the manuscript.

Acknowledgments

Not applicable.

Authors' Contributions

Dr Sreetama Bandyopadhyay contributed to data curation, formal analysis, investigation, resources, and software. Dr Chandan Kumar Shit was involved in investigation, writing the original draft, and review and editing of the manuscript. Dr Surajit Chatterjee contributed to project administration. Dr Subhankar Chatterjee was responsible for methodology and supervision. Dr Biplab Chandra contributed to validation and visualization. Dr Amitabha Sengupta was responsible for conceptualization of the study.

Orcid

Sreetama Bandyopadhyay https://orcid.org/0009-0007-4641-4806
Chandan Kumar Shit https://orcid.org/0000-0002-4173-2377
Surajit Chatterjee https://orcid.org/0000-0002-3908-5254

References

1. Shah W, Hillman T, Playford E, et al. Managing the long-term effects of COVID-19: Summary of NICE, SIGN, and RCGP rapid guideline. BMJ. 2021;372:n136. DOI: 10.1136/bmj.n136.
2. Huang C, Wang Y, Li X, et al. Clinical features of patients infected with 2019 novel coronavirus in Wuhan, China. Lancet. 2020;395:497–506. DOI: 10.1016/S0140-6736(20)30183-5.
3. Zhao Y, Yang C, An X, et al. Follow-up study on COVID-19 survivors one year after discharge from hospital. Int J Infect Dis. 2021;112:173–182. DOI: 10.1016/j.ijid.2021.09.017.
4. Chong WH, Saha BK, Ramani A, et al. State-of-the-art review of secondary pulmonary infections in patients with COVID-19 pneumonia. Infection. 2021;49:591–605. DOI: 10.1007/s15010-021-01602-z.
5. Koehler P, Bassetti M, Chakraborty A, et al. Defining and managing COVID-19-associated pulmonary aspergillosis: 2020 ECMM/ISHAM consensus criteria. Lancet Infect Dis. 2021;21(6):e149–e162. DOI: 10.1016/S1473-3099(20)30847-1.
6. Garg B, Jindal N. A Pulmonologist Perspective in Post-COVID-19 Fungal Lung Infection. Indian J Chest Dis Allied Sci 2024;66(1):57–60.
7. Muthu V, Agarwal R, Patel A, et al. Definition, diagnosis, and management of COVID-19-associated pulmonary mucormycosis: Delphi consensus statement from the Fungal Infection Study Forum and Academy of Pulmonary Sciences, India. Lancet Infect Dis. 2022;22(9):e240–e253. DOI: 10.1016/S1473-3099(22)00124-4.
8. RECOVERY Collaborative Group. Dexamethasone in hospitalized patients with Covid-19. N Engl J Med. 2021;384:693–704. DOI: 10.1056/NEJMoa2021436.
9. Wauters J, Baar I, Meersseman P, et al. Invasive pulmonary aspergillosis is a frequent complication of critically ill H1N1 patients: A retrospective study. Intensive Care Med. 2012;38:1761–1768. DOI: 10.1007/s00134-012-2673-2.
10. Patel A, Agarwal R, Rudramurthy SM, et al. Multicenter epidemiologic study of coronavirus disease–associated mucormycosis, India. Emerg Infect Dis. 2021;27(9):2349–2359. DOI: 10.3201/eid2709.210934.

11. Zhu X, Ge Y, Wu T, et al. Co-infection with respiratory pathogens among COVID-2019 cases. Virus Res. 2020;285:198005. DOI: 10.1016/j.virusres.2020.198005.
12. Muthu V, Gandra RR, Dhooria S, et al. Role of flexible bronchoscopy in the diagnosis of invasive fungal infections. Mycoses. 2021;64:668–677. DOI: 10.1111/myc.13263.
13. Kariyawasam RM, Dingle TC, Kula BE, et al. Defining COVID-19-associated pulmonary aspergillosis: Systematic review and meta-analysis. Clin Microbiol Infect. 2022;28(7):920–927. DOI: 10.1016/j.cmi.2022.01.027.
14. Donnelly JP, Chen SC, Kauffman CA, et al. Revision and update of the consensus definitions of invasive fungal disease from the EORTC/MSGERC. Clin Infect Dis. 2020;71(6):1367–1376. DOI: 10.1093/cid/ciz1008.
15. Zou M, Tang L, Zhao S, et al. Systematic review and meta-analysis of detecting galactomannan in bronchoalveolar lavage fluid for diagnosing invasive aspergillosis. PLoS One. 2012;7(8):e43347. DOI: 10.1371/journal.pone.0043347.
16. Moni M, John TMM, Moosa AR, et al. Risk factors of COVID-19 associated pulmonary aspergillosis in a high endemic setting and development of a bedside clinical risk prediction score. Open Forum Infect Dis 2022;9(Suppl 2):ofac492.372. DOI: 10.1093/ofid/ofac492.372.
17. Moni M, Sathyapalan DT, Edathadathil F, et al. Predicting COVID-19-associated pulmonary aspergillosis risk in low- and middle-income countries: A matched case-control study. Open Forum Infect Dis 2024;11(7):ofae406. DOI: 10.1093/ofid/ofae406.
18. Gupta R, Kesavadev J, Krishnan G, et al. COVID-19 associated mucormycosis: A descriptive multisite study from India. Diabetes Metab Syndr 2021;15(6):102322. DOI: 10.1016/j.dsx.2021.102322.
19. Patel AK, Bakshi H, Shah K, et al. Risk factors for COVID-19 associated mucormycosis in India: A case control study. Med Mycol 2022;60(7):myac044. PMID: 35709394.

CASE REPORT

The Benign Imposter: When Cancer is not the Answer

Manu Chopra[1], Siddhartha Chakraborty[2], Prerna Guleria[3], Rahul Tyagi[4], Kislay Kishore[5], Aseem Yadav[6], Srishti Tripathi[7]

Received on: 27 June 2026; *Accepted on:* 20 August 2026; *Published on:* 26 September 2026

Abstract

A 43-year-old man presented with cough, fever, and unintentional weight loss of 3 months' duration, raising suspicion of pulmonary infection or malignancy. Contrast-enhanced computed tomography (CECT) of the chest revealed a mass causing complete occlusion of the right upper lobe (RUL) bronchus. Initial endobronchial biopsy (EBB) was inconclusive but raised concern for lung cancer. To obtain a definitive diagnosis, intralesional cryobiopsy was performed via flexible bronchoscopy under conscious sedation using intravenous midazolam and fentanyl with continuous cardiopulmonary monitoring, after creating a controlled access tunnel into the lesion using a monopolar electrocautery probe. Histopathological examination (HPE) confirmed the diagnosis of an endobronchial leiomyoma, a rare benign tumor of smooth muscle origin. The patient subsequently underwent therapeutic bronchoscopic management using a flexible bronchoscope under conscious sedation, employing cryotherapy-based endobronchial ablation combined with electrocautery for devitalization of the tumor base. Treatment was delivered over six sessions performed over several days, resulting in restoration of airway patency and avoidance of surgical resection. This case highlights the diagnostic value of cryobiopsy in submucosal endobronchial lesions and demonstrates that advanced therapeutic bronchoscopy can provide an effective lung-preserving treatment option for selected patients with benign airway tumors when performed in experienced centers with appropriate airway backup.

Keywords: Benign airway tumors, Bronchoscopy, Case report, Cryoablation, Cryobiopsy, Leiomyoma.

Annals of Interventional Pulmonology (2026): 10.5005/annalsofip-11045-0051

Introduction

Endobronchial leiomyomas are rare benign tumors originating from smooth muscle cells of the bronchial tree. They may pose a diagnostic challenge by mimicking malignant or other benign endobronchial lesions such as carcinoid, fibroma, and hamartoma. Conventional endobronchial biopsy (EBB) may occasionally be non-diagnostic, particularly in lesions with a submucosal component where superficial sampling yields inadequate tissue. In such situations, cryobiopsy can facilitate deeper core tissue sampling with improved preservation of histological architecture. In addition, advances in therapeutic bronchoscopy have enabled minimally invasive endobronchial treatment options that allow airway recanalization while preserving lung parenchyma. We present a rare case of endobronchial leiomyoma that remained undiagnosed despite multiple endobronchial biopsies and was ultimately diagnosed using cryobiopsy, followed by successful bronchoscopic therapy.

[1,2,4–7]Department of Respiratory Medicine, Army Institute of Cardiothoracic Sciences, Pune, Maharashtra, India

[3]Department of Pathology, Armed Forces Medical College, Pune, Maharashtra, India

Corresponding Author: Manu Chopra, Department of Respiratory Medicine, Army Institute of Cardiothoracic Sciences, Pune, Maharashtra, India, Phone: +91 9199881977, e-mail: drmanuchopra@gmail.com

How to cite this article: Chopra M, Chakraborty S, Guleria P, *et al*. The Benign Imposter: When Cancer is not the Answer. Ann Interv Pulmonol 2026;2(2):86–89.

Source of support: Nil

Conflict of interest: None

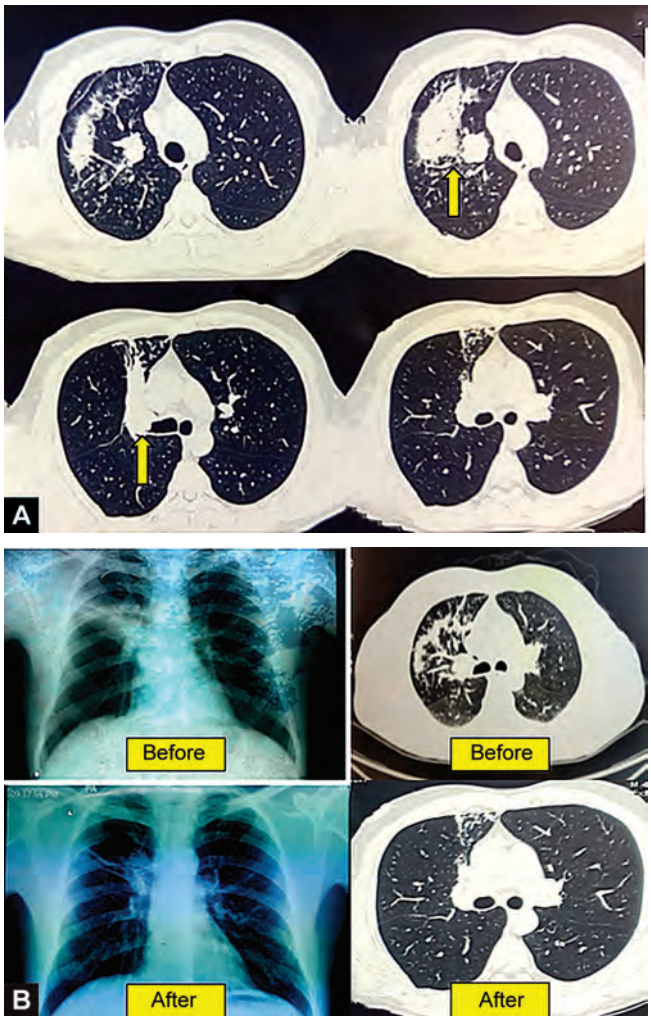
Patient consent statement: The author(s) have obtained written informed consent from the patient for publication of the case report details and related images.

Case Description

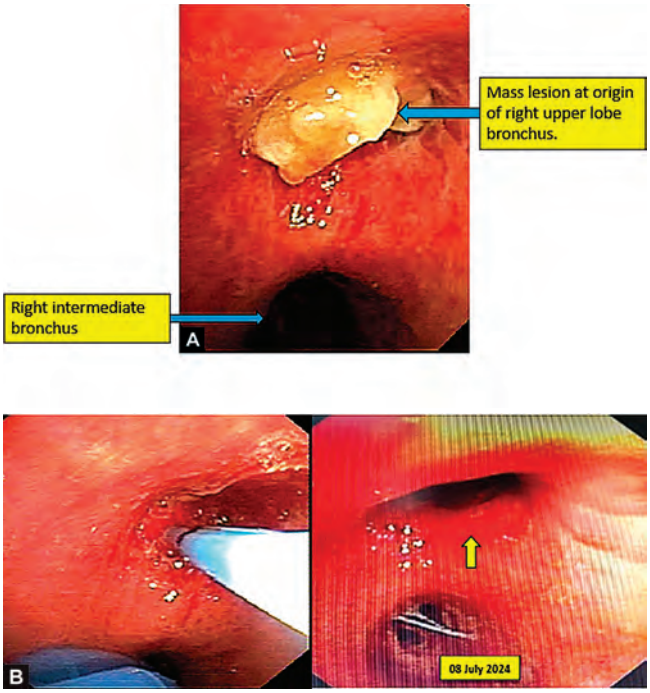
A 43-year-old male, lifetime nonsmoker, with no prior comorbidities, presented with fever and cough of 15 days' duration along with unintentional weight loss of 5 kg over 3 months. On examination, a monophonic wheeze was heard over the right infraclavicular area. Chest radiograph revealed nonhomogeneous opacities in the right upper zone. Further evaluation with contrast-enhanced computed tomography (CECT) of the chest revealed a well-defined lobulated mass lesion measuring 30 × 22 × 30 mm at the origin of the segmental bronchi of the right upper lobe (RUL), causing occlusion of the anterior, posterior, and apical segmental bronchi (Fig. 1A). There was subsegmental atelectasis and consolidation in the anterior segment of the right upper lobe with foci of calcification. The lesion did not infiltrate adjacent mediastinal structures. There were multiple subcentimetric mediastinal lymph nodes, the largest being at the subcarinal level. Whole-body positron emission tomography-computed tomography scan (PET-CT) showed a low-grade fluorodeoxyglucose (FDG) avid soft tissue density lesion measuring 21 × 27 × 38 mm with spiculated margins at the right suprahilar region (SUV max 2.63). His sputum investigations for Gram stain, pyogenic culture, and Ziehl-Neelsen (ZN) stain were negative.

He underwent flexible bronchoscopy, which revealed a wide-based, smooth lobular mass in the right upper lobe bronchus, almost completely occluding it (Fig. 2A). Endobronchial biopsy for HPE was inconclusive. Endobronchial ultrasound-guided transbronchial needle aspiration (EBUS-TBNA) from station 7 lymph nodes was also inconclusive. He underwent a repeat EBB, which was inconclusive, leading to a diagnostic dilemma. Block reviews were done at a tertiary care center, and a diagnosis of malignancy

© The Author(s). 2026 Open Access. This article is distributed under the terms of the Creative Commons Attribution-NonCommercial 4.0 International License (https://creativecommons.org/licenses/by-nc/4.0/). This license permits non-commercial use, distribution, and reproduction in any medium, provided the original author and source are credited, a link to the license is included, and any changes are indicated.



Figs 1A and B: (A) Lung window CT Chest showing endobronchial mass at origin of RUL bronchus; (B) Follow-up chest X-ray and CT showing resolution after therapy



Figs 2A and B: (A) Initial bronchoscopy showing mass occluding RUL bronchus; (B) Follow-up bronchoscopy showing restored RUL segmental openings

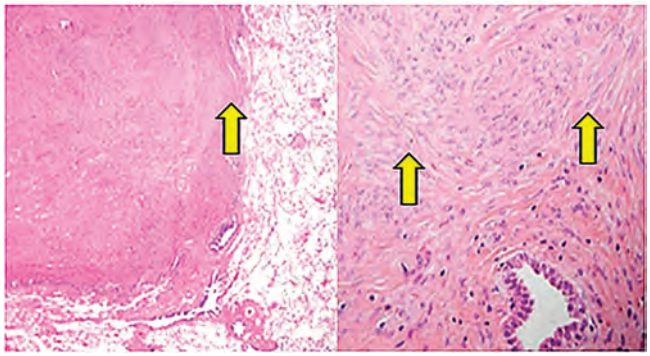


Fig. 3: Histopathology showing spindle cells with blunt nuclei consistent with leiomyoma

was suspected. A multidisciplinary discussion was held, and given the slow-growing tumor with low FDG avidity and no conclusive evidence of malignancy on HPE, initially, a diagnosis of carcinoid was considered. He underwent a Gallium-68 1,4,7,10-tetra-azacyclododecane-1,4,7,10-tetra-acetic acid-1-Nal-octreotide scan (Ga-68 DOTANOC scan), which was negative.

In view of repeated inconclusive superficial biopsies, a controlled 5 mm deep tunnel was created using monopolar electrocautery to access the submucosal core of the lesion, as the tumor appeared predominantly subepithelial. Cryobiopsy was performed using a 1.7 mm cryoprobe under conscious sedation with intravenous midazolam and fentanyl. Continuous ECG, pulse oximetry, and blood pressure monitoring were maintained. In anticipation of possible complications, the option of rigid bronchoscopy under general anesthesia was kept immediately available as a backup airway control strategy. The procedure was performed via the nasal route using a flexible bronchoscope without any conduit or Laryngeal Mask Airway. Approximately 10 mL of bleeding occurred during cryobiopsy, which was mild and self-limited. Bleeding was controlled using suction and topical measures. Topical adrenaline, cold saline, electrocautery, and rigid bronchoscopy were kept ready. Histopathological examination revealed a spindle-cell lesion composed of cells arranged in sheets and fascicles with elongated nuclei having blunt ends, suggestive of leiomyoma (Fig. 3). Immunohistochemistry demonstrated positivity for smooth muscle actin and desmin, confirming the diagnosis.

As the patient declined surgical resection but remained symptomatic, therapeutic bronchoscopy was planned. Cryotherapy was applied using repeated freeze–thaw cycles (cryoablation) to induce tumor necrosis rather than mechanical extraction. Each session lasted approximately 30 minutes and was performed at 3-day intervals to allow clearance of sloughed necrotic tissue. A total of six cryoablation sessions were performed. Monopolar electrocautery was additionally used to devitalize the tumor base and achieve hemostasis; a snare was not used. He showed radiological resolution (Fig. 1B), and follow-up bronchoscopy at 1 month showed near-complete resolution of the lesion with restoration of the right upper lobe segmental openings (Fig. 2B).

The patient has remained asymptomatic during 2 years of follow-up, with no radiological evidence of recurrence. The patient continues to remain under periodic surveillance.

Discussion

Primary endobronchial leiomyoma is an uncommon benign tumor, although an increasing number of cases have been reported in the literature in recent years.[1] The condition was first described by Forkel in 1909.[2] Leiomyomas are benign neoplasms arising from smooth muscle cells of the mesenchymal layer, including those of the bronchioles and vascular structures. While these tumors are commonly encountered in the uterus, their occurrence in extrauterine sites such as the respiratory tract is extremely rare. Pulmonary leiomyomas account for <2% of benign lung tumors, of which approximately 33–45% are reported to be endobronchial, around 50% intrapulmonary, and about 16% tracheal.[1,3–5] Endobronchial leiomyomas are generally reported to show a female preponderance; however, some studies suggest that they may occur in young to middle-aged individuals without a clear sex predilection.[6,7] Because these tumors are rare and often present with non-specific symptoms, diagnosis may be delayed or initially mistaken for malignant airway lesions.

Clinical presentation depends on tumor location, size, and the degree of airway obstruction. Patients may present with cough, breathlessness, wheezing, recurrent pneumonia, or hemoptysis. In some cases, symptoms may mimic bronchial asthma; however, the presence of a localized monophonic wheeze should raise suspicion of an alternative endobronchial pathology.[8] Endobronchial leiomyomas are typically described as smooth, round, oval, or lobulated lesions with a broad base on bronchoscopic examination.

Radiological findings are often non-specific, and imaging alone rarely establishes the diagnosis. Findings may range from normal imaging to features such as atelectasis, solitary pulmonary nodules, obstructive pneumonitis, or unilateral hyperinflation resulting from airway obstruction.[7] Calcification within the lesion is extremely uncommon, with only a few cases reported in the literature, as was seen in the present case, further complicating the diagnostic evaluation.[9,10] In addition, increased FDG uptake on PET-CT has occasionally been reported in benign leiomyomas, potentially mimicking malignant lesions.[11]

In our patient, the FDG uptake was low; however, initial histopathological evaluation raised suspicion of malignancy, resulting in a diagnostic dilemma. Multiple conventional endobronchial biopsies were inconclusive, likely due to the predominantly submucosal nature of the lesion. In such situations, cryobiopsy can provide larger and deeper tissue samples with better preservation of histological architecture and minimal crush artefact, thereby improving diagnostic yield compared with conventional forceps biopsy.[12–15] The use of cryobiopsy in this case enabled adequate tissue acquisition and facilitated definitive diagnosis. To the best of our knowledge, this represents one of the few reported cases of endobronchial leiomyoma in a male patient diagnosed using cryobiopsy. This case therefore highlights the potential role of cryobiopsy in establishing a definitive diagnosis in submucosal endobronchial lesions when conventional superficial biopsies remain inconclusive, while simultaneously demonstrating the feasibility of bronchoscopic therapy as a lung-preserving management strategy.

On HPE, leiomyomas are characterized by intersecting bundles of spindle-shaped cells with elongated nuclei and minimal mitotic activity. Immunohistochemical staining typically demonstrates positivity for smooth muscle markers such as smooth muscle actin and desmin, which helps differentiate leiomyoma from other spindle-cell tumors including fibroma, neurofibroma, and schwannoma.[3]

Traditionally, surgical resection—such as lobectomy, sleeve resection, and pneumonectomy was considered the standard treatment for these tumors, particularly in cases with significant airway obstruction.[3,16] However, advances in interventional pulmonology have enabled minimally invasive bronchoscopic treatment modalities, including electrocautery, laser therapy, cryotherapy, and argon plasma coagulation.[3,17] These approaches can restore airway patency while preserving lung parenchyma in selected patients where the tumor is entirely endo-luminal.

In the present case, therapeutic bronchoscopy using cryoablation combined with electrocautery resulted in substantial tumor devitalization and restoration of airway patency, thereby avoiding surgical resection. Such bronchoscopic interventions may therefore serve as effective lung-preserving therapeutic options in appropriately selected patients.

However, therapeutic airway procedures performed under conscious sedation should be undertaken only in experienced centers with immediate availability of rigid bronchoscopy and facilities for general anesthesia. Careful patient selection is essential, particularly in cases where the tumor appears highly vascular, shows evidence of vascular invasion, or has significant extraluminal extension. In our patient, the lesion was predominantly endoluminal without radiological evidence of vascular invasion, and the procedure was associated with minimal bleeding. This case highlights the dual role of advanced bronchoscopic techniques in both establishing a definitive diagnosis and providing effective lung-preserving treatment for selected benign endobronchial tumors.

Limitation(s)

This report is limited by its single-case design, which precludes generalization of the diagnostic and therapeutic approach to all endobronchial leiomyomas. Therapeutic airway procedures such as cryotherapy and electrocautery performed under conscious sedation should be undertaken only in experienced centers with immediate availability of rigid bronchoscopy and facilities for general anesthesia. The cryoablation protocol in managing this case was based on clinical judgement and the optimal duration and number of sessions remains undefined. Additionally, as the tumor was devitalized *in situ* rather than surgically excised, complete histological clearance could not be confirmed on a resected specimen and long-term recurrence beyond the 2 year follow up period cannot be entirely excluded.

Clinical Significance

This case highlights cryobiopsy as a valuable diagnostic adjunct in submucosal endobronchial lesions where conventional forceps biopsy is repeatedly non-diagnostic, potentially reducing diagnostic delay and the need for more invasive procedures. It further demonstrates that cryoablation combined with electrocautery can serve as an effective lung –parenchyma preserving alternative to surgical resection in select patient group. Finally, it reinforces the value of maintaining strong clinical suspicion for endobronchial pathology in patients with localized monophonic wheeze to avoid misdiagnosis.

Ethical Approval

Not applicable as this is a single case report. Consent was obtained from patient as per guidelines.

Data Availability Declaration

The data supporting the findings of this case report are included within the article. Additional de-identified data are available from the corresponding author upon reasonable request.

Artificial Intelligence (AI) Disclosure

No generative AI tools were used for this manuscript.

Acknowledgment

The authors would like to acknowledge the technicians and support staff of Department of Respiratory Medicine, AICTS, Pune, who played a valuable role during the procedures.

Authors' Contribution

Manu Chopra conceptualized and performed the bronchoscopic procedures. Siddhartha Chakraborty and Srishti Tripathi contributed to manuscript writing and data collection. Rahul Tyagi, Kislay Kishore and Aseem Yadav contributed to procedural assistance and critical review. Prerna Guleria contributed to histopathological interpretation and image acquisition. All authors reviewed and approved the final manuscript.

Conclusion

Endobronchial leiomyomas are rare benign tumors that can closely mimic malignant airway lesions both clinically and radiologically. Cryobiopsy may play an important role in the diagnostic evaluation of such lesions when conventional forceps biopsy is non-diagnostic. In selected patients, bronchoscopic therapy using cryoablation and electrocautery can serve as an effective lung-preserving treatment option when performed in experienced centers with appropriate airway backup.

Orcid

Manu Chopra https://orcid.org/0000-0001-7596-7564
Siddhartha Chakraborty https://orcid.org/0009-0005-0824-5250
Kislay Kishore https://orcid.org/0009-0003-6628-0332
Aseem Yadav https://orcid.org/0000-0001-8176-2709
Srishti Tripathi https://orcid.org/0000-0002-5507-1485

References

1. Sharifi N, Massoum SHF, Shahri MK, et al. Endobronchial leiomyoma: Report of a case successfully treated by bronchoscopic resection. J Res Med Sci 2010;15(6):364–370. PMID: 21526110.
2. Forkel W. Ein Fall von Fibromyom der Lunge. Z Krebsforsch 1909;8(2):390–393. DOI: 10.1007/BF02015238.
3. Bawaadam H, Ivanick N, AlShelli I, et al. Endobronchial leiomyoma: A case report with cryoprobe extraction and review of literature. Respir Med Case Rep 2021;33:101467. DOI: 10.1016/j.rmcr.2021.101467.
4. Wu P, Venkatachalam J, Lee VKM, et al. Primary pulmonary leiomyoma. Respirol Case Rep 2016;4(3):e00153. DOI: 10.1002/rcr2.153.
5. Al-Kindi AH, Al-Ibrahim MT, Al-Marhoon MM, et al. Bronchial leiomyoma: Importance of preoperative biopsy for lung preserving surgery. Oman Med J 2022;37(6):e445. DOI: 10.5001/omj.2023.02.
6. Swarnakar R, Sinha S. Endobronchial leiomyoma: A rare and innocent tumour of the bronchial tree. Lung India 2013;30(1):57–60. DOI: 10.4103/0970-2113.106175.
7. Cárdenas-García J, Lee-Chang A, Chung V, et al. Bronchial leiomyoma: A case report and review of literature. Respir Med Case Rep 2014;12:59–62. DOI: 10.1016/j.rmcr.2014.04.004.
8. Öztürk A, Aktaş Z, Yılmaz A, et al. A case of tracheal leiomyoma misdiagnosed as asthma. Tuberk Toraks 2016;64(4):306–309. DOI: 10.5578/tt.27665.
9. Ko SM, Han SB, Lee SK, et al. Calcified endobronchial leiomyoma. Br J Radiol 2007;80(953):e91–e93. DOI: 10.1259/bjr/25631438.
10. Rodriguez E, Pombo F, Aguilera C, et al. Recurring tracheal leiomyoma presenting as a calcified mediastinal mass. Eur J Radiol 1996;23(1):82–84. DOI: 10.1016/0720-048x(95)00718-6.
11. Song KS, Keum DY, Hwang IS. Malignant transformation of pulmonary benign metastasizing leiomyoma. Korean J Thorac Cardiovasc Surg 2017;50(1):59–63. DOI: 10.5090/kjtcs.2017.50.1.59.
12. Hetzel J, Eberhardt R, Herth FJF, et al. Cryobiopsy increases the diagnostic yield of endobronchial biopsy: A multicentre trial. Eur Respir J 2012;39(3):685–690. DOI: 10.1183/09031936.00033011.
13. Stastna N, Brat K, Heroutova M, et al. Endobronchial cryobiopsy may shorten the time to cancer diagnosis: A retrospective study. ERJ Open Res 2023;9(4):00179–2023. DOI: 10.1183/23120541.00179-2023.
14. Aktas Z, Gunay E, Hoca NT, et al. Endobronchial cryobiopsy or forceps biopsy for lung cancer diagnosis. Ann Thorac Med 2010;5(4):242–246. DOI: 10.4103/1817-1737.69117.
15. Rubio ER, le SR, Whatley RE, et al. Cryobiopsy: Should this be used in place of endobronchial forceps biopsies? Biomed Res Int 2013;2013:730574. DOI: 10.1155/2013/730574.
16. Nakamura Y, Hata Y, Koezuka S, et al. Tracheal leiomyoma resected with endobronchial electrocautery snare. J Bronchol Interv Pulmonol 2015;22(1):90–93. DOI: 10.1097/LBR.0000000000000107.
17. Wang Y, Zhang Y, Tong R. Successful bronchoscopic interventional treatment of endobronchial leiomyomas. Open Life Sci 2024;19(1):20220845. DOI: 10.1515/biol-2022-0845.

CASE REPORT

Invasive Pulmonary Aspergillosis in an Apparently Immunocompetent Host: A Diagnostic Challenge

Athul Francis

Received on: 19 November 2025; *Accepted on:* 15 February 2026; *Published on:* 26 September 2026

Abstract

Invasive pulmonary aspergillosis (IPA) is classically associated with immunocompromised states; however, it is increasingly recognized in individuals without overt immunodeficiency. We report a case of IPA in an apparently immunocompetent adult male who presented with acute respiratory symptoms and progressive radiological consolidation. The diagnosis was established through bronchoscopy and histopathological confirmation following clinical deterioration despite empirical antimicrobial therapy. This case highlights the importance of maintaining a high index of suspicion for invasive fungal infections even in immunocompetent hosts and emphasizes the role of early tissue diagnosis.

Keywords: Acute respiratory distress syndrome, Bronchoscopy, Case report, Galactomannan, Invasive pulmonary aspergillosis.

Annals of Interventional Pulmonology (2026): 10.5005/annalsofip-11045-0041

Introduction

Aspergillus species are ubiquitous environmental fungi that primarily cause invasive disease in patients with impaired host immunity, including those with hematological malignancies, prolonged neutropenia, solid organ transplantation, or long-term immunosuppressive therapy.[1,2] Invasive pulmonary aspergillosis in immunocompetent individuals is traditionally considered uncommon and is frequently under-recognized due to nonspecific clinical and radiological features.[3]

Over the past two decades, increasing reports have documented invasive aspergillosis in patients without classical immunosuppressive conditions, particularly in critically ill individuals and those with transient pulmonary or systemic immune dysfunction.[4–6] Delayed diagnosis in this population is common and is associated with inappropriate antimicrobial escalation and worse outcomes. We report a case of invasive pulmonary aspergillosis in an apparently immunocompetent adult male, highlighting the diagnostic challenges and reviewing the relevant literature.

Case Presentation

A 45-year-old male presented with an acute onset of fever, productive cough, and progressive dyspnea for 1 week duration. He had no prior diagnosis of chronic respiratory disease, including chronic obstructive pulmonary disease, bronchiectasis, or asthma. There was no history of diabetes mellitus, chronic kidney disease, chronic liver disease, malignancy, connective tissue disease, or prior pulmonary tuberculosis. There was no history of frequent oral corticosteroid use or long-term inhaled corticosteroid therapy. The patient had a smoking history of approximately 10 pack-years, predominantly cigarette smoking, and had quit smoking 2 years ago. He denied alcohol and other substance abuse and had no significant occupational or environmental exposure. There was no history suggestive of any recent viral infection.

On examination, the patient was febrile (101° F), with a pulse rate of 120/min, BP—140/90 mm Hg, SpO_2—80% on room air, and bilateral inspiratory crackles on auscultation. Initial laboratory evaluation revealed a total leukocyte count of 23,000 cells/mm3 (normal 4,000–11,000 cells/mm^3), with neutrophilic predominance (88%) and elevated CRP—315 mg/L (0–6 mg/L). Renal and hepatic function tests were within normal limits. Human immunodeficiency virus 1 and 2 serology was negative. Chest radiograph showed bilateral multilobar consolidatory changes on presentation, with worsening of the consolidatory changes after 48 hours (Figs 1A and B).

The patient was initiated on empirical broad-spectrum antimicrobial therapy at admission. After 48 hours of hospitalization, there was persistent fever, worsening hypoxemia, and radiological progression with increasing bilateral consolidations (Fig. 1B), prompting further diagnostic evaluations. High-resolution computed tomography (HRCT) of the thorax was performed, which demonstrated innumerable nodules involving both lungs, distributed along bronchovascular, perilymphatic, centriacinar, and subpleural regions, with a few nodules exhibiting a tree-in-bud pattern suggestive of endobronchial spread. Multiple coalescent air-space opacities were noted along the bronchovascular bundles, displaying both solid and ground-glass attenuation. Areas of mosaic attenuation were present, along with patchy ground-glass opacities involving the right middle lobe and bilateral lower lobes. Subpleural fibrosis in the right lower lobe and patchy peripheral

Department of Pulmonary and Sleep Medicine, Mar Augustine Jubilee Hospital, Ernakulam, Kerala, India

Corresponding Author: Athul Francis, Department of Pulmonary and Sleep Medicine, Mar Augustine Jubilee Hospital, Ernakulam, Kerala, India, Phone: +91 8547873763, e-mail: athulfrancis48@gmail.com

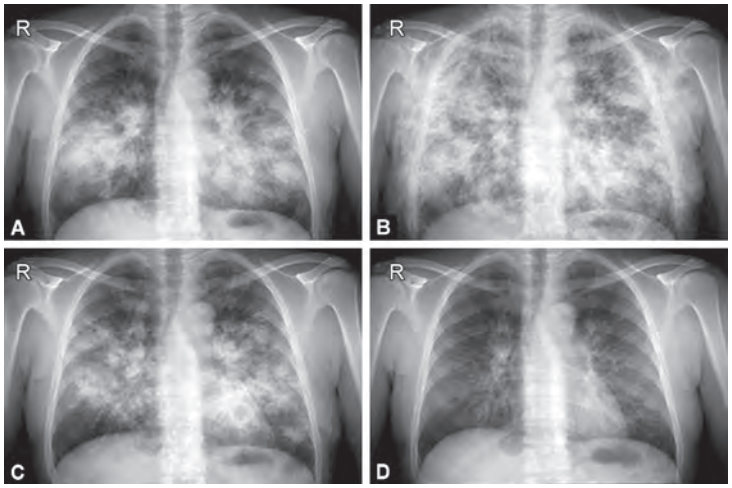
How to cite this article: Francis A. Invasive Pulmonary Aspergillosis in an Apparently Immunocompetent Host: A Diagnostic Challenge. Ann Interv Pulmonol 2026;2(2):90–93.

Source of support: Nil

Conflict of interest: None

Patient consent statement: A written informed consent was obtained from the patient for the publication of details, which can include photographs and/or videos and/or case history to be published in any printed/online journals.

© The Author(s). 2026 Open Access. This article is distributed under the terms of the Creative Commons Attribution-NonCommercial 4.0 International License (https://creativecommons.org/licenses/by-nc/4.0/). This license permits non-commercial use, distribution, and reproduction in any medium, provided the original author and source are credited, a link to the license is included, and any changes are indicated.



Figs 1A to D: Chest X-rays. (A) On admission—showing bilateral consolidatory changes; (B) Worsening of consolidatory changes; (C) Resolving consolidatory changes after treatment with IV Voriconazole; (D) Chest X-ray after 2 weeks showing significant resolution of consolidatory changes

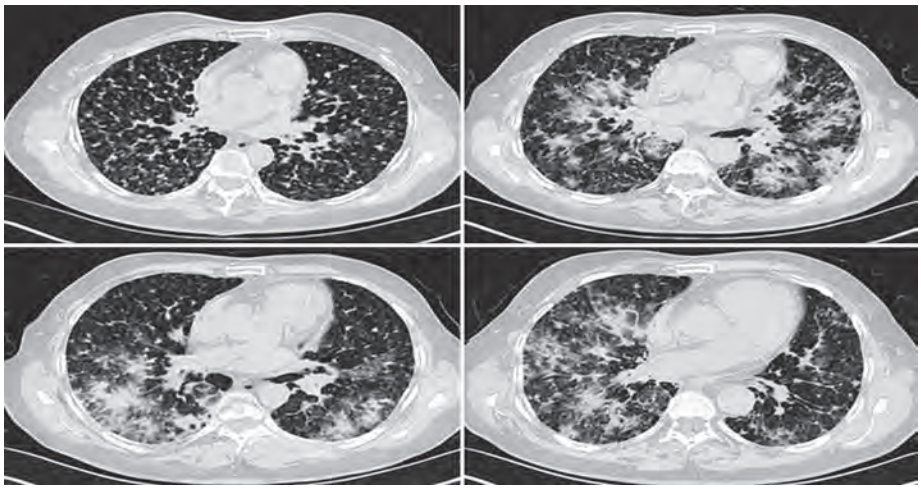


Fig. 2: HRCT thorax demonstrating widespread bilateral centrilobular and peribronchovascular nodules with areas of ground-glass attenuation and confluent consolidation, reflecting progressive diffuse pulmonary involvement

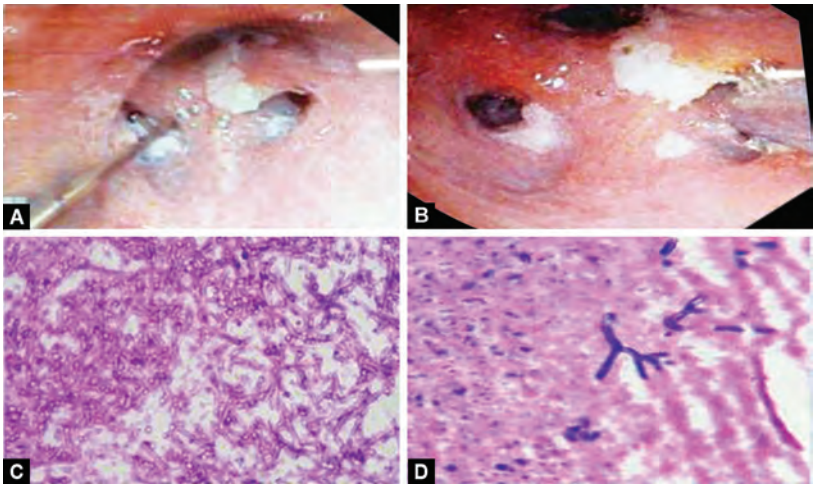
fibrosis in the right middle lobe were also noted, likely representing postinfectious changes. Overall, the imaging features favored an infectious etiology (Fig. 2).

A flexible bronchoscopy was then performed. Bronchoscopic examination revealed inflamed bronchial mucosa with purulent secretions. Necrotic material was visualized in the carina, the right upper and middle lobes, and the left lower lobe. Bronchoalveolar lavage and endobronchial lung biopsy were obtained during the same procedure, and adequate tissue samples were secured (Figs 3A and B). The specimens were sent for bacterial, mycobacterial, and fungal evaluation.

Histopathological examination of the endobronchial biopsies demonstrated septate hyphae with acute-angle branching consistent with *Aspergillus* species (Figs 3C and D). Fungal cultures subsequently confirmed *Aspergillus* growth. Bronchoalveolar lavage samples were negative for acid-fast bacilli, GeneXpert MTB/RIF, and pyogenic organisms. Cytological analysis showed no evidence of malignancy.

A comprehensive evaluation was then undertaken to exclude an underlying immunodeficiency state. Lymphocyte subset analyses were normal, which ruled out idiopathic CD4 lymphocytopenia. Dihydrorhodamine (DHR) flow cytometry assay was done and was found to be normal, hence ruling out chronic granulomatous disease. Serum immunoglobulin levels (IgG, IgA, and IgM) were normal. Glycated hemoglobin was within normal range, excluding occult diabetes mellitus. Renal and hepatic function tests were normal. There was no history of immunosuppressive medication use, chemotherapy, or prolonged corticosteroid therapy. Based on clinical history and laboratory evaluation, the patient was considered apparently immunocompetent.

Given the clinical deterioration, antibiotics were escalated after 48 hours as per institutional protocol. Sputum cultures collected at admission showed no growth on the final report at 48 hours. Following confirmation of invasive pulmonary aspergillosis, antibacterial agents were de-escalated, and antifungals, IV



Figs 3A to D: (A) Bronchoscopic image of necrotic material in the right upper lobe bronchus; (B) Bronchoscopy image (with biopsy forceps) showing necrotic material in the right upper lobe; (C) Histopathology image showing *Aspergillus* species; (D) Histopathology of endobronchial biopsy showing numerous entangled *Aspergillus* fungi

voriconazole was given at a dose of 400 mg IV twice a day on day 1 as a loading dose and then 200 mg IV twice a day for 4 days. The patient showed gradual clinical improvement with resolution of fever, reduction in oxygen requirement, and radiological improvement (Fig. 1C). IV Voriconazole was changed to oral voriconazole-200 mg twice a day, and the patient was discharged on the same. Follow-up imaging was done 2 weeks after discharge, which showed significant resolution (Fig. 1D).

Discussion

Invasive pulmonary aspergillosis is traditionally regarded as a disease confined to profoundly immunocompromised hosts; however, a growing body of literature over the past two decades has clearly demonstrated that invasive pulmonary aspergillosis (IPA) can occur in individuals without classical immunosuppressive risk factors.[3–7] In immunocompetent or apparently immunocompetent patients, the diagnosis is frequently delayed because clinical manifestations are nonspecific and overlap considerably with bacterial pneumonia, tuberculosis, or viral infections, often resulting in inappropriate escalation of antibacterial therapy and delayed antifungal initiation.[4,5]

The pathogenesis of IPA in immunocompetent hosts appears to differ from that in neutropenic patients. Rather than systemic immunodeficiency, localized pulmonary immune dysfunction plays a pivotal role. Structural epithelial injury, impaired mucociliary clearance, and dysfunctional alveolar macrophage responses facilitate fungal invasion and tissue penetration.[6,8] Cigarette smoking, as observed in the present case, is a well-recognized contributor to impaired innate pulmonary immunity. Experimental and clinical studies have demonstrated that smoking reduces macrophage phagocytosis, impairs oxidative burst activity, and alters cytokine signaling, thereby diminishing effective clearance of inhaled *Aspergillus* conidia.[9,10] Importantly, this susceptibility may exist even in the absence of clinically overt COPD.

Another increasingly recognized population at risk comprises critically ill and acutely unwell patients without traditional immunosuppression. Sepsis, severe pneumonia, and systemic inflammatory states can induce a phenomenon termed immunoparalysis, characterized by functional impairment of neutrophils and monocytes despite normal cell counts.[4,7,11] This transient immune dysfunction is sufficient to permit angioinvasive fungal disease and explains the occurrence of IPA in patients with normal baseline immune investigations.

Radiological manifestations of IPA in immunocompetent hosts are often atypical and lack the classical halo sign or air-crescent sign typically seen in neutropenic patients.[3,12] Instead, imaging frequently reveals centrilobular nodules, tree-in-bud opacities, patchy consolidations, or miliary nodules, which closely mimic tuberculosis or atypical bacterial infections.[3–5] Such nonspecific appearances contribute significantly to diagnostic delay, as occurred in the present case.

Microbiological diagnosis of IPA in non-neutropenic hosts remains challenging. Sputum cultures are frequently negative, and serum fungal biomarkers such as galactomannan and β-D-glucan demonstrate reduced sensitivity outside neutropenic populations.[13,14] Consequently, bronchoscopy with bronchoalveolar lavage and tissue biopsy assumes critical diagnostic importance. Histopathological demonstration of tissue invasion by septate hyphae with acute-angle branching remains the gold standard and allows definitive differentiation between colonization and invasive disease.[13]

Timely initiation of antifungal therapy is the most important determinant of outcome. Several studies have demonstrated that delays in antifungal treatment are independently associated with increased mortality in IPA, even among immunocompetent patients.[4,7,15] Voriconazole remains the recommended first-line agent, with alternative therapies reserved for intolerance or resistance. Compared to immunocompromised populations, outcomes in immunocompetent hosts are generally more favorable when diagnosis is established early.[16]

This case underscores several important clinical lessons. First, IPA should be considered in the differential diagnosis of non-resolving or rapidly progressive pneumonia irrespective of immune

status. Second, smoking and acute pulmonary insults may act as sufficient predisposing factors in otherwise immunocompetent individuals. Finally, early bronchoscopy with tissue diagnosis is essential to avoid diagnostic delay, unnecessary antibiotic escalation, and adverse outcomes.

Conclusion

Invasive pulmonary aspergillosis can occur in apparently immunocompetent individuals and may present with nonspecific clinical and radiological features. Early bronchoscopy with tissue diagnosis and prompt antifungal therapy are essential for favorable outcomes.

AI Disclosure

The authors confirm that no AI was used.

Acknowledgment

Nil.

References

1. Kousha M, Tadi R, Soubani AO. Pulmonary aspergillosis: A clinical review. Eur Respir Rev 2011;20:156–174. DOI: 10.1183/09059180.00001011.
2. Segal BH. Aspergillosis. N Engl J Med 2009;360:1870–1884. DOI: 10.1056/NEJMra0808853.
3. Park SY, Lim C, Lee SO, et al. Invasive pulmonary aspergillosis in a immunocompetent patient after congenital heart disease surgery: A case report - Taehan Yongsang Uihakhoe Chi 2020;81(6):1529–1536. DOI: 10.3348/jksr.2020.0014.
4. Meersseman W, Vandecasteele SJ, Wilmer A, et al. Invasive aspergillosis in critically ill patients without malignancy. Am J Respir Crit Care Med 2004;170:621–625. DOI: 10.1164/rccm.200401-093OC.
5. Vandewoude KH, Blot SI, Benoit D, et al. Invasive aspergillosis in critically ill patients: Attributable mortality and excesses in length of ICU stay and ventilator dependence. J Hosp Infect 2004;56(4):269–276. DOI: 10.1016/j.jhin.2004.01.006.
6. Soubani AO, Chandrasekar PH. The clinical spectrum of pulmonary aspergillosis. Chest 2002;121:1988–1999. DOI: 10.1378/chest.121.6.1988.
7. Taccone FS, Van den Abeele AM, Bulpa P, et al. Epidemiology of invasive aspergillosis in critically ill patients: Clinical presentation, underlying conditions, and outcomes. Crit Care 2015:12;19(1):7. DOI: 10.1186/s13054-014-0722-7.
8. Latgé JP. Aspergillus fumigatus and aspergillosis. Clin Microbiol Rev 1999;12:310–350. DOI: 10.1128/CMR.12.2.310.
9. Bulpa P, Dive A, Sibille Y. Invasive pulmonary aspergillosis in patients with COPD. Eur Respir J 2007;30:782–800. DOI: 10.1183/09031936.00062206.
10. Hunninghake GW, Gadek JE, Fales HM, et al. Human alveolar macrophage-derived chemotactic factor for neutrophils: Stimuli and partial characterization. J Clin Invest 1980;66(3):473–483. DOI: 10.1172/JCI109878.
11. Bassetti M, Righi E, De Pascale G, et al. How to manage aspergillosis in non-neutropenic intensive care unit patients. Crit Care 2014:25;18(4):458. DOI: 10.1186/s13054-014-0458-4.
12. Franquet T, Müller NL, Giménez A, et al. Spectrum of pulmonary aspergillosis: Histologic, clinical, and radiologic findings. Radiographics 2001;21(4):825–837. DOI: 10.1148/radiographics.21.4.g01jl03825.
13. Hope WW, Walsh TJ, Denning DW. Laboratory diagnosis of invasive aspergillosis. Lancet Infect Dis 2005;5:609–622. DOI: 10.1016/S1473-3099(05)70238-3.
14. Pfeiffer CD, Fine JP, Safdar N. Diagnosis of invasive aspergillosis using galactomannan. Clin Infect Dis 2006;42:1417–1427. DOI: 10.1086/503427.
15. Denning DW. Invasive aspergillosis. Clin Infect Dis 1998;26:781–803. DOI: 10.1086/513943.
16. Matsuda S, Fushimi K, Kamochi M. Association between early diagnosis of and inpatient mortality from invasive pulmonary aspergillosis among patients without immunocompromised host factors: A nationwide observational study. Int J Infect Dis 2022;122:279–284. DOI: 10.1016/j.ijid.2022.05.048.

INNOVATION CORNER

Flip Y Self-expanding Metallic Stent Deployment for Complex Right-sided Malignant Central Airway Obstruction: A Two-patient Case Series

Shivalingaswamy Salimath[1], Rajendra Rao KM[2]

Received on: 10 August 2026; *Accepted on:* 03 September 2026; *Published on:* 26 September 2026

Abstract

Y-shaped self-expanding metallic stents (Y-SEMS) are conventionally deployed with the longer bronchial limb directed into the left main bronchus (LMB). This configuration may be suboptimal in malignant central airway obstruction (CAO) predominantly involving the right main bronchus (RMB) and bronchus intermedius. We describe anatomy-guided reverse deployment of a commercially available Y-SEMS, termed "flip Y-SEMS," corresponding to previously described reverse or inverted Y-stenting. A 74-year-old man with pulmonary adenocarcinoma had >60% obstruction of the RMB and bronchus intermedius. A 60-year-old woman with acinar-type adenocarcinoma had approximately 60% lower-tracheal, 90% right-main-bronchial, and 40% bronchus-intermedius obstruction, with room-air oxygen saturation of 88%. Covered nitinol Y-SEMS were deployed in reverse orientation, directing the longer limb into the right bronchial tree. Technical success was achieved in both cases without immediate major complications. Symptoms improved in both patients. Seven days bronchoscopy demonstrated patent stents without migration, significant secretions, granulation tissue, or tumor ingrowth. Reverse Y-SEMS deployment may provide effective individualized airway coverage in selected right-predominant malignant obstruction.

Keywords: Airway stenting, Case report, Case series, Central airway obstruction, Interventional pulmonology, Self-expanding metallic stent.

Annals of Interventional Pulmonology (2026): 10.5005/annalsofip-11045-0053

Introduction

Malignant central airway obstruction (CAO) involving the trachea, carina, or main bronchi causes substantial morbidity and may require urgent therapeutic bronchoscopy. Contemporary guidelines emphasize individualized, multimodality treatment of symptomatic CAO using tumor debulking, ablative therapies, dilation, and airway stenting according to the mechanism, anatomical distribution, and clinical context of obstruction.[1–3] Y-shaped stents are particularly useful for carinal disease because they stabilize the distal trachea and both main bronchi.[4–6]

Commercial Y-shaped self-expanding metallic stents (Y-SEMS) conventionally direct the longer bronchial limb toward the left main bronchus (LMB). This geometry may be suboptimal when malignant disease extends predominantly from the lower trachea or carina through the right main bronchus (RMB) into the bronchus intermedius; in such patients, directing the longer limb toward the right bronchial tree may provide more appropriate coverage.

Intentional reversal of Y-stent orientation has been described as reverse, inverted, or reversed Y-stenting.[7,8] We use the descriptive term "flip Y-SEMS" in this report for intentional reverse orientation of a commercially available Y-SEMS; this configuration corresponds to reverse or inverted Y-stenting previously described in the literature. We report two cases of malignant CAO managed using flip Y-SEMS, with emphasis on anatomy-based selection and the technical modification used to reverse the bronchial limbs.

Case Description

Flip Y-SEMS Deployment Technique

Following detailed computed tomography (CT) assessment and bronchoscopic evaluation of airway anatomy and the extent of obstruction, guidewires are placed into the RMB and LMB under combined bronchoscopic and fluoroscopic guidance.

External radiopaque skin markers, such as needles or intravenous cannulae, are placed on the anterior chest wall and aligned with the carina, RMB, and LMB by correlating bronchoscopic visualization with fluoroscopic imaging. These markers provide external reference points for depth and level during deployment.

To achieve the flip orientation, the guidewire positioned in the LMB is inserted into the right bronchial limb of the Y-SEMS deployer, while the guidewire positioned in the RMB is inserted into the left bronchial limb of the deployer. This deliberate cross-loading reverses the conventional orientation of the bronchial limbs and directs the longer limb of the Y-SEMS into the right bronchial tree.

Under continuous fluoroscopic guidance, with the external radiopaque markers used as adjunctive anatomical references, the

[1,2]Department of Interventional Pulmonology, Trustwell Hospitals, Bengaluru, Karnataka, India

Corresponding Author: Rajendra Rao KM, Department of Interventional Pulmonology, Trustwell Hospitals, Bengaluru, Karnataka, India, Phone: +91 9880634914, e-mail: rajendra.rao.5494@gmail.com

How to cite this article: Salimath S, Rajendra Rao KM. Flip Y Self-expanding Metallic Stent Deployment for Complex Right-sided Malignant Central Airway Obstruction: A Two-patient Case Series. Ann Interv Pulmonol 2026;2(2):94–99.

Source of support: Nil

Conflict of interest: None

Patient consent statement: A written informed consent was obtained from the patient for the publication of details, which can include photographs and/or videos and/or case history to be published in any printed/online journals.

© The Author(s). 2026 Open Access. This article is distributed under the terms of the Creative Commons Attribution-NonCommercial 4.0 International License (https://creativecommons.org/licenses/by-nc/4.0/). This license permits non-commercial use, distribution, and reproduction in any medium, provided the original author and source are credited, a link to the license is included, and any changes are indicated.

delivery system is carefully advanced and the Y-SEMS is deployed in the "FLIP" orientation, ensuring alignment of the stent bifurcation with the carina.

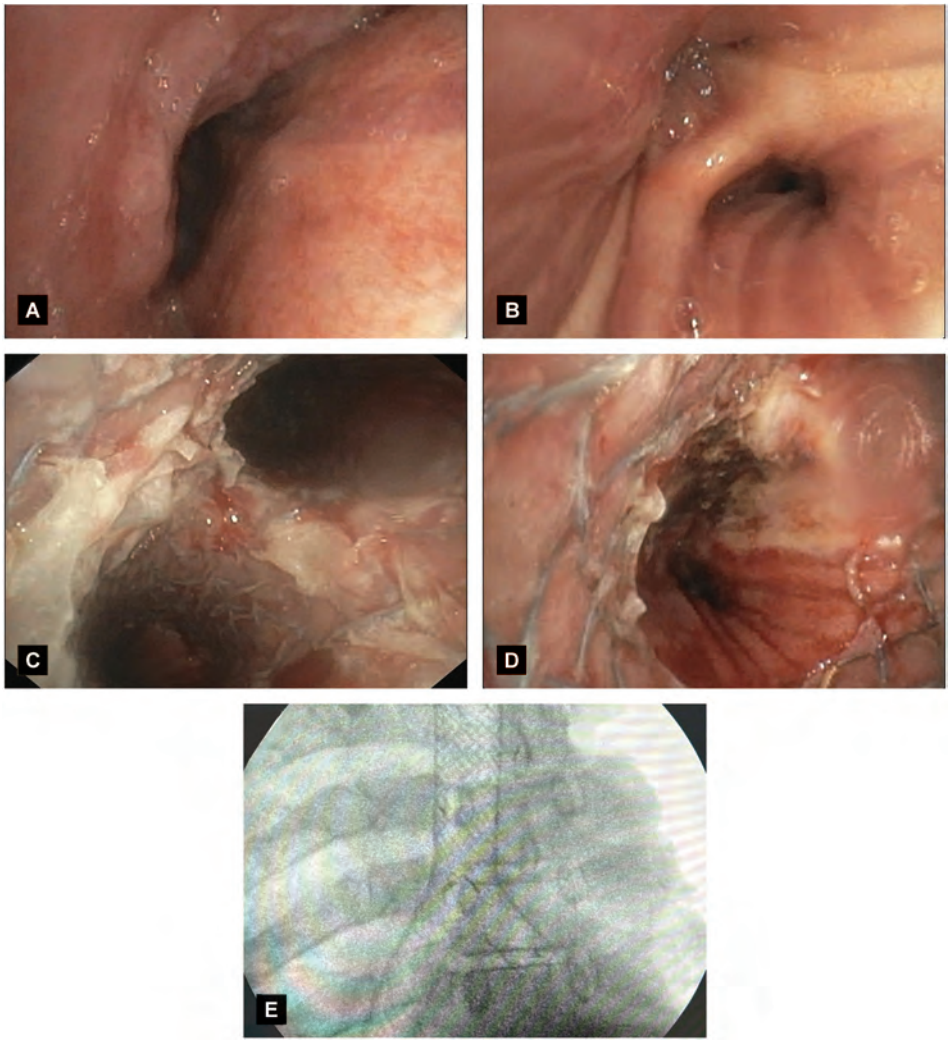
After deployment, bronchial limb position, expansion, and orientation are reconfirmed using both bronchoscopy and fluoroscopy, with attention to carinal seating and distal airway patency.

Case 1

A 74-year-old man, ex-smoker with type 2 diabetes mellitus, presented with progressively worsening dyspnea of 1 week's duration (modified Medical Research Council grade III), orthopnea, and recurrent cough and breathlessness over 6 years. Oxygen saturation was 98% on room air. Electrocardiography was normal. Echocardiography showed preserved left-ventricular systolic function, no regional wall-motion abnormality, and mild pulmonary hypertension (estimated pulmonary artery systolic pressure, 46 mm Hg).

Contrast-enhanced CT of the thorax showed a large right hilar mass with central airway involvement. Flexible bronchoscopy demonstrated tumor infiltration beginning at the carina, involving the entire RMB and extending into the bronchus intermedius, with greater than 60% obstruction at both levels. The anterior segment of the right upper lobe (B3) was completely obstructed by endobronchial tumor, while CT demonstrated external compression of the remaining right-upper-lobe segments. Multiple endobronchial biopsies confirmed adenocarcinoma. The obstruction was classified as mixed malignant CAO.

Because of extensive longitudinal infiltration, associated extrinsic compression, and persistent obstruction, superficial endobronchial tumor ablation was performed using electrocautery, with fraction of inspired oxygen (FiO_2) maintained below 40% during thermal treatment. A Mitra BRAVO covered nitinol tracheobronchial Y-stent was selected to provide radial force and maintain patency. It comprised a 60 × 18 mm tracheal component, a 15 × 14 mm nominal right bronchial limb, and a 30 × 14 mm



Figs 1A to E: Case 1 bronchoscopic and fluoroscopic sequence. (A) Preintervention bronchoscopy at the level of the right main bronchus showing tumor-related obstruction; (B) Preintervention bronchoscopy at the level of the bronchus intermedius showing tumor-related obstruction; (C) Post-deployment view at the carina showing the Y-SEMS in flip configuration; (D) View at the right-main-bronchial stent opening showing satisfactory expansion and patency; (E) Fluoroscopy showing final Flip Y-SEMS position with the longer bronchial limb directed into the right bronchial tree

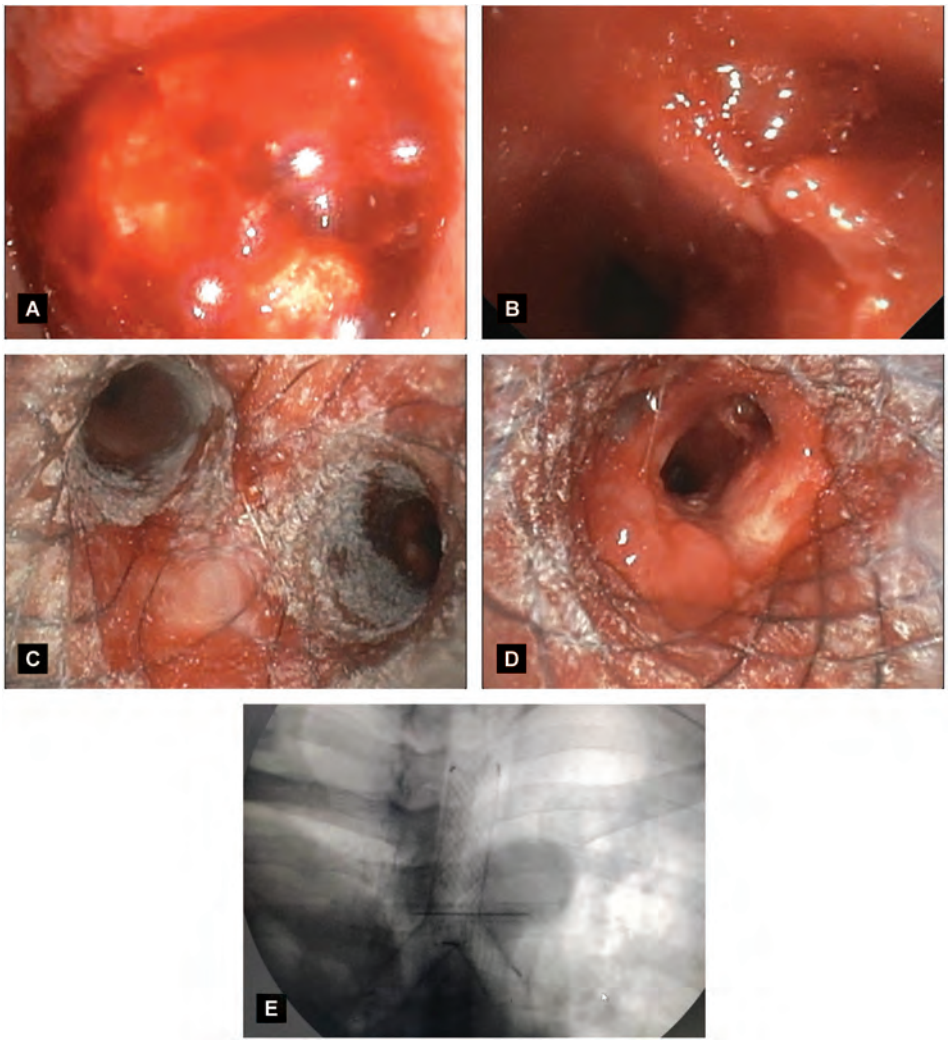
nominal left bronchial limb (dimensions reported as length × diameter). The stent was deployed using the flip Y-SEMS technique described above, directing the longer nominal left limb into the right bronchial tree.

The longer limb traversed the RMB toward the bronchus intermedius and intentionally occluded the right-upper-lobe orifice. This trade-off was accepted because the right upper lobe was already severely compromised, whereas CT and bronchoscopy confirmed patent distal airways and potentially recruitable functional middle- and lower-lobe lung. Postdeployment bronchoscopy and fluoroscopy confirmed satisfactory expansion and bronchus-intermedius patency (Fig. 1). Dyspnea improved, and the patient was discharged the following day. Surveillance bronchoscopy at 7 days showed a patent stent with minimal secretions and no migration, granulation tissue, or tumor ingrowth. Chemotherapy was subsequently initiated with palliative intent. His dyspnea did not worsen during follow-up. Subsequent bronchoscopies showed a patent RMB and bronchus intermedius, without granulation tissue or tumor ingrowth. The patient survived for more than 8 months without recurrent breathlessness.

Case 2

A 60-year-old woman with a seizure disorder presented with a 6 months history of persistent dry cough and 2–3 episodes of blood-tinged sputum. She denied fever, chest pain, or significant hemoptysis. At presentation, inspiratory stridor and bilateral expiratory wheeze were present; oxygen saturation was 88% on room air. Echocardiography showed preserved left-ventricular systolic function (ejection fraction, 55–60%).

Positron emission tomography (PET)-CT showed a complex cystic right-lung mass measuring approximately 9.0 × 8.0 × 9.4 cm and crossing the major fissure, with contiguous endobronchial involvement of the right upper-lobe bronchus, RMB, and lower trachea. Other findings included postobstructive changes, right hilar, subcarinal, and paratracheal lymphadenopathy, pulmonary-vein infiltration with tumor thrombus extending into the left atrium, and pulmonary and rib metastases.



Figs 2A to E: Case 2 bronchoscopic and fluoroscopic sequence. (A) Preintervention bronchoscopy showing tumor-related obstruction at the level of the carina and right main bronchus; (B) Postdebulking bronchoscopy showing a patent bronchus intermedius and persistent obstruction of the right-upper-lobe bronchus; (C) Postdebulking and postdeployment view at the carina showing the bronchial limbs; (D) Right-main-bronchial stent opening after deployment, with restored distal patency; (E) Final fluoroscopic configuration with the longer bronchial limb directed into the right bronchial tree

Initial flexible bronchoscopy showed a large lobulated tumor arising from the lower trachea above the carina, producing approximately 60% lower-tracheal, 90% right-main-bronchial, and 40% bronchus-intermedius obstruction. Rigid bronchoscopic intubation was performed using an 11 mm rigid bronchoscope, followed by flexible bronchoscopy. Mechanical debulking with an electrosurgical snare was followed by cryodebulking and recanalization using an ERBE 1.7 mm cryoprobe and rigid coring. Further RMB tumor debulking was performed, achieving airway patency. An electrocautery ball-tip probe was used for coagulation and hemostasis. Fraction of inspired oxygen was maintained below 40% during electrocautery. Histopathological examination of tumor tissue obtained during the procedure confirmed pulmonary adenocarcinoma, acinar type.

Given the advanced metastatic disease, therapeutic bronchoscopy was performed with palliative intent to relieve critical airway obstruction, facilitate liberation from ventilatory support, and enable subsequent oncological treatment. After recanalization, CT and bronchoscopy supported the presence of patent distal airways and potentially recruitable functional lung. A Mitra BRAVO covered nitinol tracheobronchial Y-stent was selected for its radial force and covering. It comprised a 60 × 16 mm tracheal component, a 15 × 12 mm nominal right bronchial limb, and a 30 × 12 mm nominal left bronchial limb (length × diameter). It was deployed using the flip Y-SEMS technique, with the longer nominal left limb directed into the right bronchial tree. Bronchoscopy and fluoroscopy confirmed expansion and distal patency (Fig. 2).

There were no immediate complications. The patient was electively ventilated overnight and extubated the following day. Dyspnea and stridor improved, and room-air peripheral oxygen saturation (SpO_2) increased from 88 to 92%. She was discharged after 2 days. Surveillance bronchoscopy at 7 days showed a patent stent with minimal secretions and no migration, granulation tissue, or tumor ingrowth. The patient was referred to a medical oncologist for further palliative treatment. This case demonstrates that the stent is used to maintain a lumen achieved by recanalization rather than serving as the primary recanalization procedure.

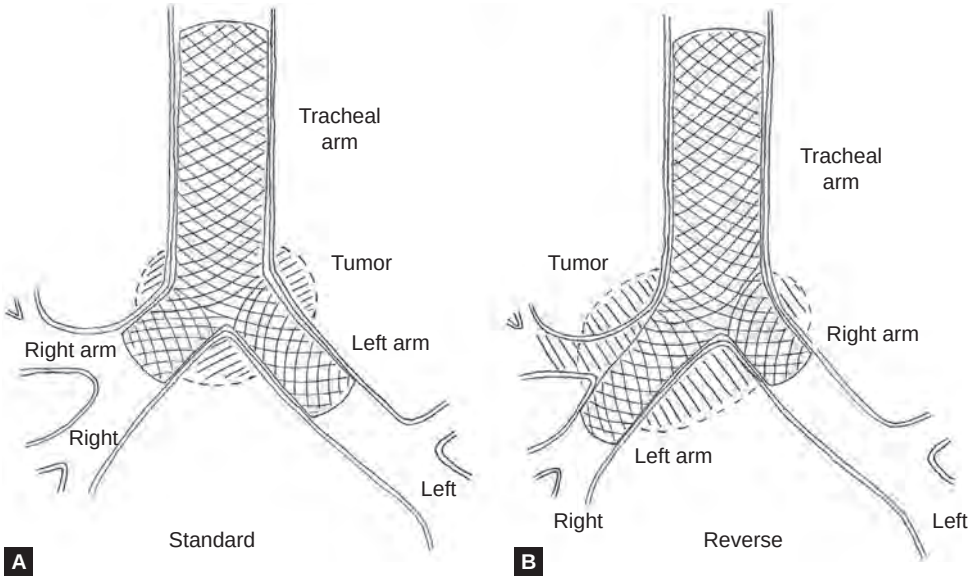
Discussion

The two cases illustrate an anatomy-driven modification of Y-SEMS for malignant CAO with marked right-sided predominance. The relevant question was not simply whether the carina was involved, but which diseased bronchial pathway required greater longitudinal support. In asymmetric carinal disease, Y-stent orientation should be determined by the longitudinal extent of the airway requiring support rather than by the conventional left–right assignment of the bronchial limbs (Fig. 3).

Reverse Y-stenting is not a new intervention. A 15-patient series described the "Y reverse" technique with the longer limb directed into the right bronchial tree, and reversed orientation has also been reported with a customized Dumon silicone Y-stent.[7,8] The contribution of the present cases is an educational demonstration of anatomy-based selection and procedural decision-making in two distinct right-predominant malignant obstructions, rather than a claim of inventing reverse orientation. To our knowledge, this is the first reported case series from India describing reverse ("flip") Y-SEMS deployment for right-sided CAO. Other customized and multiple-stent strategies have been described for complex carinal obstruction.[9,10]

Patient selection requires integration of cross-sectional imaging and bronchoscopic mapping.[2,3,11,12] Operators should determine which side requires greater longitudinal coverage, whether the conventional shorter limb is adequate, whether the distal airway can be recanalized, whether functional distal lung is recruitable, whether the relationship to the right-upper-lobe orifice and contralateral bronchus is acceptable, and whether suitable stent dimensions are available.

A covered nitinol Y-SEMS was chosen in both cases to provide sufficient radial force to maintain malignant-airway patency, while the covering was intended to limit tumor in growth through the stent mesh. In these patients these features were considered preferable to a silicone Y-stent; however, no stent type is universally superior, and selection should remain individualized according to anatomy, obstruction mechanism, device availability, and operator



Figs 3A and B: Standard vs reverse (flip) Y-SEMS configuration. (A) Standard Y-SEMS configuration with the longer bronchial limb directed toward the LMB; (B) Reverse (flip) configuration with the longer limb directed toward the right bronchial tree

experience. Tumor overgrowth at the stent margins remains possible despite covering.

The two cases illustrate related but distinct objectives. In case 1, superficial electrocautery was followed by stenting to maintain bronchus-intermedius patency despite intentional occlusion of an already compromised right-upper-lobe orifice. In case 2, multimodality tumor reduction first established a viable distal lumen; the stent then maintained the achieved patency. Thus, airway preparation, distal-lung viability, and stent orientation must be considered together.

Reverse orientation changes the relationship of both bronchial limbs to their recipient bronchi. Increased right-sided coverage must not cause unacceptable contralateral extension, poor seating, or obstruction of a functional lobar airway. Other relevant risks include migration, tumor ingrowth or marginal overgrowth, granulation tissue, and mucus impaction. Post-stent surveillance should be individualized; either scheduled surveillance bronchoscopy or symptom-driven bronchoscopic reassessment may be used according to the clinical context.[2,3,12]

For this report, technical success was defined as deployment in the intended reverse orientation with adequate expansion and target coverage, bronchoscopic and fluoroscopic confirmation of positioning, patency of the intended distal airways, and no immediate major procedural complication. Clinical success was defined as improvement in obstruction-related respiratory symptoms, with improved oxygenation where applicable. Technical and clinical success were achieved in both patients.

Limitations include the small two-patient series, absence of a comparator arm, and relatively short follow-up duration. The findings therefore demonstrate feasibility rather than comparative effectiveness. Larger multicenter studies are required to determine selection criteria, comparative efficacy, durability, and complication rates.

Conclusion

The two cases demonstrate the feasibility of anatomy-guided reverse ("flip") Y-SEMS deployment in selected right-predominant malignant CAO when conventional orientation would provide inadequate right-sided longitudinal coverage. To our knowledge, this is the first reported case series from India describing reverse ("flip") Y-SEMS deployment for right-sided CAO. Careful CT assessment, bronchoscopic mapping, confirmation of functional distal lung, and individualized stent sizing are essential. Larger studies are required to determine comparative efficacy, durability, and complication rates.

Clinical Significance

Y-stent orientation should be tailored to the longitudinal distribution of airway disease rather than assumed from the conventional left–right limb arrangement. Reverse orientation may be considered when right-sided disease exceeds the coverage afforded by the conventional shorter limb. Selection should confirm that the distal right airway is recanalizable and supplies functional lung, and that suitable individualized stent dimensions are available.

Declarations

Ethics Approval and Patient Consent to Participate

Ethics approval was not applicable because this report describes two anonymized clinical cases treated during routine care and does not constitute a research study. Consent to participate in research was therefore not applicable.

Animal Studies

Not applicable; this manuscript reports human clinical cases and no animal research.

Availability of Data and Materials

Data supporting this case series are contained within the article. Additional de-identified clinical information may be available from the corresponding author on reasonable request, subject to institutional and patient-privacy requirements.

Clinical Trial Registry Number

Not applicable; this case series is not a clinical trial.

PROSPERO Registry Number

Not applicable; this manuscript is not a systematic review.

Supplementary Materials

CARE reporting checklist to be supplied separately. No other supplementary material is included with this manuscript.

Copies of Permissions

Not applicable. Figure 3 is wholly original artwork created by the authors.

Reporting Guidelines Checklist

The CARE reporting checklist is to be submitted as a separate supplementary file.

Artificial Intelligence (AI) Disclosure:

No AI was used in any step of preparing/writing of the manuscript.

Acknowledgments

The authors gratefully acknowledge Dr NS Chandrashekar, Director and Head of the Department of Anaesthesiology, and his team, including Dr Jaydev, Dr Jyothsna and Dr Lalitha, for their valuable support in the management of these patients.

Authors' Contributions (CRediT)

Dr Shivalingaswamy Salimath - Conceptualization, Methodology, Investigation, Visualization, Writing - Review and editing, Supervision.
Dr Rajendra Rao KM - Investigation, Data curation, Visualization, Writing - Original draft, Writing - Review and editing.

Orcid

Shivalingaswamy Salimath https://orcid.org/0009-0003-7505-9218
Rajendra Rao KM https://orcid.org/0000-0002-2855-0018

References

1. Colt HG, Harrell J. Therapeutic rigid bronchoscopy allows levels of care changes in patients with acute respiratory failure from central airways obstruction. Chest 1997;112:202–206. DOI: 10.1378/chest.112.1.202.
2. Mahmood K, Frazer-Green L, Gonzalez AV, et al. Management of central airway obstruction: An American College of Chest Physicians clinical practice guideline. Chest 2025;167(1):283–295. DOI: 10.1016/j.chest.2024.06.3804.

3. Chaddha U, Agrawal A, Kurman J, et al. World Association for Bronchology and Interventional Pulmonology (WABIP) guidelines on airway stenting for malignant central airway obstruction. Respirology 2024;29(7):563–573. DOI: 10.1111/resp.14764.
4. Dutau H, Toutblanc B, Lamb C, et al. Use of the Dumon Y-stent in the management of malignant disease involving the carina: A retrospective review of 86 patients. Chest 2004;126(3):951–958. DOI: 10.1378/chest.126.3.951.
5. Shiraishi T, Kawahara K, Shirakusa T, et al. Stenting for airway obstruction in the carinal region. Ann Thorac Surg 1998;66(6): 1925–1929. DOI: 10.1016/S0003-4975(98)01059-5.
6. Hauck RW, Born P, Helmberger H, et al. Y-nitinol airway stent for management of central airway compression due to metastatic colon cancer. Endoscopy 2003;35(10):858–860. DOI: 10.1055/s-2003-42615.
7. Messina G, Natale G, Pica DG, et al. Y reverse: Modified technique in challenging airway management. Thorac Cancer 2024;15(34): 2428–2436. DOI: 10.1111/1759-7714.15440.
8. Takigawa Y, Sato K, Watanabe H, et al. Customised Dumon Y-stent with reversed orientation for management of complex airway obstruction in endobronchial non-small-cell lung cancer: Clinical image of a successful airway salvage. Respirol Case Rep 2025;13(6):e70240. DOI: 10.1002/rcr2.70240.
9. Oki M, Saka H. Double Y-stenting for tracheobronchial stenosis. Eur Respir J 2012;40:1483–1488. DOI: 10.1183/09031936.00015012.
10. Breen DP, Dutau H. On-site customization of silicone stents: Towards optimal palliation of complex airway conditions. Respiration 2009;77:447–453. DOI: 10.1159/000205396.
11. Mitchell PD, Kennedy MP. Bronchoscopic management of malignant airway obstruction. Adv Ther 2014;31(5):512–538. DOI: 10.1007/s12325-014-0122-z.
12. Sabath BF, Casal RF. Airway stenting for central airway obstruction: A review. Mediastinum 2023;7:18. DOI: 10.21037/med-22-65.

INNOVATION CORNER

Targeted Thoracoscopic Autologous Blood Patch for Persistent Air Leak in Secondary Spontaneous Pneumothorax: A Case Report

Avinash Anil Nair[1], Rennis Davis Kizhakkepeedika[2], Ajaykumar Kurumpelil Karunakaran[3], Akhila Joboy[4]

Received on: 20 July 2026; *Accepted on:* 19 August 2026; *Published on:* 26 September 2026

Abstract

Persistent air leak (PAL) is a challenging complication of secondary spontaneous pneumothorax (SSP), particularly in patients with advanced structural lung disease who are poor surgical candidates. We report a case of successful thoracoscopically guided autologous blood patching for PAL in an elderly patient with SSP. A 78-year-old man with smoking-related chronic lung disease presented with a left-sided SSP and a continuous, high-grade air leak (Cerfolio grade IV) that persisted despite prolonged chest drainage. Surgical repair was considered high risk and was declined by the patient. Flexible bronchoscopy with sequential balloon occlusion localized the dominant air leak to the basal segments of the left lower lobe. Medical thoracoscopy was subsequently performed and demonstrated a focal visceral pleural defect corresponding to the suspected leak site. Fifty milliliters of freshly drawn autologous blood was applied directly over the defect under thoracoscopic visualization. The air leak decreased substantially within 24 hours, from Cerfolio grade IV to grade I, with complete radiographic lung re-expansion. The chest tube was removed after 48 hours, and the patient was discharged in stable condition. At 1-month follow-up, he remained asymptomatic without clinical or radiographic evidence of recurrence. Thoracoscopically guided direct autologous blood patching may represent a simple, targeted, and pragmatic salvage option for PAL in selected patients with SSP, particularly when surgery is contraindicated or declined and bronchoscopic occlusion alone is insufficient. Further experience is required to establish its safety, reproducibility, and role among available PAL management strategies.

Keywords: Autologous blood patch, Case report, Medical thoracoscopy, Persistent air leak, Pleural intervention, Secondary spontaneous pneumothorax.

Annals of Interventional Pulmonology (2026): 10.5005/annalsofip-11045-0050

Introduction

Persistent air leak (PAL) is a frequent and clinically significant complication of secondary spontaneous pneumothorax (SSP), particularly in patients with underlying chronic lung disease.[1,2] Persistent air leak is commonly considered as an air leak that persists for several days; many sources use a threshold of >5–7 days to label an air leak as "persistent/prolonged," while some guidance—particularly for SSP—recommends early thoracic surgical discussion if an air leak persists or the lung fails to re-expand, including discussion at approximately 48 hours in SSP.[1,2] Prolonged air leak is associated with extended chest tube duration, increased morbidity, higher healthcare utilization, and delayed recovery.[1,3]

Surgical repair remains the definitive treatment for refractory PAL and typically involves resection of blebs or bullae with pleural symphysis.[1,3] However, advanced age, comorbid illness, frailty, and patient refusal frequently preclude operative management.[3] In such settings, interventional pulmonology-based alternatives assume greater importance. Bronchoscopic strategies, including balloon occlusion testing and endobronchial valve/spigot or glue placement, have expanded the therapeutic armamentarium but are limited by collateral ventilation, incomplete fissures, distal air leaks, and restricted availability of specialized devices.[4,5]

Pleural-based approaches, including chemical pleurodesis and autologous blood patch pleurodesis, are commonly employed when surgery is not feasible.[3,5] Autologous blood pleurodesis has demonstrated encouraging success rates in observational studies and systematic reviews, with air leak cessation reported in most patients within 24–72 hours.[5,6] Nevertheless, this technique is usually performed without direct visualization of the pleural defect, and outcomes may be influenced by variability in blood volume, distribution, and pleural apposition.[5,6]

Medical thoracoscopy provides direct access to the pleural space, enabling visual identification of focal pleural defects and targeted therapeutic intervention.[7] Despite its established role in

[1,2,4]Department of Pulmonary Medicine, Amala Institute of Medical Sciences, Thrissur, Kerala, India

[3]Department of Cardiovascular and Thoracic Surgery, Amala Institute of Medical Sciences, Thrissur, Kerala, India

Corresponding Author: Avinash Anil Nair, Department of Pulmonary Medicine, Amala Institute of Medical Sciences, Thrissur, Kerala, India, Phone: +91 9159143854, e-mail: avinash444@hotmail.com

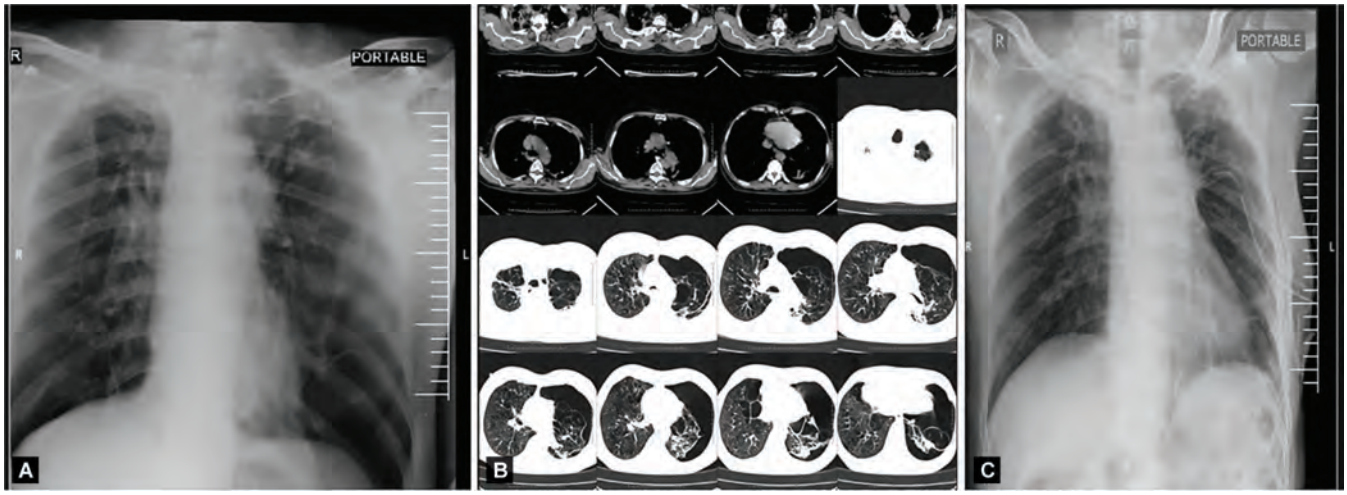
How to cite this article: Nair AA, Kizhakkepeedika RD, Karunakaran AK, *et al*. Targeted Thoracoscopic Autologous Blood Patch for Persistent Air Leak in Secondary Spontaneous Pneumothorax: A Case Report. Ann Interv Pulmonol 2026;2(2):100–103.

Source of support: Nil

Conflict of interest: None

Patient consent statement: A written informed consent was obtained from the patient for the publication of details, which can include photographs and/or videos and/or case history to be published in any printed/online journals.

© The Author(s). 2026 Open Access. This article is distributed under the terms of the Creative Commons Attribution-NonCommercial 4.0 International License (https://creativecommons.org/licenses/by-nc/4.0/). This license permits non-commercial use, distribution, and reproduction in any medium, provided the original author and source are credited, a link to the license is included, and any changes are indicated.



Figs 1A to C: (A) Chest radiograph at presentation demonstrating a left-sided SSP with partial lung collapse; (B) Computed tomography of the thorax revealing bilateral bullous lung disease with emphysematous changes, consistent with SSP and predisposing to persistent air leak; (C) Chest radiograph following intercostal chest drain insertion showing partial lung re-expansion with residual pneumothorax, correlating with a continuous high-grade air leak (Cerfolio grade IV)

pleural disease, thoracoscopic autologous blood patching for PAL has been infrequently described, and its position within current management algorithms remains undefined.[7]

We report the feasibility of a targeted, thoracoscopically guided autologous blood patch applied directly to a visually identified visceral pleural defect in a patient with SSP and continuous air leak who was a poor surgical candidate.

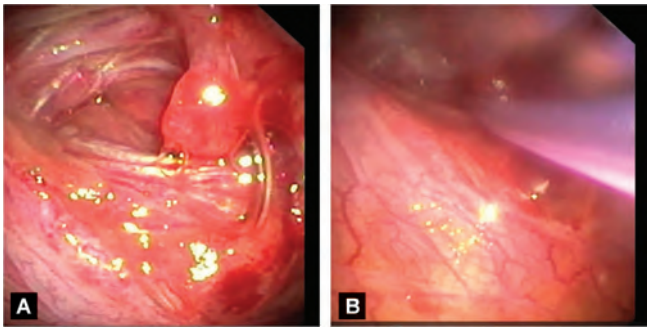
Case Presentation

A 78-year-old male farmer with a smoking history exceeding 40 pack-years presented with acute-onset left-sided chest pain, progressive dyspnea, and cough following physical exertion. Initial evaluation confirmed a left-sided SSP, for which an intercostal chest drain was inserted (Fig. 1A). Computed tomography of the thorax revealed bilateral bullous lung disease, supporting the diagnosis of SSP (Fig. 1B).

Following tube thoracostomy, the patient experienced symptomatic improvement; however, there was continuous air leak through the chest drain. Air leak severity was assessed using the bedside underwater seal system and categorized using the Cerfolio leak pattern classification as grade IV (continuous bubbling during both inspiration and expiration). Serial chest radiographs demonstrated incomplete resolution of the pneumothorax despite appropriate drain position and function. After 1 week of continuous drainage, the air leak persisted (Fig. 1C).

Thoracic surgical consultation was obtained. In view of the patient's advanced age, significant comorbidities, and high anticipated operative risk, surgical intervention was considered unfavorable. After detailed discussion, the patient and family declined operative management, prompting consideration of alternative interventional strategies.

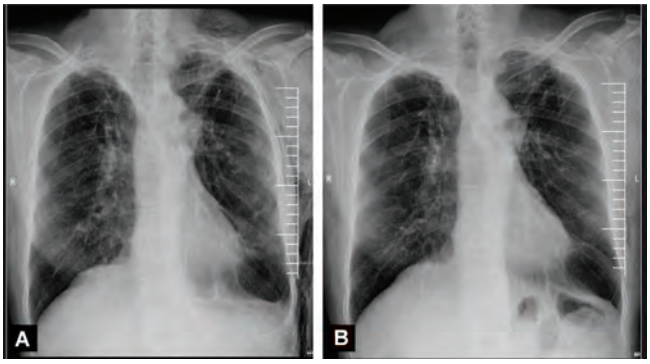
Flexible bronchoscopy was performed to localize the source of the air leak. Sequential balloon occlusion was performed using a balloon catheter passed through the working channel of the flexible bronchoscope. Occlusion was maintained for several respiratory cycles while observing changes in bubbling in the underwater seal chamber; the most pronounced reduction occurred when occluding the left lower lobe lateral basal segment (LB9), suggesting this as the dominant contributor. Balloon occlusion of the LB9 segment led to a reduction, but not cessation, of the air leak. Localization was performed without using fluoroscopy and airway or pleural contrast instillation. Objective assessment of collateral ventilation and fissural completeness using the CHARTIS system could not be performed due to unavailability.



Figs 2A and B: (A) Thoracoscopic view of the visceral pleura demonstrating a focal pleural defect with active air leakage identified during medical thoracoscopy; (B) Thoracoscopic instillation of autologous blood directly over the identified pleural defect using a feeding catheter, illustrating targeted blood patch application

Given the persistence of a high-grade air leak, absence of surgical options, and limitations of bronchoscopic therapy, a medical thoracoscopic approach was planned to allow direct pleural visualization and targeted intervention.

Medical thoracoscopy was performed with the patient in a right lateral decubitus position, using a single-port approach. Port placement was guided by identification of a safe access site and standard positioning principles under real-time ultrasound guidance. Single-port medical thoracoscopy was performed, which revealed a focal pleural defect with active air leakage on the visceral pleura (Fig. 2). Under thoracoscopic guidance, an autologous blood patch was performed by instilling approximately 2 aliquots of 25 mL each (total 50 mL) of freshly drawn autologous



Figs 3A and B: (A) Postprocedure chest radiograph showing complete lung re-expansion with no residual pneumothorax following thoracoscopic autologous blood patching; (B) Follow-up chest radiograph after 4 weeks

blood directly onto the identified pleural defect using a 6 Fr infant feeding catheter (length 50 cm), to maximize local coverage while minimizing dispersion. A small blood volume was considered, as it was applied directly over the visualized defect.

Adjunctive ice-cold saline, 500 mg tranexamic acid, and 1 mL botropase were applied locally (as routinely used for intraluminal bleeds during bronchoscopic procedures), followed by tamponade with scope over the defect for 3–4 minutes to promote local clot stabilization. A new 24 Fr intercostal drain was positioned to ensure optimal pleural apposition.

Within 24 hours of the procedure, there was a marked reduction in air leak from Cerfolio grade IV to grade I. Follow-up chest radiography demonstrated complete lung re-expansion without residual pneumothorax (Fig. 3A). Mild subcutaneous emphysema was noted but remained clinically insignificant and required no intervention. The chest drain was removed after 48 hours.

The patient remained clinically stable and was discharged shortly thereafter. At 1-month follow-up, he was asymptomatic, with no radiographic evidence of recurrent pneumothorax (Fig. 3B).

Discussion

Persistent air leak in SSP represents a complex therapeutic challenge, particularly when definitive surgical management is not feasible.[1,2] In elderly patients with underlying structural lung disease, prolonged air leak is common and frequently refractory to conservative chest tube drainage alone. Current management algorithms emphasize early identification of patients unlikely to respond to conservative measures, as delayed intervention is associated with prolonged hospitalization and increased morbidity.[1–3]

Surgical repair remains the gold standard for refractory PAL, offering high success rates through resection of blebs or bullae combined with pleural symphysis.[1,3] However, real-world practice often necessitates alternative approaches, as advanced age, comorbidities, frailty, or patient preference may preclude surgery.[3] In such scenarios, interventional pulmonology-based strategies assume a vital role. Bronchoscopic interventions may be considered when surgery is not feasible, particularly after localization of the dominant leaking segment.[4,5] Options reported include one-way valves, silicone spigots, and occlusive strategies using sealants, coils, occluder devices, or covered airway stents. Indian experience has described bronchoscopic device closure using endobronchial coils with sealant, ductal occluder devices, and covered self-expandable metallic stents and customized silicone stents, with successful closure reported in most cases in that series.[8] They are particularly useful when a proximal airway source can be reliably localized. Nevertheless, their effectiveness may be limited by collateral ventilation, incomplete fissures, distal pleural defects, and restricted access to specialized devices, all of which may compromise durable air leak control.[4,5]

Autologous blood patch pleurodesis has emerged as a pragmatic, low-cost option for PAL, most often administered through an indwelling chest drain. Several observational studies and a systematic review have reported high rates of air leak cessation, often within 24–72 hours, with an acceptable safety profile.[6] However, the technique is typically performed without direct visualization of the pleural defect, and reported methodologies vary with respect to blood volume, clamping protocols, patient positioning, and adjunctive measures. These factors may influence both efficacy and reproducibility, particularly in patients with focal visceral pleural defects.[5,6]

Medical thoracoscopy provides a unique advantage by allowing direct visualization of the pleural cavity and visceral pleural surface.[7] In the present case, thoracoscopic inspection enabled precise identification of a focal pleural defect responsible for the persistent, high-grade air leak. Targeted delivery of autologous blood directly over the defect, rather than blind instillation through a chest tube, may facilitate immediate sealing of the leak, optimize clot localization, and enhance pleural apposition. The rapid reduction in air leak severity observed in this patient supports the potential utility of this targeted approach.

Reports describing thoracoscopic autologous blood patching remain limited, confined to small case series and isolated reports.[7,9] A recent case series and systematic review examining thoracoscopic blood patch instillation suggested favorable outcomes in selected patients, although heterogeneity in technique and patient selection precludes definitive conclusions.[7] Importantly, thoracoscopic autologous blood patch (ABP) should not be viewed as a replacement for surgery or established bronchoscopic therapies, but rather as a salvage strategy in carefully selected patients where other options are unavailable, contraindicated, or declined.[3–5,7]

This case illustrates several practical considerations relevant to interventional practice. First, thoracoscopic ABP may be particularly suited for patients with peripheral, focal pleural defects identified under direct visualization. Second, the procedure can be cost-effective and performed using readily available equipment without the need for specialized bronchoscopic devices. Third, rapid air leak control may facilitate early chest tube removal and discharge, reducing hospital length of stay in a vulnerable patient population compared to large volume blood instillation through chest tube.[6,7]

Limitations

The limitations of this report are inherent to its single-patient design. Objective digital air leak quantification and assessment of collateral ventilation were not available, and the index case reports only a 1-month follow-up. Additionally, standardized protocols for thoracoscopic blood volume, adjunctive agents, and

post-procedure management remain undefined. Given the use of supportive local measures and the single-patient design, the independent contribution of each step cannot be determined. Even though our patient did not have any adverse events – fever, chest pain, hemoptysis, and respiratory failure – these are ones that need to be considered. Larger prospective studies are required to better delineate patient selection criteria, procedural standardization, and comparative effectiveness relative to other interventional modalities for the management of PAL.

Conclusion

Thoracoscopically guided autologous blood patching may be considered a useful salvage option in carefully selected non-surgical candidates for PAL in SSP.[5,7] Direct pleural visualization allows precise localization and targeted treatment of focal pleural defects, potentially enabling rapid air leak control and early chest tube removal (Fig. 3B). While this approach should not replace established surgical or bronchoscopic therapies, it may be feasible in only selected patients within a tertiary interventional pulmonology setting.[3–5,7] Further prospective and comparative studies are needed to define standardized techniques and optimal patient selection.

Clinical Significance

Targeted thoracoscopic autologous blood patching may be a feasible salvage option for persistent air leak in selected patients with secondary spontaneous pneumothorax who are unsuitable for or decline surgery. Direct visualization of the pleural defect allows precise application of autologous blood and may facilitate rapid air leak control and earlier chest tube removal.

Declarations

Ethical Approval

Ethics committee approval was not required for this single-patient case report in accordance with institutional policy. Written informed consent was obtained from the patient for publication of clinical details and accompanying images.

Data Availability Declaration

All relevant clinical data supporting the findings of this case report are included within the article. Additional details are available from the corresponding author upon reasonable request, subject to patient confidentiality.

Artificial Intelligence (AI) Disclosure

Generative AI tools were used for language editing and formatting assistance. All clinical information, scientific content, interpretation, references, and the final manuscript were reviewed and verified by the authors.

Acknowledgment

The authors would like to thank Mrs Remya, Nursing Assistant, and Miss Nima, Physician Assistant, for their assistance in collecting patient records and facilitating correspondence. The authors also thank the patient and his family for providing consent for publication of this case.

Authors' Contribution

Avinash Anil Nair contributed to the conception of the report, clinical management, and manuscript preparation.
Rennis Davis Kizhakkepeedika clinically managed and performed the procedure, supervised the work and critically revised the manuscript.
Ajaykumar Kurumpelil Karunakaran and Akhila Joboy contributed to clinical management and critical revision of the manuscript.
All authors reviewed and approved the final manuscript.

Orcid

Avinash Anil Nair https://orcid.org/0000-0002-2062-0376

References

1. Dugan KC, Laxmanan B, Murgu S, et al. Management of persistent air leaks. Chest 2017;152(2):417–423. DOI: 10.1016/j.chest.2017.02.020.
2. Roberts ME, Rahman NM, Maskell NA, et al. British thoracic society guideline for pleural disease. Thorax 2023;78(Suppl 3):s1–s42. DOI: 10.1136/thorax-2022-219784.
3. Mundanchira G, Frye L, Reisenauer J, et al. The persistent problem of persistent air-leaks: Approach to management. Curr Opin Pulm Med 2025;31(1):28–34. DOI: 10.1097/MCP.0000000000001134.
4. Lazarus DR, Casal RF. Persistent air leaks: A review with an emphasis on bronchoscopic management. J Thorac Dis 2017;9(11):4660–4670. DOI: 10.21037/jtd.2017.10.122.
5. Ruenwilai P. Bronchoscopic management in persistent air leak: A narrative review. J Thorac Dis 2024;16(6):4030–4042. DOI: 10.21037/jtd-24-46.
6. Hugen N, Hekma EJ, Claessens NJM, et al. Efficacy of an autologous blood patch for prolonged air leak: A systematic review. Ann Thorac Surg 2022;114(3):1064–1071. DOI: 10.1016/j.athoracsur.2021.05.047.
7. Kedia Y, Madan M, Kaushik R, et al. Thoracoscopic blood patch instillation for persistent air leak in pneumothorax: A case series and systematic review. Monaldi Arch Chest Dis 2025;95(2). DOI: 10.4081/monaldi.2024.2994.
8. Marwah V, Katoch CDS, Kumar K, et al. Bronchoscopic device closure of postoperative bronchopleural fistulae: Novel devices and innovative techniques. Lung India 2020;37(2):107–113. DOI: 10.4103/lungindia.lungindia_179_19.
9. Mishra G, Marwah V, Tiwari P, et al. Innovative thoracoscopic management of empyema thoracis with alveolopleural fistula using laparoscopic instruments in a peripheral hospital setting: A case report. Ann Interv Pulmonol 2025;1(2):134–137. DOI: 10.5005/annalsofip-11045-0026.

CASE LETTER

A Surprise beyond Bronchiectasis: Tracheobronchopathia Osteochondroplastica

Sai Sindhu Naru[1], Virender Pratibh Prasad[2], Venkata Nagarjuna Maturu[3]

Received on: 07 August 2026; *Accepted on*: 09 September 2026; *Published on*: 26 September 2026

Keywords: Bronchoscopy, Case report, Chronic cough, Tracheobronchopathia osteochondroplastica.
Annals of Interventional Pulmonology (2026): 10.5005/annalsofip-11045-0057

Dear Editor,

Tracheobronchopathia Osteochondroplastica (TPO) is an uncommon, benign and indolent airway disorder characterized by multiple submucosal osseous and cartilaginous nodules involving the trachea and main bronchi, without affecting the posterior membranous wall.[1–3] Due to the nonspecific clinical presentation, the disease remains unidentified and is often detected while evaluating for other respiratory symptoms.[1,2]

A 78-year-old man, carpenter by occupation and a reformed smoker (smoking index 120), with no known concurrent illnesses, developed a dry cough in the year 2000 and was managed with symptomatic therapy with no relief. Ten years later, he developed new-onset intermittent low-grade fever and an evening rise in temperature for 2 months. He was clinically diagnosed with pulmonary tuberculosis and was initiated on weight-based antitubercular therapy for a period of 6 months. His fever resolved, but he continued to have a dry cough. Since 2023, he developed dyspnea [modified Medical Research Council (mMRC) grade II] and a productive cough, for which he was initiated on inhalers (inhaled bronchodilators and inhaled steroids) along with multiple courses of antibiotics; despite this, his symptoms didn't improve. He was referred to our center for further evaluation.

He presented to us with complaints of dyspnea (mMRC grade III) and cough with mucoid expectoration. On examination, he was tachypneic (24 breaths/min) while the rest of the vital parameters were stable. Diffuse inspiratory coarse crackles were heard all over the chest on auscultation. Initial laboratory work-up showed hemoglobin 12.6 gm/dL, white blood cell count 9,300/µL, and platelet count 3.42×10^5/µL. High-resolution computed tomography of the chest showed fibrocavitatory and bronchiectatic changes predominantly in the bilateral upper lobes, with multiple calcified nodules noted in the trachea and both main bronchi (Fig. 1A).

Video bronchoscopy performed using Olympus Video bronchoscope (BF-1TH1100; Olympus Corporation, Tokyo, Japan) revealed multiple firm, sessile nodular lesions involving anterior and lateral walls of the trachea and both main bronchi (Fig. 1B). The nodules were extremely hard to biopsy, raising concern for a calcified or bony process, and biopsy was done using Olympus EndoJaw fenestrated forceps. Histopathology revealed subepithelial mature bony trabeculae in a fibrous stroma, with no evidence of inflammation or malignancy, suggestive of TPO (Fig. 1C). Bronchoalveolar lavage (BAL) fluid obtained from the right upper lobe apical segment yielded *Pseudomonas aeruginosa* and *Klebsiella pneumoniae* subspecies *ozaenae*. Acid-fast bacilli (AFB) staining, mycobacterial culture and Xpert MTB/RIF Ultra were negative.

[1–3]Department of Pulmonary Medicine, Yashoda Super Specialty Hospitals, Hyderabad, Telangana, India

Corresponding Author: Virender Pratibh Prasad, Department of Pulmonary Medicine, Yashoda Super Specialty Hospitals, Hyderabad, Telangana, India, Phone: +91 9814917788, e-mail: vpratibh712@yahoo.co.in

How to cite this article: Naru SS, Prasad VP, Maturu VN. A Surprise beyond Bronchiectasis: Tracheobronchopathia Osteochondroplastica. Ann Interv Pulmonol 2026;2(2):104–105.

Source of support: Nil

Conflict of interest: Dr Venkata Nagarjuna Maturu is associated as Editor-in-Chief of this journal and this manuscript was subjected to this journal's standard review procedures, with this peer review handled independently of the Editor-in-Chief and his research group.

Patient consent statement: A written informed consent was obtained from the patient for the publication of details, which can include photographs and/or videos and/or case history to be published in any printed/online journals.

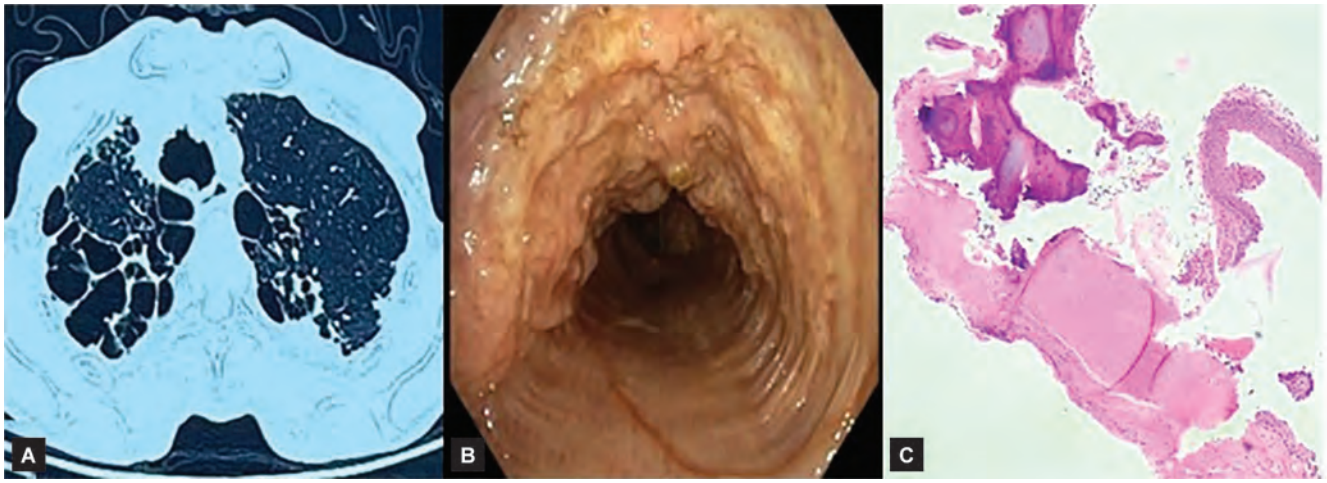
While TPO is often discovered incidentally during the evaluation of a patient with chronic respiratory symptoms, treatment depends on the severity of the symptoms and underlying lung pathology. In a patient with mild symptoms, symptomatic management is given, whereas in patients with significant airway obstruction, interventional bronchoscopic modalities may be considered.

In our patient, given the absence of significant respiratory impairment attributable to TPO, the patient was started on antibiotics as per susceptibility and treatment for underlying post-tuberculous bronchiectasis was initiated using airway clearance techniques like postural drainage, a positive expiratory pressure device and bronchodilator inhaler therapy.

Tracheobronchopathia Osteochondroplastica predominantly affects the age group between 60 and 80 years, with a slight propensity towards the male gender.[2,3] The etiology and pathogenesis are still unknown. Several factors such as genetic predisposition, developmental disorders, chronic respiratory infections, and metabolic diseases are thought to predispose to this condition. It has been reported that undifferentiated pleuripotent embryonic cells, mediated by bone morphogenetic protein 2 (BMP-2) and transforming growth factor-β1(TGF-β_1) pathways, differentiate into osteocytes and chondrocytes, leading to the formation of calcific foci.[4]

A literature review highlighted that 44.5% of TPO cases had history of smoking and 55.5% of patients had reported with

© The Author(s). 2026 Open Access. This article is distributed under the terms of the Creative Commons Attribution-NonCommercial 4.0 International License (https://creativecommons.org/licenses/by-nc/4.0/). This license permits non-commercial use, distribution, and reproduction in any medium, provided the original author and source are credited, a link to the license is included, and any changes are indicated.



Figs 1A to C: (A) High-resolution computed tomography of chest shows fibrocavitatory and bronchiectatic changes predominantly in bilateral upper lobes with multiple nodules in the trachea; (B) Bronchoscopic findings showed multiple sessile nodular opacities involving anterior and lateral wall of trachea; (C) Histopathological image shows subepithelial mature bony trabeculae in a fibrous stroma, with no evidence of inflammation or malignancy

coexisting medical conditions such as malignancies (20.4%) (predominantly lung, breast, and prostate cancer); cardiovascular diseases (coronary artery disease, hypertension, atrial fibrillation, and valvular heart diseases); respiratory diseases (pulmonary tuberculosis, asthma, chronic obstructive pulmonary disease); autoimmune diseases (Behçet's disease, CREST syndrome, sarcoidosis, Sjögren's syndrome); hepatobiliary diseases; metabolic disorders and miscellaneous diseases (amyloidosis, myasthenia gravis, IgA deficiency). An association between TPO and atrophic rhinitis has been reported, with *Klebsiella pneumoniae* subspecies *ozaenae* occasionally isolated in patients with both conditions. Chronic infection and impaired mucociliary clearance have therefore been proposed as potential contributors to TPO pathogenesis; however, the direction of this relationship remains uncertain, and a causal association has not been established.[2]

High-resolution computed tomography (HRCT) chest is more sensitive than chest radiography in detecting TPO, as it can demonstrate nodules as small as 3 mm.[3] Bronchoscopic characteristic findings include sessile submucosal nodules involving the anterior and lateral walls of the trachea and main bronchi. A Chinese cohort study proposed a classification based on the bronchoscopy findings: Stage I (plaque-like infiltrations of soft whitish lesions throughout the mucosa, with hyperemia and edema), stage II (diffuse cartilaginous nodules - cobblestone appearance) and stage III (deformed and stenotic airway).[1] Although bronchoscopy findings are sufficient for diagnosis, histopathological evidence is required to rule out other mimicking conditions such as amyloidosis, relapsing polychondritis, mucoepidermoid carcinoma, sarcoidosis, and silicosis.[2]

Treatment of the disease is usually symptomatic and focuses on management of the underlying respiratory condition, while interventional bronchoscopy modalities are considered in significant fixed airway obstruction. These include laser therapy, mechanical debulking, and surgical resection (when localized).[5]

To conclude, TPO is a benign and rare disease that should be considered in patients with chronic respiratory symptoms. Bronchoscopy and histopathological examination play an important role in establishing the diagnosis. The coexistence of a history of smoking and *K. ozaenae* infection in our patient is in accordance with previously reported observations in the literature on TPO, suggesting that chronic airway inflammation and recurrent infections may have a contributory role in the pathogenesis of TPO. The treatment of the patient should be individualized according to the severity of symptoms and degree of airway obstruction.

Artificial Intelligence (AI) Disclosure

No AI was used in any step of preparing/writing of the manuscript.

Acknowledgement

None.

Orcid

Sai Sindhu Naru https://orcid.org/0009-0002-0171-0752
Virender Pratibh Prasad https://orcid.org/0000-0001-8017-3697
Venkata Nagarjuna Maturu https://orcid.org/0000-0002-3679-9497

References

1. Gracia CA, Sangiovanni S, Zúñiga-Restrepo V, et al. Tracheobronchopathia osteochondroplastica—clinical, radiological, and endoscopic correlation: Case series and literature review. J Investig Med High Impact Case Rep 2020;8:2324709620921609. DOI: 10.1177/2324709620921609.
2. Devaraja K, Surendra VU. Clinicopathological features and management principles of tracheobronchopathia osteochondroplastica - a scoping review. Indian J Otolaryngol Head Neck Surg 2023;75(4):3798–3814. DOI: 10.1007/s12070-023-03998-6.
3. Jindal S, Nath A, Neyaz Z. Tracheobronchopathia osteochondroplastica—a rare or an overlooked entity? J Radiol Case Rep 2013;7(3):16–25. DOI: 10.3941/jrcr.v7i3.1305.
4. Sun J, Xie L, Su X, et al. Tracheobronchopathia osteochondroplastica: Case report and literature review. Respir Med Case Rep 2015;15:14–17. DOI: 10.1016/j.rmcr.2015.03.003.
5. Zhang X-B, Zeng H-Q, Cai X-Y, et al. Tracheobronchopathia osteochondroplastica: A case report and literature review. J Thorac Dis 2013;5(5):E182–E184. DOI: 10.3978/j.issn.2072-1439.2013.08.64.

CASE LETTER

The Rock-garden Trachea: Tracheobronchopathia Osteochondroplastica Presenting as Recurrent Respiratory Infections

Huda Shamim[1], Anil Kumar Singh[2], Shishir Kumar[3], Rahul Sharma[4]

Received on: 10 July 2026; *Accepted on:* 01 September 2026; *Published on:* 26 September 2026

Abstract

Background: Tracheobronchopathia osteochondroplastica (TBO) is a rare, benign condition marked by numerous submucosal osteocartilaginous nodules that develop from the tracheobronchial cartilaginous rings. Because of its nonspecific symptoms, diagnosis is often delayed or found incidentally during bronchoscopy.

Case presentation: A 66-year-old male with recurrent cough and dyspnea for 2 years had multiple lower respiratory infections. He previously received 6 months of empirical anti-tubercular therapy without confirmation and remained symptomatic. He was admitted with 14 days of high-grade fever and worsening respiratory symptoms. Computed tomography (CT) showed irregular nodular indentations along the tracheal wall, sparing the posterior wall, and bilateral centrilobular nodules, indicating infective bronchiolitis. Bronchoscopy revealed multiple hard, whitish osteocartilaginous nodules projecting into the trachea and main bronchi, creating a "rock-garden" appearance. These findings confirmed diffuse TBO. He was treated conservatively with antimicrobials, bronchodilators, and airway clearance, improved clinically after the infection resolved, and was discharged with follow-up advice.

Conclusion: Tracheobronchopathia osteochondroplastica is a rare but significant consideration in the differential diagnosis of patients with chronic cough, dyspnea, and recurrent respiratory infections. Identifying its distinctive CT and bronchoscopic features is essential for prompt diagnosis and preventing unnecessary tests.

Keywords: Bronchoscopy, Case report, Chronic cough, Rock-garden appearance, Tracheobronchopathia osteochondroplastica.

Annals of Interventional Pulmonology (2026): 10.5005/annalsofip-11045-0055

Dear Editor,

Tracheobronchopathia osteochondroplastica (TBO) is a rare, benign disorder of the central airways characterized by multiple submucosal cartilaginous and osseous nodules projecting into the tracheobronchial lumen. Although first described in the 19th century, the condition remains underdiagnosed, largely because its clinical manifestations are nonspecific and may mimic more common respiratory disorders. Characteristic involvement of the anterolateral tracheal walls with relative sparing of the posterior membranous wall is an important diagnostic clue.[1–4] We report a 66-year-old man with chronic cough, progressive dyspnea, and recurrent lower respiratory tract infections who had previously received empirical antitubercular therapy (ATT), highlighting the diagnostic challenges associated with this uncommon condition.

A 66-year-old male presented to our facility with recurrent productive cough and progressively worsening dyspnea for 2 years. His cough was associated with intermittent exacerbations requiring multiple courses of antibiotics, along with gradually progressive exertional dyspnea. Two years earlier, because of persistent respiratory symptoms and radiological suspicion of pulmonary infection, he had received empirical ATT for 6 months at another healthcare facility despite the absence of microbiological confirmation of tuberculosis. His symptoms persisted with minimal improvement, and he continued to experience recurrent lower respiratory tract infections.[5,6]

Fourteen days before admission, he developed high-grade fever with an increase in cough and sputum production, suggestive of an acute infective exacerbation. As his symptoms failed to improve despite empirical antimicrobial therapy administered elsewhere, he was referred to our facility for further evaluation. There was no history of hemoptysis, significant weight loss, smoking, occupational dust exposure, connective tissue disease, diabetes mellitus, or known immunodeficiency. There was also no family history of chronic respiratory illness.

On admission, he was conscious and hemodynamically stable. His temperature was 38.4°C, pulse rate 104/min, blood pressure 126/78 mm Hg, respiratory rate 24/min, and oxygen saturation 95% on room air. General physical examination was unremarkable. Respiratory examination revealed bilateral scattered coarse crackles with occasional rhonchi, predominantly over the lower

[1–4]Department of Pulmonary Medicine, Chandan Hospital, Lucknow, Uttar Pradesh, India

Corresponding Author: Huda Shamim, Department of Pulmonary Medicine, Chandan Hospital, Lucknow, Uttar Pradesh, India, Phone: +91 9793240992, e-mail: hudashamim28@yahoo.com

How to cite this article: Shamim H, Singh AK, Kumar S, *et al*. The Rock-garden Trachea: Tracheobronchopathia Osteochondroplastica Presenting as Recurrent Respiratory Infections. Ann Interv Pulmonol 2026;2(2):106–110.

Source of support: Nil

Conflict of interest: None

Patient consent statement: A written informed consent was obtained from the patient for the publication of details, which can include photographs and/or videos and/or case history to be published in any printed/online journals.

© The Author(s). 2026 Open Access. This article is distributed under the terms of the Creative Commons Attribution-NonCommercial 4.0 International License (https://creativecommons.org/licenses/by-nc/4.0/). This license permits non-commercial use, distribution, and reproduction in any medium, provided the original author and source are credited, a link to the license is included, and any changes are indicated.

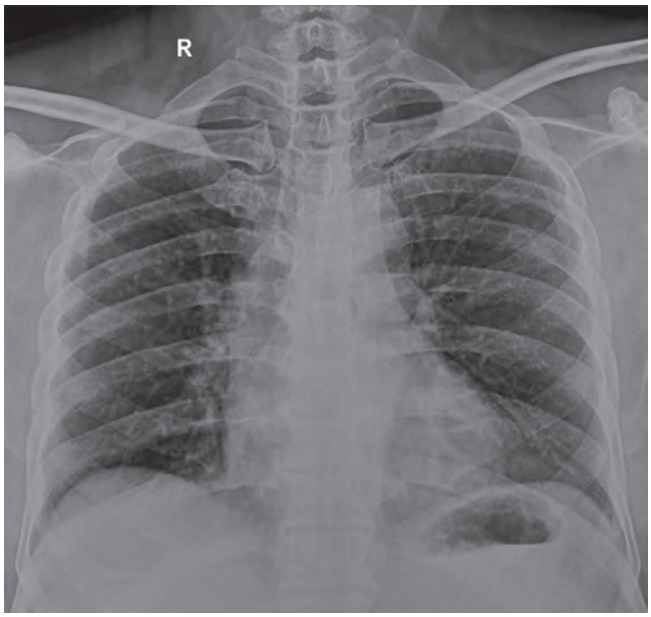


Fig. 1: Chest radiograph demonstrating no significant focal parenchymal abnormality, consolidation, cavitation, or mediastinal lymphadenopathy. The radiograph was largely unremarkable despite the patient's chronic respiratory symptoms and recurrent lower respiratory tract infections

lung fields. Cardiovascular and abdominal examinations were normal. Laboratory investigations demonstrated leukocytosis with neutrophilic predominance and elevated inflammatory markers, consistent with an ongoing respiratory infection. Sputum Gram stain, bacterial cultures, acid-fast bacilli smear, cartridge-based nucleic acid amplification test (CBNAAT), and fungal workup were negative. Routine biochemical parameters were within normal limits.

Chest radiography did not reveal any significant abnormality (Fig. 1). However, high-resolution computed tomography (HRCT) of the chest demonstrated irregular nodular indentations along the tracheal wall with relative preservation of the posterior membranous wall. Multiple bilateral centrilobular nodules with a tree-in-bud pattern were also noted, suggestive of infective bronchiolitis (Figs 2A to D). There was no significant mediastinal lymphadenopathy or parenchymal mass lesion. In view of the persistent respiratory symptoms, recurrent infections, and unusual tracheal abnormalities on computed tomography (CT), flexible bronchoscopy was performed.

Bronchoscopy revealed numerous whitish-yellow, hard, sessile nodules protruding into the airway lumen throughout the trachea and extending into both main bronchi. The lesions appeared as multiple cartilaginous and osseous excrescences arising from the anterolateral tracheobronchial walls, with sparing of the posterior membranous wall. The intervening mucosa was mildly inflamed (Figs 3A and B). Collectively, these findings produced the characteristic "rock-garden," "cobblestone," or "stalactite cave" appearance described in TBO. Based on the highly characteristic bronchoscopic findings, a diagnosis of TBO with recurrent lower respiratory tract infections was established.

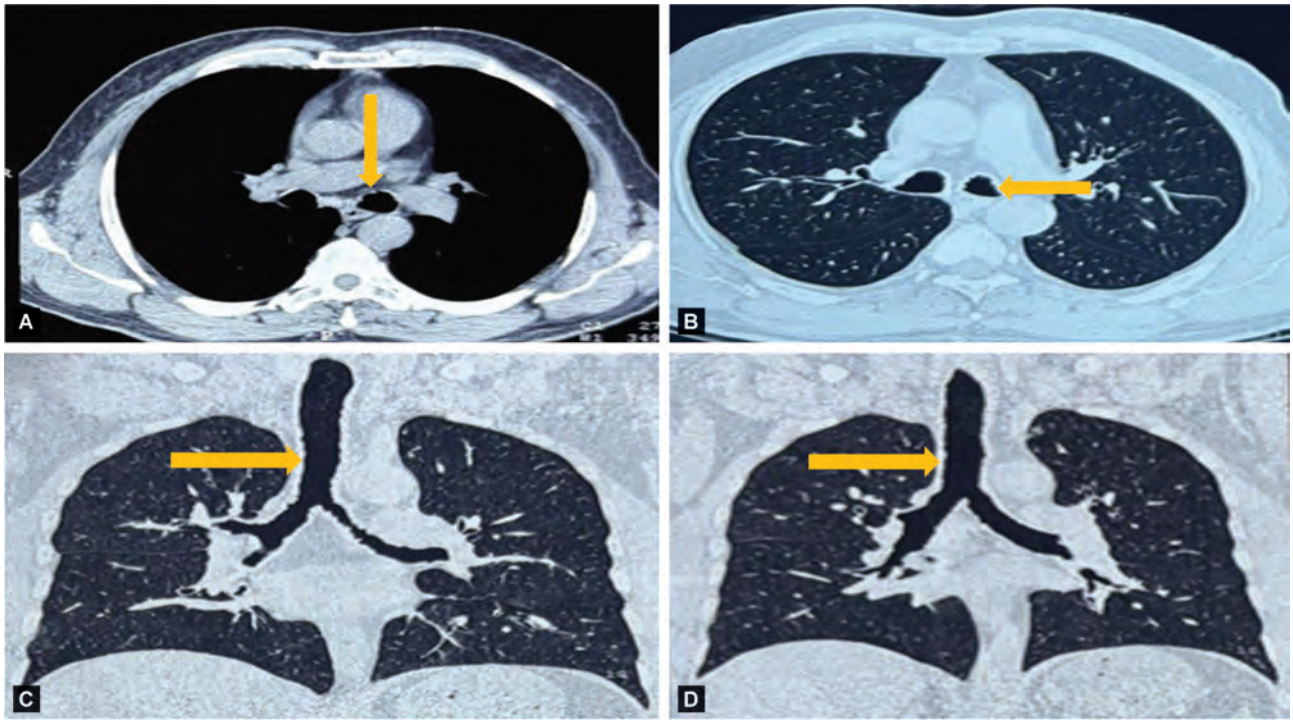
The patient was managed conservatively with culture-directed antimicrobial therapy, airway clearance measures, bronchodilator therapy, and supportive care. Following resolution of the infectious episode, he showed significant symptomatic improvement and became afebrile. He was discharged in a stable condition and advised regular follow-up for monitoring of respiratory symptoms, airway obstruction, and future infective exacerbations.

Tracheobronchopathia osteochondroplastica, also referred to as tracheopathia osteoplastica, is characterized by multiple submucosal nodules composed of cartilage and bone, predominantly involving the anterior and lateral tracheobronchial walls. The relative sparing of the posterior membranous wall is an important distinguishing feature because the lesions arise from the cartilaginous rings. Although the disease was described more than 150 years ago, its precise pathogenesis remains uncertain. Proposed mechanisms include chronic airway inflammation, metaplastic transformation of elastic connective tissue into cartilage and bone, ecchondroses and exostosis arising from tracheal cartilage, and abnormal bone formation mediated by bone morphogenetic protein-2 and transforming growth factor-beta. Chronic infection and repeated airway injury have also been proposed as possible contributing factors.[1–4,7,8]

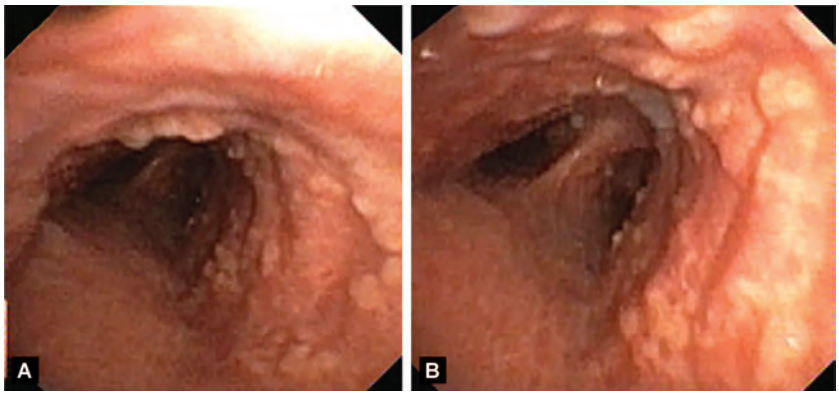
Tracheobronchopathia osteochondroplastica predominantly affects middle-aged and older individuals, with most patients being in their fifth to seventh decades. Diagnosis may be delayed because the clinical manifestations are nonspecific. Chronic cough is the most common symptom, followed by dyspnea, wheezing, recurrent respiratory infections, and occasionally hemoptysis. The clinical presentation may mimic asthma, chronic obstructive pulmonary disease, bronchitis, tuberculosis, tracheobronchial amyloidosis, or malignancy. A proportion of patients remain asymptomatic and are diagnosed incidentally during bronchoscopy or CT imaging. In our patient, the 2-year history of cough and dyspnea, accompanied by recurrent respiratory infections, is particularly noteworthy. The protruding osteocartilaginous nodules can interfere with mucociliary clearance and impair effective mucus drainage, thereby facilitating bacterial colonization and recurrent infection. Infective bronchiolitis and recurrent pneumonia have previously been described in patients with symptomatic or extensive TBO.[4,9–11]

However, HRCT plays an important role in suggesting the diagnosis. Typical findings include irregular nodular thickening and calcified protrusions arising from the anterolateral tracheal wall, variable degrees of luminal narrowing, and preservation of the posterior membranous wall. Calcification may not always be evident, particularly in early disease. In our patient, the combination of irregular tracheal wall indentations and posterior wall preservation raised the possibility of TBO and prompted bronchoscopy. The tree-in-bud nodules were considered likely to represent infective bronchiolitis related to impaired airway clearance rather than direct pulmonary involvement by TBO.[12,13]

Bronchoscopy remains the diagnostic gold standard. The characteristic finding is multiple hard, whitish, sessile nodules projecting into the tracheobronchial lumen, producing the classic rock-garden or cobblestone appearance. The lesions commonly involve the distal two-thirds of the trachea and may extend into the main and lobar bronchi. Our patient had diffuse involvement of the trachea and both main bronchi, representing extensive disease. The widespread cartilaginous growths observed bronchoscopically were essentially diagnostic of TBO. Histologically, TBO lesions contain mature cartilage, calcified cartilage, lamellar bone, and occasionally bone marrow elements beneath an intact respiratory epithelium. However, biopsy can be technically difficult because the nodules are extremely hard, and tissue obtained may be inadequate. Consequently, in the presence of characteristic



Figs 2A to D: Computed tomography chest findings. (A) Axial mediastinal window image showing irregular nodular protrusions arising from the tracheal wall (yellow arrow) causing luminal indentation; (B) Axial lung window image demonstrating nodular thickening of the tracheobronchial wall with preservation of the posterior membranous wall (yellow arrow); (C and D) Coronal lung window images showing multiple nodular excrescences projecting into the tracheal lumen along the anterolateral walls (yellow arrows), producing characteristic tracheal irregularity while sparing the posterior wall, a feature suggestive of TBO



Figs 3A and B: Bronchoscopic appearance of TBO. (A and B) Flexible bronchoscopy shows multiple hard, sessile, whitish osteocartilaginous nodules projecting into the tracheal lumen from the anterolateral walls, producing the characteristic "rock-garden" or "cobblestone" appearance. The nodules cause diffuse mucosal irregularity and luminal narrowing while relatively sparing the posterior membranous wall, a hallmark of TBO

radiological and bronchoscopic findings, histological confirmation may not always be necessary.[4,8,14–16]

The principal differential diagnosis is tracheobronchial amyloidosis, which more commonly involves the posterior membranous wall and produces circumferential airway thickening. Relapsing polychondritis can also spare the posterior wall but is generally associated with diffuse cartilage inflammation and dynamic airway collapse rather than discrete osteocartilaginous nodules. Endobronchial tuberculosis, papillomatosis, granulomatosis with polyangiitis, sarcoidosis, and tracheal malignancy should also be considered. The combination of posterior wall sparing and hard nodular lesions on bronchoscopy strongly favors TBO.[4,8]

There is currently no specific medical treatment for TBO. Management is primarily directed toward symptom control and prevention or treatment of complications. Respiratory infections should be appropriately treated, while airway humidification, mucolytics, pulmonary rehabilitation, and airway clearance techniques may provide symptomatic benefit. In patients with severe airway obstruction or significant symptomatic stenosis, interventional bronchoscopic procedures such as laser ablation, cryotherapy, mechanical debulking, balloon dilation, or airway stenting may be considered. Surgical resection is rarely required. The overall prognosis is generally favorable because TBO usually progresses slowly over several years.[4]

Table 1: Differential diagnosis of nodular tracheal diseases

Disorder	Posterior wall involvement	HRCT findings	Bronchoscopy
Tracheobronchopathia osteochondroplastica	Typically spared	Calcified nodules from cartilaginous rings	Hard whitish nodules, cobblestone appearance
Tracheobronchial amyloidosis	Common	Circumferential wall thickening, calcification	Diffuse infiltrative plaques
Relapsing polychondritis	Usually spared, but diffuse cartilage involvement	Tracheal thickening and airway collapse	Inflamed cartilaginous rings
Endobronchial tuberculosis	Variable	Focal stenosis, nodularity	Ulcerative or granular lesions
Tracheal malignancy	Variable	Focal mass lesion	Irregular friable growth

HRCT, high-resolution computed tomography

This case emphasizes that TBO should be considered in older patients with chronic cough, recurrent respiratory infections, or unexplained respiratory symptoms, particularly when imaging demonstrates nodular tracheal abnormalities with posterior membranous wall sparing. The diagnosis is especially important in tuberculosis-endemic regions, where nonspecific respiratory symptoms and radiological abnormalities may lead to empirical ATT, as occurred in our patient. Recognition of the characteristic CT and bronchoscopic appearances can prevent diagnostic delay and unnecessary treatment (Table 1).

Key Learning Points

- Tracheobronchopathia osteochondroplastica should be suspected in patients with chronic cough, recurrent respiratory infections, and unexplained tracheal abnormalities on imaging.
- Sparing of the posterior membranous tracheal wall on CT and bronchoscopy helps differentiate TBO from other tracheal diseases.
- Bronchoscopy remains the gold standard for diagnosis, revealing the characteristic "rock-garden" appearance of multiple osteocartilaginous nodules.
- Tracheobronchopathia osteochondroplastica may mimic pulmonary tuberculosis and other chronic airway disorders, leading to delayed diagnosis and unnecessary therapy.

Limitation(s) of the Study

This report represents a single case and therefore cannot establish the broader clinical spectrum or natural history of TBO.

Clinical Significance

Consider tracheobronchopathia osteochondroplastica in patients presenting with chronic cough, unexplained dyspnea, or recurrent respiratory infections, especially when CT reveals nodular irregularities of the tracheal wall with sparing of the posterior membranous wall. Early identification of this distinctive radiological and bronchoscopic pattern can prevent diagnostic delays, prevent unnecessary treatments such as empirical antitubercular therapy, and enable appropriate management of associated airway obstruction and recurrent infections.

Declarations

Ethics Approval

Not applicable.

Availability of Data and Materials

Not applicable.

Artificial Intelligence (AI) Disclosure

AI tools were used for grammatical correction.

Clinical Trial Registry Number

Not applicable.

Acknowledgment

None.

Authors' Contributions

Huda Shamim was the lead author for this case article. Huda Shamim, Anil K Singh, Shishir Kumar, and Rahul Sharma played a significant role in drafting the manuscript. Anil K Singh, Shishir Kumar, and Rahul Sharma were involved in the final review and submission of the article. All authors read and approved the final manuscript.

Orcid

Huda Shamim https://orcid.org/0009-0003-7717-5482
Anil Kumar Singh https://orcid.org/0009-0008-1815-9331
Shishir Kumar https://orcid.org/0009-0004-4223-7353
Rahul Sharma https://orcid.org/0009-0008-6550-330X

References

1. Dalgaard JB. Tracheopathia chondro-osteoplastica. A case elucidating the problems concerning development and ossification of elastic cartilage. Acta Pathologica Microbiologica Scandinavica 1947;24:118–134. DOI: 10.1111/j.1699-0463.1947.tb00581.x.
2. Moersch HJ, Broders AC, Havens FZ. Tracheopathia osteoplastica (osteoma of the trachea). Arch Otolaryngol 1937;26(3):291–293. DOI: 10.1001/archotol.1937.00650020319004.
3. Wilks S. Ossific deposits on the larynx, trachea and bronchi. Trans Pathol Soc Lond 1857;8:88. Available from: https://journals.sagepub.com/doi/epdf/10.1177/003591577606900524. Last accessed on: 10th September 2026.
4. Dumazet A, Launois C, Lebargy F, et al. Tracheobronchopathia osteochondroplastica: Clinical, bronchoscopic, and comorbid features in a case series. BMC Pulm Med 2022;22(1):423. DOI: 10.1186/s12890-022-02225-2.
5. Hussain K, Gilbert S. Tracheopathia osteochondroplastica. Clin Med Res 2003;1(3):239–242. DOI: 10.3121/cmr.1.3.239.
6. Liu Q, Hu Y, Lei M, et al. Clinical characteristics of tracheobronchopathia osteochondroplastica: A retrospective study of 33 patients. Int J Gen Med 2023:16:3447–3455. DOI: 10.2147/IJGM.S418394.
7. Wang H, Li S, Chen P, et al. Tracheobronchopathia osteochondroplastica: A case report and literature review. Zhong Nan Da Xue Xue Bao Yi Xue Ban 2020;45(2):208–215. DOI: 10.11817/j.issn.1672-7347.2020.180804.

8. García CA, Sangiovanni S, Zúñiga-Restrepo V, et al. Tracheobronchopathia osteochondroplastica—clinical, radiological, and endoscopic correlation: Case series and literature review. J Investigative Med High Impact Case Rep 2020;8:2324709620921609. DOI: 10.1177/2324709620921609.
9. Zhu Y, Wu N, Huang H-D, et al. A clinical study of tracheobronchopathia osteochondroplastica: Findings from a large Chinese cohort. PLoS One 2014;9(7):e102068. DOI: 10.1371/journal.pone.0102068.
10. Cho HK, Jeong B-H, Kim H. Clinical course of tracheobronchopathia osteochondroplastica. J Thorac Dis 2020;12(10):5571–5579. DOI: 10.21037/jtd-20-1898.
11. Abouda M, Jomni T, Charfi MR. Tracheobronchopathia osteochondroplastica: An unusual cause of chronic cough. QJM 2016;109(3):193–194. DOI: 10.1093/qjmed/hcv166.
12. Cai ZG, Quan GM, Zhang HF. Tracheobronchopathia osteochondroplastica: Diagnostic value of computed tomography. Am J Med Sci 2015;349(4):357. DOI: 10.1097/MAJ.0000000000000199.
13. White BD, Kong A, Khoo E, et al. Computed tomography diagnosis of tracheobronchopathia osteochondroplastica. Australas Radiol 2005;49(4):319–321. DOI: 10.1111/j.1440-1673.2005.01444.x.
14. Nielsen SW, Stevens JR, Dion GR, et al. Dyspnea, dysphonia, and cough: Varied presentations of tracheobronchopathia osteochondroplastica. Ann Otol Rhinol Laryngol 2015;124(10):829–833. DOI: 10.1177/0003489415586845.
15. Riva G, Girolami I, Luchini C, et al. Tracheobronchopathia osteochondroplastica: A case report illustrating the importance of multilevel workup clinical, endoscopic and histological assessment in diagnosis of an uncommon disease. Am J Case Rep 2019;20:74–77. DOI: 10.12659/AJCR.911859.
16. Prince JS, Duhamel DR, Levin DL, et al. Nonneoplastic lesions of the tracheobronchial wall: Radiologic findings with bronchoscopic correlation. Radiographics 2002;22:S215–S230. DOI: 10.1148/radiographics.22.suppl_1.g02oc02s215.

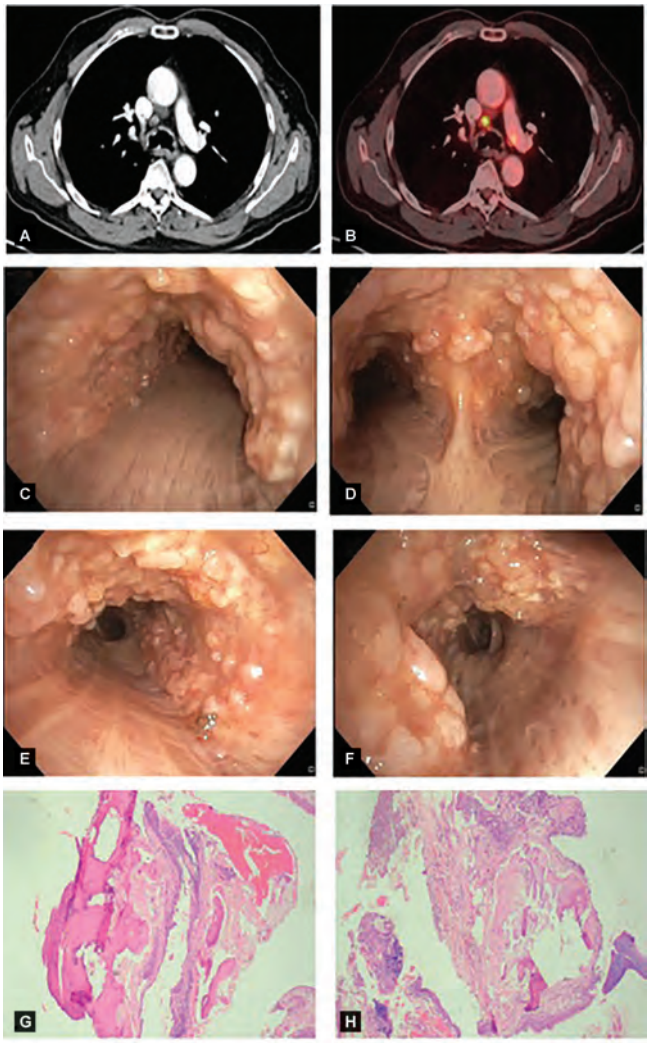
IMAGE OF THE ISSUE

When the Trachea Hardens: "Rock Garden Trachea"

Spurthi K[1], Virender Pratibh Prasad[2], Venkata Nagarjuna Maturu[3]

Received on: 06 July 2026; *Accepted on*: 18 August 2026; *Published on*: 26 September 2026

Annals of Interventional Pulmonology (2026): 10.5005/annalsofip-11045-0049



Figs 1A to H: (A and B) Contrast-enhanced computed tomography of chest (CECT chest) and PET-CT images demonstrating mild diffuse nodular thickening with intermittent calcific densities noticed at the level of carina respectively. Lesions show no demonstrable FDG uptake. Bronchoscopic findings; (C to F) Multiple submucosal nodular lesions protruding from anterolateral wall into tracheobronchial lumen at different levels: (C) Subglottic region; (D) Carina; (E) Left main bronchus, (F) Right main bronchus; Histopathological examination from tracheal nodule biopsy shows: (G) Tracheal mucosa with submucosal nodules composed of cartilage and bone; (H) Submucosal cartilage nodule

[1]Department of Respiratory Medicine, Manipal Hospitals, Mysuru, Karnataka, India

[2,3]Department of Pulmonary Medicine, Yashoda Hospital, Hyderabad, Telangana, India

Corresponding Author: Venkata Nagarjuna Maturu, Department of Pulmonary Medicine, Yashoda Hospital, Hyderabad, Telangana, India, Phone: +91 9000060507, e-mail: arjunjipmer@yahoo.co.in

How to cite this article: Spurthi K, Prasad VP, Maturu VN. When the Trachea Hardens: "Rock Garden Trachea". Ann Interv Pulmonol 2026;2(2):111–112.

Source of support: Nil

Conflict of interest: Venkata Nagarjuna Maturu is associated as Editor-in-Chief of this journal and this manuscript was subjected to this journal's standard review procedures, with this peer review handled independently of the Editor-in-Chief and his research group.

Tracheobronchopathia osteochondroplastica (TO) is a rare benign disorder of unknown etiology, characterized by multiple, submucosal osseocartilaginous nodules protruding from the anterolateral wall into the tracheobronchial lumen, sparing the posterior wall.[1] The exact prevalence of TO is underestimated due to subtle or absent symptoms. The clinical manifestations are nonspecific respiratory tract symptoms such as cough, hemoptysis, dyspnea on exertion, and wheezing.[2] The disease generally has an indolent course, but in rare cases, it may progress rapidly, resulting in clinically significant airway stenosis or life-threatening airway obstruction.[3] Histopathological examination remains the gold standard for establishing the diagnosis. Management is predominantly conservative, with bronchoscopic intervention reserved for symptomatic or progressive disease.[3,4]

We present a case of a male patient in his early seventies with no known comorbidities or addictions. He presented to us with a 4-week history of cough associated with scanty expectoration and fever. He received treatment at multiple healthcare facilities, with antibiotics and bronchodilators; despite this, his symptoms persisted. He was referred to our institution for further management. At presentation to our center, his vitals were stable, but he reported multiple episodes of hemoptysis (approximately 20 mL) over the last 5 days. Laboratory investigations, including complete blood count, inflammatory markers, renal and liver function tests, and coagulation parameters, were within normal limits. Respiratory examination revealed bilaterally diminished breath sounds on auscultation.

Contrast-enhanced computed tomography (CT) and positron emission tomography (PET)-CT demonstrated diffuse nodular thickening of the tracheal wall with scattered calcifications, without significant fluorodeoxyglucose (FDG) uptake. Additionally, imaging revealed a hypermetabolic cavitary lesion in the left lower lobe measuring 43 × 35 × 27 mm (SUV max 8.8), a subsolid lesion in

© The Author(s). 2026 Open Access. This article is distributed under the terms of the Creative Commons Attribution-NonCommercial 4.0 International License (https://creativecommons.org/licenses/by-nc/4.0/). This license permits non-commercial use, distribution, and reproduction in any medium, provided the original author and source are credited, a link to the license is included, and any changes are indicated.

the right upper lobe with surrounding ground-glass opacities measuring 32 × 21 × 17 mm (SUV max 4.9), and FDG-avid right paratracheal and subcarinal mediastinal lymphadenopathy.

Flexible bronchoscopy was performed, which showed numerous hard, whitish nodules projecting from the anterolateral walls of the trachea and bilateral main bronchi, imparting a characteristic "rock garden" appearance. The posterior tracheal wall was relatively spared. Multiple endobronchial biopsies were obtained from the tracheal nodules, which demonstrated submucosal chondro-osseous nodules with mild chronic inflammatory infiltrates, establishing the diagnosis of TO (Fig. 1).

During the same procedure, radial endobronchial ultrasound (EBUS) biopsy of the left lower lobe lesion and linear EBUS sampling of the mediastinal lymph nodes were also performed, which confirmed lung adenocarcinoma with nodal metastases. A CT-guided biopsy from the right upper lobe lesion was later performed, which also confirmed it to be metastatic lung adenocarcinoma. Following a multidisciplinary team discussion, palliative treatment was recommended for the underlying malignancy, while the tracheal pathology was managed conservatively in view of its benign nature and the absence of significant airway compromise.

The coexistence of TO with primary lung malignancy has only occasionally been reported in the literature.[5] Whether this association is incidental or reflects a shared pathogenic mechanism remains unclear. Although infrequently encountered, TO has a remarkably characteristic phenotype. Recognition of its pathognomonic bronchoscopic appearance and posterior wall sparing, in conjunction with supportive imaging and histopathology, enables accurate diagnosis and prevents it from being mistaken for diffuse tracheobronchial malignancy or other infiltrative airway disorders. Nevertheless, recognition of TO is important to avoid misdiagnosis.

Ethical Approval

Not applicable.

Data Availability

Not applicable as it is a case report.

AI Disclosure

No AI used in preperation of manuscript.

Patient Consent Statement

The author(s) have obtained written informed consent from the patient for publication of the related images.

Acknowledgments

None.

Authors' Contributions

Spurthi K: Drafted the manuscript and managed the patient.
Virender Pratibh Prasad: Performed the procedure.
Venkata Nagarjuna Maturu: Performed the procedure and revised the manuscript.

Orcid

Virender Pratibh Prasad https://orcid.org/0000-0001-8017-3697
Venkata Nagarjuna Maturu https://orcid.org/0000-0002-3679-9497

References

1. Silveira MGM, de Oliveira Castellano MVC, Fuzi CE, et al. Tracheobronchopathia osteochondroplastica. J Bras Pneumol 2017;43(2):151–153. DOI: 10.1590/S1806-37562016000000143.
2. Luo S, Wu L, Zhou J, et al. Tracheobronchopathia osteochondroplastica: Two cases and a review of the literature. Int J Clin Exp Pathol 2015;8(7):8585–8590. PMID: 26339438.
3. Abali H. A rare case of rapidly progressive tracheobronchopathia osteochondroplastica. Respir Med Case Rep 2023;43:101853. DOI: 10.1016/J.RMCR.2023.101853.
4. Sun J, Xie L, Su X, et al. Tracheobronchopathia osteochondroplastica: Case report and literature review. Respir Med Case Rep 2015;15:14–17. DOI: 10.1016/J.RMCR.2015.03.003.
5. Feng Y, Wang L, Jia R, et al. Tracheobronchopathia osteochondroplastica concurrent with peripheral lung cancer: A case report and perioperative considerations. Transl Cancer Res 2024;13(4):2064–2072. DOI: 10.21037/tcr-24-410.

VIDEO OF THE ISSUE

Emergency Airway Rescue with Self-expandable Metallic Y Stent for Malignant Distal Tracheobronchial Compression in a Young Adult with Soft Tissue Sarcoma

Yasho Vardhan Mangisetty[1], Koripi Kondala Rao[2], Khazi Mohammed Athar[3]

Keywords: Airway stenting, Carinal obstruction, Interventional pulmonology, Malignant central airway obstruction, Rigid bronchoscopy, Self-expandable metallic stent, Soft tissue sarcoma, Tracheal compression.

Annals of Interventional Pulmonology (2026): 10.5005/annalsofip-11045-0052

Malignant central airway obstruction (MCAO) is a potentially fatal complication of thoracic malignancy that may present with respiratory failure, hemodynamic instability, and difficulty in mechanical ventilation. While endoluminal or mixed lesions may respond to conventional endobronchial debulking, obstruction due to pure extrinsic compression of the distal trachea and carina cannot be relieved by debulking, as there is no endoluminal tumor to resect; airway stenting is the only means of restoring luminal patency and can be lifesaving in such patients.

A 22-year-old male with soft tissue sarcoma of the right foot presented in an unconscious state with poor Glasgow Coma scale (GCS), severe respiratory distress, and hypotension. Arterial blood gas revealed type I respiratory failure, necessitating emergency intubation and mechanical ventilation. Persistently elevated peak airway pressures prompted urgent bronchoscopic evaluation. Flexible bronchoscopy showed critical narrowing of the distal trachea, carina, and right main bronchus, with thick mucopurulent secretions from the left main bronchus; bronchoscopic toileting was performed. Contrast-enhanced computed tomography (CECT) chest confirmed a large right thoracic mass causing extrinsic compression of the distal trachea and central airways, along with a left lower lobe mass.

Given critical airway obstruction and persistent ventilatory compromise, the patient underwent rigid bronchoscopy under general anesthesia, with deployment of a 16 × 60 mm self-expandable metallic Y stent (SEMS) across the narrowed segment. Airway patency and ventilation improved immediately, and the patient was extubated within 24 hours.

This case underscores the importance of early recognition of MCAO in patients with unexplained ventilatory difficulty and elevated airway pressures and demonstrates that rigid bronchoscopy with SEMS placement can rapidly and effectively restore central airway patency, even in critically ill young patients with advanced malignancy.

Clinical Significance

This case illustrates a systematic, stepwise approach to an unrecognized MCAO presenting as ventilatory failure. Persistently elevated airway pressures after intubation prompted diagnostic flexible bronchoscopy and cross-sectional imaging, which together localized a critical obstruction at the distal trachea, carina, and right main bronchus arising from pure extrinsic compression, with no endoluminal tumor component. As the obstruction was purely compressive rather than infiltrative, conventional endobronchial debulking had no role, and airway stenting remained the only means of restoring luminal patency. Rigid bronchoscopy under general anesthesia allowed safe airway control and precise deployment of a self-expandable metallic stent across this technically demanding segment, achieving immediate restoration of airway patency and permitting extubation within 24 hours. This case underscores rigid bronchoscopy with SEMS placement as the definitive rescue strategy for pure extrinsic distal and carinal MCAO, and highlights the importance of prompt bronchoscopic and radiological evaluation whenever unexplained ventilatory compromise persists after intubation.

Ethical Approval

This case video does not report a new intervention, drug, or device outside standard practice, and was performed as part of routine emergency clinical care. Institutional ethics committee approval was therefore not required for this single-case report/video, in accordance with institutional policy; a formal waiver is enclosed as per journal requirements.

Patient Consent Statement

Written informed consent for the use of procedural video and case details for publication was obtained from the patient.

[1,2]Department of Pulmonology, KIMS Group of Hospitals, Anantapur, Andhra Pradesh, India

[3]Department of Radiology, KIMS Group of Hospitals, Anantapur, Andhra Pradesh, India

Corresponding Author: Yasho Vardhan Mangisetty, Department of Pulmonology, KIMS Group of Hospitals, Anantapur, Andhra Pradesh, India, Phone: +91 9642317642, e-mail: dr.yashvardha@gmail.com

How to cite this article: Mangisetty YV, Rao KK, Athar KM. Emergency Airway Rescue with Self-expandable Metallic Y Stent for Malignant Distal Tracheobronchial Compression in a Young Adult with Soft Tissue Sarcoma. Ann Interv Pulmonol 2026;2(2):113–114.

Source of support: Nil

Conflict of interest: None

© The Author(s). 2026 Open Access. This article is distributed under the terms of the Creative Commons Attribution-NonCommercial 4.0 International License (https://creativecommons.org/licenses/by-nc/4.0/). This license permits non-commercial use, distribution, and reproduction in any medium, provided the original author and source are credited, a link to the license is included, and any changes are indicated.

Data Availability Statement

The data supporting the findings of this case video (de-identified imaging and procedural records) are available from the corresponding author upon reasonable request.

Artificial Intelligence (AI) Disclosure Statement

No AI or AI-assisted technologies were used in the generation of clinical data, image/video content, or in the analysis and interpretation of this case.

Acknowledgments

The authors would like to sincerely thank the Department of Anesthesia and Critical Care and the Emergency Department at KIMS Saveera Hospital for their invaluable support in the emergency management of this patient. The authors also thank Dr Kalyan Ram at KIMS Saveera Hospital for his contribution to the care of this patient.

Access this video online	
Quick Response Code:	**Website:**
	tinyurl.com/Annals0052-vid

OLYMPUS

EVIS X1 VIDEO SYSTEM & Pleura videoscope

(CV-1500 & LTF-H290)



Features



EVIS X1 (CV-1500)

- **5 LED System** Longer Life, Improved image
- **TXI** Texture, Color and Brightness optimization
- **RDI** Visibility of blood vessels and bleeding point
- **Full Screen** Enhances Broncoscopy experience
- **BAI-MAC** Improves brightness in darker regions

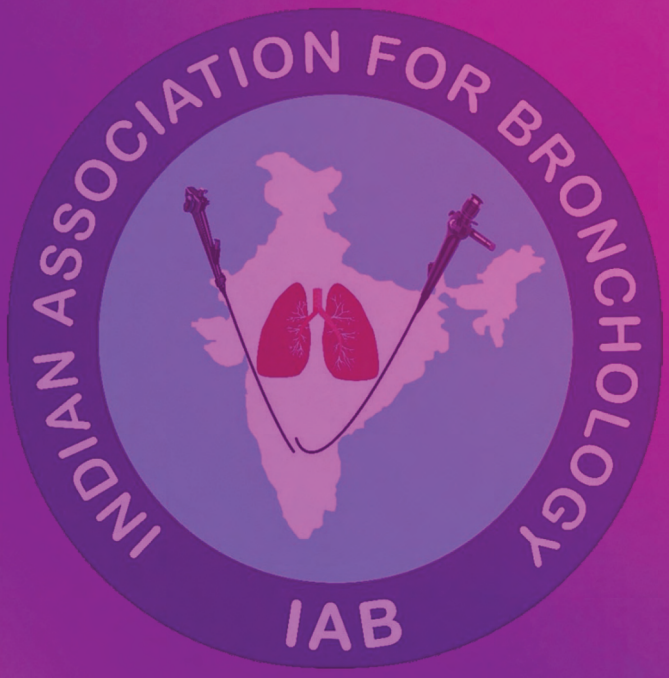
Pleura Videoscope (LTF-H290)

- **HDTV** Bright, clear observation with HD imaging
- **NBI** Enhanced Imaging of vascular structures
- **EVIS X1 Features** TXI, RDI, BAI-MAC compatible
- **Angulation** UP Angulation of 180 Degree
- **Channel** Larger 3.0 mm Channel

Information

www.olympusmedical.co.in

SAS Tower, Ground Floor, Sec-38
Gurugram, Haryana- 122001


INDIAN ASSOCIATION FOR BRONCHOLOGY
IAB